eCAM Evidence-Based Complementary and Alternative Medicine

Translational Research in Complementary and Alternative Medicine 2014

Guest Editors: Wei Jia, Aiping Lu, Kelvin Chan, Mats G. Gustafsson, and Ping Liu

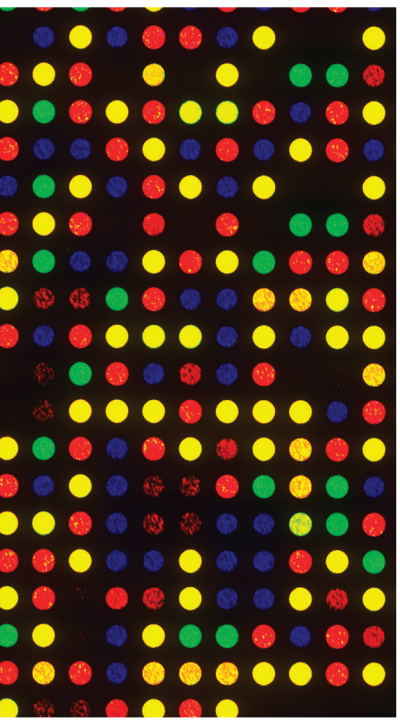

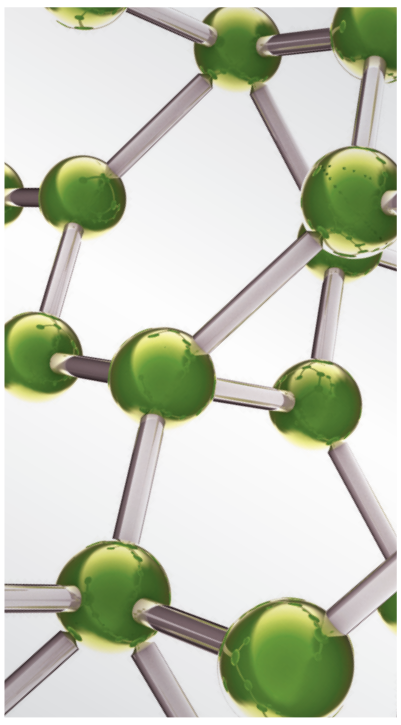


Translational Research in Complementary and Alternative Medicine 2014

Evidence-Based Complementary and Alternative Medicine

Translational Research in Complementary and Alternative Medicine 2014

Guest Editors: Wei Jia, Aiping Lu, Kelvin Chan, Mats G. Gustafsson, and Ping Liu

Editorial Board

Hindawi Publishing Corporation
Evidence-Based Complementary and Alternative Medicine
Volume 2015, Article ID 427508, 2 pages
http://dx.doi.org/10.1155/2015/427508

Editorial

Translational Research in Complementary and Alternative Medicine 2014

Wei Jia,[1,2] Aiping Lu,[3] Kelvin Chan,[4,5] Mats G. Gustafsson,[6] and Ping Liu[7]

[1]*Center for Translational Medicine, Shanghai Jiao Tong University Affiliated Sixth People's Hospital, Shanghai 200233, China*
[2]*Cancer Epidemiology, University of Hawaii Cancer Center, Honolulu, HI 96813, USA*
[3]*School of Chinese Medicine, Hong Kong Baptist University, Kowloon Tong, Hong Kong*
[4]*Faculty of Pharmacy, The University of Sydney, NSW 2006, Australia*
[5]*The National Institute of Complementary Medicine, School of Science & Health, University of Western Sydney, NSW 2791, Australia*
[6]*Cancer Pharmacology and Computational Medicine, Department of Medical Sciences, Uppsala University, Uppsala Academic Hospital, 751 85 Uppsala, Sweden*
[7]*Key Laboratory of Liver and Kidney Diseases (Ministry of Education), E-institute of Shanghai Municipal Education Commission, Institute of Liver Diseases, Shuguang Hospital Affiliated to Shanghai University of Traditional Chinese Medicine, Shanghai 201203, China*

Correspondence should be addressed to Wei Jia; wjia@cc.hawaii.edu

Received 16 September 2014; Accepted 16 September 2014

Complementary and alternative medicine (CAM) has often been regarded as a practical, holistic, and personalized medical approach. However, the CAM research community in the past two decades has witnessed a huge disconnection between clinical studies and preclinical studies including authentication, quality control, pharmacology, and toxicology of CAM agents. Meanwhile, novel translational research approaches, including cutting-edge-omics technologies, new bioinformatics tools, novel imaging modalities, well-designed clinical trial metrics, protocols, and outcome measures, are still lacking in the CAM research. In this special issue, we aim to promote research that can translate from bench to bedside in CAM diagnosis and treatments.

This issue contains seven papers, where two papers reported novel approaches to human metabolic disease diagnosis using metabolomics technology. X. Wang et al. reported a novel syndrome differentiation strategy investigated in a clinical study. A group of liver cirrhosis patients ($n = 63$) who were classified into two TCM syndromes, "Liver-Kidney Yin Deficiency" or "Dampness-Heat Internal Smoldering," and healthy subjects ($n = 31$) were recruited, and a combined gas chromatography, as well as liquid chromatography mass spectrometry, was used to profile the urine samples of the study participants. The results underscored several key urinary metabolite markers, including glycoursodeoxycholate, cortolone-3-glucuronide, and L-aspartyl-4-phosphate, that can readily differentiate between the two TCM syndromes. T. Wu et al. applied a mass spectrometry-based metabolomics approach to characterize the distinct alterations of serum metabolites among diabetes patients who can be classified into "excess" and "deficiency" TCM syndromes. The results suggest that patients with the excess syndrome have more oxidative stress than the deficiency syndrome, highlighting a novel diabetic patient subtyping method using a metabolomics approach.

Dr. G. H. Seol's group reported an interesting clinical trial to investigate the effects of inhalation of the essential oil of *Citrus aurantium L. var. amara* (neroli oil) on menopausal symptoms, stress, and estrogen in postmenopausal women. Sixty-three healthy postmenopausal women were randomized to inhale 0.1% or 0.5% neroli oil (v/v in almond oil) or almond oil (control) for 5 minutes twice daily for 5 days. They report that systolic blood pressure and diastolic blood pressure were significantly lower among participants inhaling

neroli oil than the control group, suggesting that neroli oil may have potential as an effective intervention to reduce stress and improve the endocrine system.

J. Qi et al. evaluated the therapeutic effect and mechanisms of a traditional Chinese medicine, Apocynum Tablet (AT), on cardiac hypertrophy in a mouse model of cardiac hypertrophy. AT is formulated mainly with *Apocynum*, *Chrysanthemum*, and *Fangchi* and widely used in China to treat patients with hypertension. Their experimental data provided evidence that AT inhibits cardiac hypertrophy from pressure overload and thus explained a possible mechanism of the effective AT treatment in patients with cardiac hypertrophy. The authors also suggested that selective ERK1/2 and AKT modulation for cardioprotection as possible therapeutic targeting may be feasible.

In the paper entitled "*The traditional kampo medicine tokishakuyakusan increases ocular blood flow in healthy subjects*," S. Takayama et al. reported a clinical study with healthy volunteers to examine the effects of oral administration of kampo medical formulas on ocular blood flow. A crossover protocol was used to randomly administer 5 grams of one of the 4 kampo medical formulas to 13 healthy subjects (mean age: 37.3 ± 12.3 years). Laser speckle flowgraphy was used and blood pressure and intraocular pressure were also recorded in the study. The authors concluded that one of the kampo formulas, tokishakuyakusan, can significantly increase ocular blood flow, at 30 to 60 minutes after administration, without affecting blood pressure or intraocular pressure in healthy subjects.

T. Kakegawa et al. conducted a translatome analysis to investigate the mechanisms and modes of action of three diarylheptanoids isolated from a medicinal plant, *Alpinia officinarum*. The authors comprehensively identified the polysome-associated mRNAs in a human B lymphoblastoid cell line and examined changes to the mRNA profile caused by each of three *A. officinarum* diarylheptanoids. The microarray-based translatome analysis was able to reveal the inhibitory effects on proinflammatory mediators and cytotoxic and antiviral activity of plant bioactives, highlighting the application of omics technologies in advancing our understanding of molecular effects of CAM agents.

In the paper entitled "*A review of botanical characteristics, traditional usage, chemical components, pharmacological activities, and safety of Pereskia bleo (kunth) DC*" S. Zareisedehizadeh et al. provided an up-to-date and comprehensive review of the botanical characteristics, traditional usage, phytochemistry, pharmacological activities, and safety of *P. bleo*. The review highlighted the association between the traditional usage of the plant and the anticancer, antibacterial, and antinociceptive effects reported in different studies.

In summary, these 7 papers represent exciting CAM research activities with translational strategies embedded in design and context. The articles will help readers to follow translational research in CAM with a wide range of topics, from clinical trials to omics technologies and bioinformatics that will collectively contribute to an improved understanding of mechanisms and pharmacology of the CAM treatments.

Acknowledgments

We would like to thank all authors and reviewers for making this special issue possible.

Wei Jia
Aiping Lu
Kelvin Chan
Mats G. Gustafsson
Ping Liu

Hindawi Publishing Corporation
Evidence-Based Complementary and Alternative Medicine
Volume 2015, Article ID 464969, 11 pages
http://dx.doi.org/10.1155/2015/464969

Research Article

Urinary Metabolite Profiling Offers Potential for Differentiation of Liver-Kidney Yin Deficiency and Dampness-Heat Internal Smoldering Syndromes in Posthepatitis B Cirrhosis Patients

Xiaoning Wang,[1,2] Guoxiang Xie,[3] Xiaoyan Wang,[4] Mingmei Zhou,[1,5] Huan Yu,[6,7] Yan Lin,[1,2] Guangli Du,[1,2] Guoan Luo,[6] and Ping Liu[1,2]

[1] *E-Institute of Shanghai Municipal Education Committee, Shanghai University of Traditional Chinese Medicine, Shanghai 201203, China*
[2] *Key Laboratory of Liver and Kidney Diseases, Ministry of Education, Institute of Liver Diseases, Shuguang Hospital, Shanghai University of Traditional Chinese Medicine, Shanghai 201203, China*
[3] *University of Hawaii Cancer Center, Honolulu, HI 96813, USA*
[4] *Key Laboratory of Systems Biomedicine, Ministry of Education, Shanghai Center for Systems Biomedicine, Shanghai Jiao Tong University, Shanghai 200240, China*
[5] *Center for Chinese Medical Therapy and Systems Biology, Shanghai University of Traditional Chinese Medicine, Shanghai 201203, China*
[6] *Key Laboratory of Bioorganic Phosphorus Chemistry and Chemical Biology, Ministry of Education, Department of Chemistry, Tsinghua University, Beijing 100083, China*
[7] *School of Traditional Chinese Medicine, Beijing University of Chinese Medicine, Beijing 100102, China*

Correspondence should be addressed to Ping Liu; liuliver@vip.sina.com

Received 23 June 2014; Accepted 29 July 2014

Academic Editor: Wei Jia

Zheng is the basic theory and essence of traditional Chinese medicine (TCM) in diagnosing diseases. However, there are no biological evidences to support TCM Zheng differentiation. In this study we elucidated the biological alteration of cirrhosis with TCM "Liver-Kidney Yin Deficiency (YX)" or "Dampness-Heat Internal Smoldering (SR)" Zheng and the potential of urine metabonomics in TCM Zheng differentiation. Differential metabolites contributing to the intergroup variation between healthy controls and liver cirrhosis patients were investigated, respectively, and mainly participated in energy metabolism, gut microbiota metabolism, oxidative stress, and bile acid metabolism. Three metabolites, aconitate, citrate, and 2-pentendioate, altered significantly in YX Zheng only, representing the abnormal energy metabolism. Contrarily, hippurate and 4-pyridinecarboxylate altered significantly in SR Zheng only, representing the abnormalities of gut microbiota metabolism. Moreover, there were significant differences between two TCM Zhengs in three metabolites, glycoursodeoxycholate, cortolone-3-glucuronide, and L-aspartyl-4-phosphate, among all differential metabolites. Metabonomic profiling, as a powerful approach, provides support to the understanding of biological mechanisms of TCM Zheng stratification. The altered urinary metabolites constitute a panel of reliable biological evidence for TCM Zheng differentiation in patients with posthepatitis B cirrhosis and may be used for the potential biomarkers of TCM Zheng stratification.

1. Introduction

Cirrhosis is scarring of the liver and also is the final stage of many chronic liver diseases, leading to portal hypertension and end-stage liver disease [1]. Over the past decades, a series of methods, including serum biochemical tests [2], abdominal imaging scan [3], and liver biopsy [4], have been developed for the diagnosis of liver cirrhosis. To date, liver biopsy is still considered to be a golden standard for diagnosing cirrhosis, although it is a high-risk invasive surgery [5–8]. In

clinic, imaging scan such as computed tomography (CT) and ultrasound or transient elastography are noninvasive methods, getting more and more attention due to the excellent diagnostic accuracy in assessing the pathological stage of liver fibrosis [9–11]. Although noninvasive, none of them can provide the information on inflammatory activity, steatosis, or other findings derived from liver biopsy [12]. Child-Pugh (CP) scores classification is a widespread method to grade the liver function levels in cirrhotic patients [13, 14]. It can reasonably predict survival in many chronic liver conditions and the likelihood of major complications such as bleeding from varices and spontaneous bacterial peritonitis and is still considered to be a cornerstone in prognostic evaluation of cirrhosis [15, 16]. However, the CP score does not provide direct evidence of the pathological stage or state of cirrhosis [2]. Moreover, it has some drawbacks such as the limited discriminatory ability as well as the fact that it depends greatly on the clinician's experience [3, 4].

Zheng (Chinese character transliteration) is a temporary state at one time and is also known as a traditional Chinese medicine (TCM) syndrome [17]. It is, in essence, a characteristic profile of all clinical manifestations, such as signs, symptoms, and all other presentative information, even psychology, emotion, feeling, and so forth that can be identified by a TCM practitioner. Syndrome differentiation (TCM Zheng) is an important element in TCM theories and is the basis for the treatments of all diseases, including cirrhosis. In TCM, patients with posthepatitis B cirrhosis will usually be classified into different Zhengs, "Liver-Kidney Yin Deficiency," "Dampness-Heat Internal Smoldering," "Stasis-Heat Internal Smoldering," "Liver Depression and Spleen Deficiency," and "Spleen-Kidney Qi Deficiency" [18–21], by clustering and merging the uniform or analogical clinical evidences. Importantly, clinical investigations reveal that the total effective rate is significantly higher in those subject to integrated traditional Chinese and western medicine treatment based on TCM Zheng stratification than those only subject to western medicine [22–24]. Since TCM Zheng stratification significantly improves the clinical therapeutic outcome of liver cirrhosis, the TCM syndromes (Zheng) of patients with cirrhosis are necessary to characterize [25]. However, in clinic, TCM Zheng identification commonly relied on the experience of TCM practitioners. Recent advance in systems biology provides a panel of platform for the joint development of multidisciplinary partnerships. Metabonomics, a quantitative determination of the multiparametric metabolic response of living systems [26, 27], has been widely accepted as an effective approach for the study of pathophysiological changes associated with or resulting from disease or injury [28]. It can provide abundant mechanistic information to achieve the diagnosis of disease and the curative effect evaluation of drugs [29–31] by a variety of endogenous substances differentially expressed in tissues or biofluids such as blood and urine [32–34]. In our recent study [35], metabonomics approach showed that urinary metabolite variation is closely associated with pathological progression of liver cirrhosis in posthepatitis B cirrhosis patients.

In this study, we conduct a urinary metabonomic study on a group of liver cirrhosis patients ($n = 63$) and healthy subjects ($n = 31$), the same participants used in our previous study [35], using a combined gas chromatography-mass spectrometry (GC-MS) and ultraperformance liquid chromatography quadrupole time-of-flight mass spectrometry (UPLC-QTOFMS). Our study is aimed at (1) comparing the urinary metabolic profiles of participants with and without cirrhosis, (2) illustrating the relationship between urine metabolic profiles and TCM syndromes in subjects with cirrhosis, and (3) determining the characteristics and differences in TCM syndrome distribution between Liver-Kidney Yin Deficiency and Dampness-Heat Internal Smoldering.

2. Materials and Methods

2.1. Participants. We used a multicenter, multistage sampling method to obtain a cohort of representative samples of male patients in the general liver cirrhosis population. Patients were eligible to enter the study if they were clinically diagnosed liver cirrhosis due to chronic hepatitis B infection according to the "Guideline on prevention and treatment of chronic hepatitis B in China (2005)." The guideline (2005 version) was jointly revised in 2007 by Chinese Society of Hepatology, Chinese Medical Association, and Chinese Society of Infectious Diseases, Chinese Medical Association [36]. In addition, patients must match the factors of TCM Zheng diagnosis criteria of posthepatitis B cirrhosis [18–20], in which "Liver-Kidney Yin Deficiency" Zheng (*shorter form: YX*) included blurred vision, tinnitus, xerophthalmia, skin itching, bitter taste and dry mouth, poor libido, soreness and flaccidity of waist and knees, constipation, rapid pulse and vexing heat in the chest, palms, and soles, while "Dampness-Heat Internal Smoldering" Zheng (*shorter form: SR*) included yellow and slimy tongue fur, jaundice in the skin and sclera, yellow urine, abdominal distension, edema of lower limbs, gynecomastia, dim facial complexion, fatigue, and heavy body.

Exclusion criteria in the study were patients having a history of hepatitis A, C infection, alcohol or drug abuse, liver cancer, neoplastic liver diseases, hepatotoxic medication, and autoimmune liver disease in the past 6 months before recruiting into the study and other conditions likely to interfere with the study, such as overt hepatic encephalopathy (West Heaven Criteria grade II through IV), spontaneous bacterial peritonitis, upper gastrointestinal haemorrhage, and hepatorenal syndrome. Those with a history of severe primary heart, brain, lung, spleen, kidney, endocrine diseases, hematological disorder, and psychosis were also excluded from the study. Meanwhile, those not matching TCM YX Zheng or SR Zheng diagnosis criteria of cirrhosis were ruled out.

A total of 63 patients, aged between 33 and 58, were enrolled in the study from Shuguang Hospital, Longhua Hospital, and Putuo District Center Hospital affiliated to Shanghai University of Traditional Chinese Medicine (Shanghai, China) and Shanghai Public Health Center affiliated to Fudan University (Shanghai, China) between January 1, 2007, and December 31, 2008. All patients were clinically stable at

Table 1: Clinical information and characteristics of human subjects.

Variable	Control	Liver cirrhosis	TCM Zhengs of liver cirrhosis	
			YX subgroup	SR subgroup
Patients (n)	31	63	33	30
Age (y)	49.70 ± 5.46	52.95 ± 8.86	52.00 ± 8.82	53.83 ± 8.91
Body height (cm)	170.8 ± 3.05	171.5 ± 5.07	171.5 ± 5.40	171.5 ± 4.92
Body weight (kg)	67.48 ± 6.37	65.91 ± 9.26	67.31 ± 8.36	65.38 ± 9.521
BMI	23.14 ± 2.14	22.73 ± 2.78	22.83 ± 2.14	22.22 ± 3.020
RBC (10^{12}/L)			3.60 ± 0.70	3.32 ± 0.68
WBC (10^9/L)			4.44 ± 1.70	4.89 ± 2.74
HB (g/L)			119.5 ± 23.94	111.5 ± 19.40
NEUT# (10^9/L)			2.41 ± 1.21	2.68 ± 1.01
LYM# (10^9/L)			1.22 ± 0.72	1.31 ± 0.90
PLT (10^9/L)			88.89 ± 45.84	85.09 ± 61.12
Alb (g/L)			32.62 ± 6.06	28.86 ± 6.18**
Glb (g/L)			35.10 ± 7.67	33.37 ± 9.0
A/G (100%)			0.98 ± 0.29	0.92 ± 0.29
ALT (IU/L)			71.73 ± 63.61	64.68 ± 52.57
AST (IU/L)			87.13 ± 67.05	79.58 ± 51.95
GGT (IU/L)			86.50 ± 75.19	73.35 ± 59.42
ALP (IU/L)			136.4 ± 94.59	110.5 ± 59.68
CHE (IU/L)			3345 ± 1296	3148 ± 1446
TBiL (μmol/L)			42.92 ± 27.17	78.71 ± 37.11**
DBiL (μmol/L)			15.59 ± 14.02	40.22 ± 35.16
PT (sec)			16.31 ± 1.99	17.41 ± 2.98
INR (%)			1.47 ± 0.24	1.62 ± 0.38
BUN (mmol/L)			5.80 ± 2.51	6.01 ± 2.91
Cr (μmol/L)			83.37 ± 31.09	86.20 ± 33.49
TCH (mmol/L)			3.32 ± 0.84	3.27 ± 0.93
TG (mmol/L)			0.81 ± 0.23	0.90 ± 0.35
APOA-1 (g/L)			0.89 ± 0.22	0.76 ± 0.17**
FPG (mmol/L)			5.81 ± 1.91	5.69 ± 2.0
AFP (ng/mL)			49.60 ± 66.67	66.37 ± 132.2

Note: The results are presented as mean ± SD and were compared by t-test. ** $P < 0.01$, TCM YX Zheng subgroup versus TCM SR Zheng subgroup.
BMI: body-mass index; RBC: red blood cell; WBC: white blood cell; HB: haemoglobin; NEUT#: absolute neutrophil Count; LYM#: absolute lymphocyte count; PLT: platelet; Alb: albumin; Glb: globulin; A/G: albumin/globulin; ALT: alanine aminotransferase; AST: aspartate aminotransferase; GGT: gamma glutamyl transferase; ALP: alkaline phosphatase; CHE: cholinesterase; TBiL: total bilirubin; DBiL: direct bilirubin; PT: prothrombin time; INR: international normalized ratio; BUN: blood urea nitrogen; Cr: creatinine; TCH: total cholesterol; TG: triglycerides; APOA-1: apolipoprotein A-1; FPG: fasting plasma glucose; AFP: alpha-fetoprotein.

the time of assessment. Patients were spontaneously divided into YX Zheng subgroup ($n = 33$) and SR Zheng subgroup ($n = 30$), according to TCM diagnosis criteria of cirrhosis.

A cohort of 31 male participants was recruited as healthy controls from the Physical Examination Center of Shuguang Hospital. There was no significant difference in age, height, body weight, and BMI between healthy controls and liver cirrhosis patients or between TCM YX Zheng and SR Zheng of cirrhosis patients (Table 1). The injury degrees of liver function in cirrhosis patients with TCM YX and SR Zheng were approximately equal according to Child-Pugh liver function classification.

Ethical approval for these studies was obtained from the ethics committees of the four hospitals mentioned above. The study was carried out in compliance with the Declaration of Helsinki (55th World Medical Association General Assembly, Tokyo, 2004). All participants have written the informed consent prior to the study.

2.2. Study Design. Before the study, all study investigators, including medical students, trained general practitioners, and nurses, had completed a training program for methods and requirements of samples collection and obtained a manual of detailed procedure that guided how to manage the questionnaires, anthropometric measurements, and biological samples (urine and serum). All participants completed a questionnaire documenting their anthropometric measurements (e.g., weight and height), sociodemographic status (e.g., age, sex, education, and career), personal and family health history (e.g., hypertension, diabetes, liver disease, and

surgery), lifestyle (e.g., smoking and alcohol consumption), and TCM Zheng scale (published in http://www.hindawi.com/journals/ecam/2012/496575/) under the guidance of the study investigators. Other information in the inclusion and exclusion criteria was noted. Serum samples of all patients were obtained under the fasting status in the morning. Clean voided midstream urine samples were obtained in the morning before breakfast and stored at −80°C condition in Key Laboratory of Liver and Kidney Diseases (Ministry of Education), until GC-MS or UPLC-QTOFMS analysis.

Serum biochemical assay was performed with an automatic biochemistry analyzer for the analysis of blood routine, liver, and renal function markers. The data were offered by clinical laboratory of each hospital participating in the study. All questionnaires and serum biochemical indices were stored and analyzed by Key Laboratory of Liver and Kidney Diseases (Ministry of Education), Institute of Liver Diseases, Shuguang Hospital, Shanghai, China.

GC-MS profiling and data analysis of urine samples completed by Center for Chinese Medical Therapy and Systems Biology, Shanghai University of Traditional Chinese Medicine, Shanghai, China. The urine sample preparation for GC-MS analysis was performed according to our previously published method with minor modification [37]. L-2-chlorophenylalanine was used as internal standard (IS) to monitor GC/MS performance and method reproducibility during a long time of run.

Raw GC-MS data were converted into AIA format (NetCDF) files by Agilent GC-MS 5975 Data Analysis software, and subsequently the data information was extracted by the XCMS toolbox using the parameters as previously described. The XCMS output (TSV file) was introduced to Matlab software version 7.0 (The MathWorks, Inc.), where internal standard (IS) peaks and impurity peaks from column bleeds and derivatization procedure were excluded. The remaining ion features with high correlation of abundance within the same retention time group were combined into a single compound so as to obtain the total numbers of compounds and simplify data matrix for multivariate statistical analysis. The intensities of ion features (area) were further normalized to the total area for each sample to eliminate the variations caused by the different volume of individual urine sample and arranged on a three-dimensional matrix consisting of arbitrary peak index (RT-m/z pair), sample names (observations), and peak area (variables).

UPLC-QTOFMS profiling and data analysis of urine samples were completed by Key Laboratory of Bioorganic Phosphorus Chemistry and Chemical Biology (Ministry of Education), Department of Chemistry, Tsinghua University, Beijing, China. The urine sample preparation for UPLC-QTOFMS was performed according to our previous works [38]. A 100 μL of each urinary sample was mixed with 400 μL of methanol and vortexed for 2 min followed by centrifugation at 6,000 rpm for 15 min at 4°C. The clear supernatant was transferred to a separate container and diluted with ultrapure water (1 : 3) before analysis.

A Waters ACQUITY UPLC system coupled with an orthogonal acceleration time-of-flight mass spectrometry equipped with an electrospray interface (Waters Corp., Milford, USA) was used for metabonomic profiling. Chromatographic separation was performed on a Waters ACQUITY BEH C18 column (100 × 2.1 mm, 1.7 μm) maintained at 50°C with a mobile phase consisting of (A) 0.1% formic acid in water and (B) acetonitrile. A linear gradient was set as follows: 0–3 min, 5% B to 50% B; 3–20 min, 50% B to 95% B; 20-21 min, 95% B to 5% B; 21–23 min, equilibration with 5% B with a flow rate of 0.4 mL/min. Mass spectrometry conditions were as follows: negative ion electrospray ionization (ESI-) mode, capillary voltage 2.5 kV, sample cone voltage 50 V, desolvation temperature 350°C, source temperature 120°C, cone gas flow 40 L/h, desolvation gas flow 700 L/h, and MCP detector voltage 2.2 kV. The data acquisition rate was set to 0.1 s, with a 0.05 s interscan delay using dynamic range enhancement (DRE). All analyses were acquired using the lock spray to ensure accuracy and reproducibility; leucine-enkephalin was used as the lock mass (m/z 554.2615) at a concentration of 50 pg/mL and an infusion flow rate of 5 μL/min. Data was collected in centroid mode from 50 to 1000 m/z.

The peak picking, peak alignment, and peak filtering of the raw UPLC-QTOFMS data were carried out with the MarkerLynx Application Manager Version 4.1 (Waters, Manchester, UK). The parameters used were retention time range 0–18 min, mass range 50–1000 m/z, mass tolerance 0.05 Da, intensity threshold 10 counts, and retention time tolerance 0.01 min; noise elimination level was set at 6.00 and isotopic peaks were excluded for processing.

Compound annotation from UPLC-QTOFMS data was performed by comparing the accurate mass (m/z) and retention time (Rt) of reference standards in our in-house library and the accurate mass of compounds obtained from the web-based resources such as the Human Metabolome Database (http://www.hmdb.ca/). For GC-TOFMS data, compound annotation was carried out by comparing the mass fragments and Rt with our in-house library or mass fragments with NIST 05 Standard mass spectral databases in NIST MS search 2.0 (NIST, Gaithersburg, MD) software with a similarity of greater than 70%.

The interpretation for data analysis derived from GC-MS and UPLC-QTOFMS was performed by Laboratory of Systems Biomedicine (Ministry of Education), Shanghai Center for Systems Biomedicine, Shanghai Jiao Tong University, Shanghai, China. The verification of data was performed by Cancer Center, University of Hawaii, Honolulu, USA, which ensured that data were complete, accurate, and verifiable from source data. The trial profile is shown in Figure 1.

2.3. Statistical Analysis. For GC-MS, the resulting three-dimensional matrix data was imported to SIMCA-P 11.0 software (Umetrics, Umea, Sweden). Principle component analysis (PCA) was performed on the mean-centered and UV-scaled data to visualize general clustering, trends, and outliers among all samples on the scores plot. Partial least squares-discriminant analysis (PLS-DA) was used to maximize the variation. These differential metabolites selected

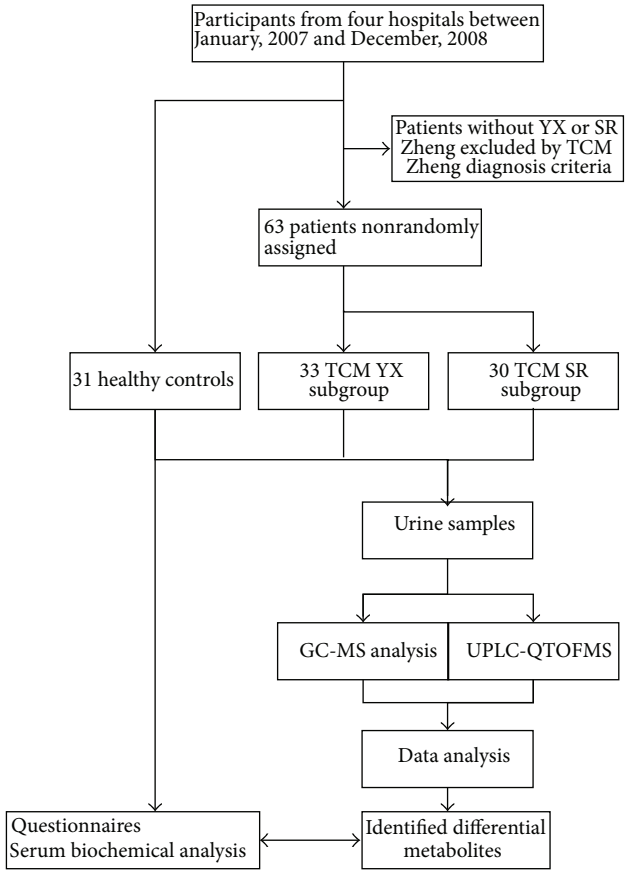

Figure 1: Scheme of the research design.

from the PLS-DA model with VIP value (VIP > 1) are validated at a univariate level with Wilcoxon-Mann-Whitney test with a critical P value usually set to 0.05.

For UPLC-QTOFMS, the resulting three-dimensional matrix, including assigned peak index (retention time-m/z pairs), sample names (observations), and normalized peak area (variables), was then exported for multivariate statistical analysis using PLS-DA with the software SIMCA-P+ 12 (Umetrics, Umea, Sweden). Significant variables (markers) were selected based on a threshold of a multivariate statistical parameter (SIMCA-P 12.0 software, Umetrics, Umea, Sweden), such as VIP value (VIP > 1) from a typical 7-fold cross-validated PLS-DA model. These differential metabolites selected from the PLS-DA model were validated at a univariate level with Wilcoxon-Mann-Whitney test with a critical P value usually set to 0.05.

GraphPad Prism software (version 6.0) was used for data entry and management. All reported P values are two-sided, and a P value of less than 0.05 was considered significant. Data analyses were performed with SAS software (version 9.1).

3. Results

3.1. Clinical Characteristics of Liver Cirrhosis Patients. The clinical characteristics of cirrhosis patients including TCM YX group and SR group were summarized in Table 1. Serum levels of albumin (Alb) and apolipoprotein A-1 (APOA-1) in SR subgroup were lower than in YX subgroup. Serum level of total bilirubin (TBiL) in SR subgroup was higher than in YX subgroup. No statistical discrepancy was found in liver function between the two groups.

3.2. GC-MS Analysis. A total of 165 ion features were obtained and 11 identified urine metabolites were differentially expressed in cirrhotic patients compared to those in healthy controls. Peak intensity comparison of the differentially expressed metabolite levels in liver cirrhosis patients compared to those in healthy controls was summarized in Table 2.

PCA and PLS-DA analysis were performed to distinguish healthy subjects from cirrhosis patients in TCM YX subgroup and SR subgroup. With the 165 features determined by GC-MS, a PCA scores plot (figure not shown) using 4 components (R2X = 0.486) and a cross-validated PLS-DA model using 1 predictive component and 2 orthogonal components (R2Xcum = 0.502, R2Ycum = 0.77, and Q2Ycum = 0.476) were constructed (Figure 2(a)). There appears to be separation between healthy controls and cirrhosis patients, reflecting the pathophysiological variations of liver cirrhosis disease. Moreover, the metabolite profiles of TCM YX or SR Zheng cirrhosis patients are also, respectively, different from the healthy controls, indicating the consistency between TCM Zheng and disease (Figure 2(a)). Compared to healthy controls, there were two urine metabolites, acetyl citrate, and 4-hydroxy-benzenepropanedioate, changed synchronously in two TCM Zheng subgroups of cirrhosis patients in all 11 identified differential expressed metabolites. Three metabolites, 2-pentendioate, citrate, and aconitate, appeared in TCM YX subgroup of liver cirrhosis patients, and two metabolites, 4-pyridinecarboxylate and hippurate, appeared in TCM SR subgroup (Table 2).

3.3. UPLC-QTOFMS Analysis. A PCA scores plot using 5 components (R2Xcum = 0.472, Q2cum = 0.058) and a cross-validated PLS-DA model using one predictive component and three orthogonal components (R2Xcum = 0.121, R2Ycum = 0.742, and Q2Ycum = 0.237) were constructed with 8,163 ion features detected on the UPLC-QTOFMS spectra. Clear separation among healthy controls, TCM YX subgroup, and SR subgroup of cirrhosis patients (Figure 2(b)) was obtained, suggesting that systemic metabolic variations in urine reflect the diversity between two TCM Zhengs.

A total of 28 characteristic urinary metabolites were identified from UPLC-QTOFMS negative ion mode for liver cirrhosis, as summarized in Table 2. Thereinto, higher peak intensity of two metabolites, L-aspartyl-4-phosphate and cortolone-3-glucuronide, were seen in TCM YX subgroup and one metabolite, glycoursodeoxycholate, was lower in SR subgroup compared to healthy controls (Table 2).

4. Discussion

Methods identifying the liver condition have been established in cirrhosis study, including the histological observations

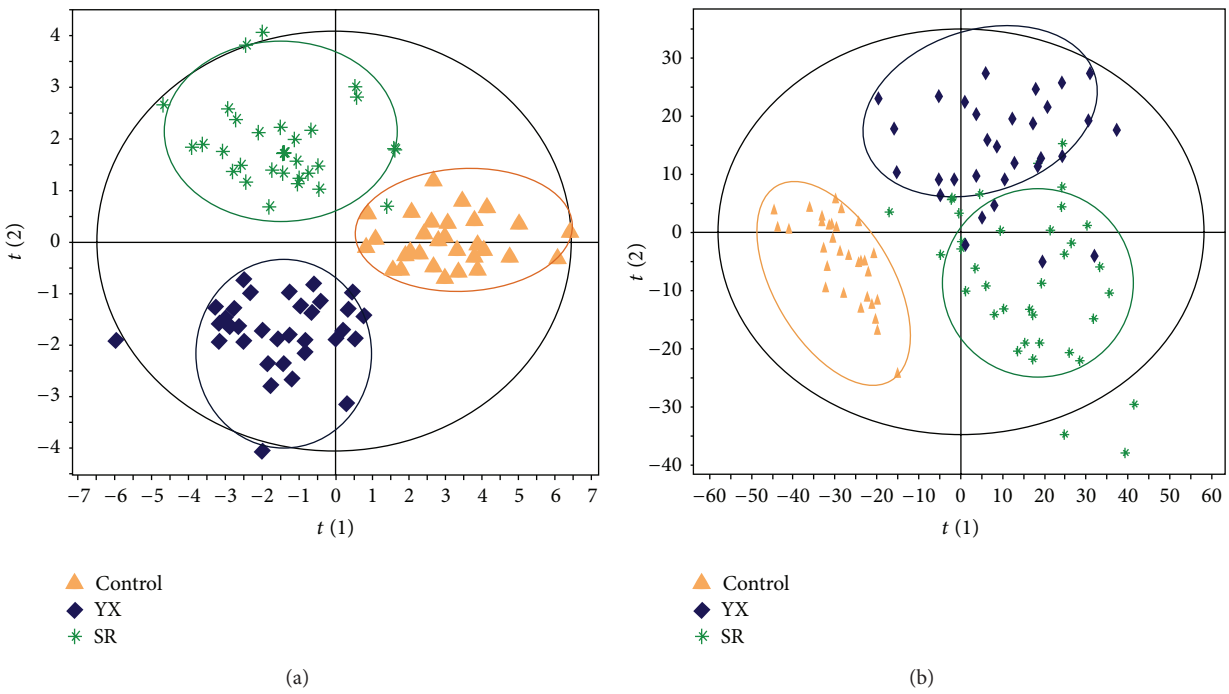

Figure 2: PLS-DA scores plot of urinary metabolites from healthy controls and TCM YX and SR Zheng patients with posthepatitis B cirrhosis using GC-MS spectral data (a) and UPLC-QTOFMS spectral data (b).

characterized by scar tissue, fibrous septa and regenerative nodules [39, 40], the clinical manifestation panels separating the compensated cirrhosis from the decompensated cirrhosis [41, 42], and CP scores classification reflecting the aggravated grade of the liver function [43]. All methods mentioned above aim to provide accurate diagnosis for disease and objective evaluation for the therapeutic schedule. With increasing requirement for the personalized treatment throughout the world, TCM Zheng stratification has become an important approach in disease diagnosis and treatment. Our previous study provided five TCM Zheng diagnostic criteria for the posthepatitis B cirrhosis according to clustering and merging of the clinical evidences [20], and, subsequently, patients with posthepatitis B cirrhosis were divided into five stratifications. Among the five TCM Zhengs, "Liver-Kidney Yin Deficiency" (YX) is a pure and representative "Deficiency Zheng," while "Dampness-Heat Internal Smoldering" (SR) is a pure and representative "Excess Zheng." "Deficiency" and "Excess," the properties being entirely opposite, are the important guiding principles in TCM for analyzing the condition of the body's resistance to pathogenic factors. "Deficiency" refers to deficient healthy Qi and "Excess" refers to excessive pathogenic Qi. The other three TCM Zhengs are of combination status composed of "Deficiency Zheng" and "Excess Zheng," although they differ in degree.

The liver is the most important metabolic organ in the human body, responsible for metabolism of a large array of substrates, such as sugar, protein, fat, and phytochemical compound [44]. The liver cirrhosis has been linked closely to metabolic disorders [45]. Metabonomics stays on the downstream terminal of system biology, contributing to an altered expression of a large number of metabolites at systemic level. Therefore, metabonomics is suitable for the study of liver disease. The present study is designed to characterize the alteration of urinary metabolite markers associated with TCM YX or SR Zheng in posthepatitis B cirrhosis and to provide the biological substance evidence for the TCM YX and SR Zheng stratification.

Two panels of markers, 11 and 28 urinary metabolites identified by GC-MS and UPLC-QTOFMS, respectively, were significantly altered in cirrhosis participants (Table 2). The PLS-DA models derived from our current GC-MS and UPLC-QTOFMS analysis showed good and similar separation between healthy controls and cirrhosis patients, or TCM YX and SR subgroups. The results in our study reflected the abnormal key metabolic pathways of energy metabolism, tricarboxylic acid (TCA) cycle, amino acid, bile acids, steroids, and intestinal microbial metabolism in the posthepatitis B cirrhosis patients. However, the abnormal alteration of metabolic pathways did not synchronously occur between TCM YX subgroup and SR subgroup patients. The abnormal alteration of aconitate, citrate, and 2-pentendioate was only found in TCM YX subgroup patients, but not in TCM SR subgroup. Aconitate is an intermediate in the tricarboxylic acid (TCA) cycle produced by the dehydration of citrate and the aconitase catalyses the stereospecific isomerization of citrate to isocitrate via cis-aconitate in the TCA cycle. The significantly elevated level of citrate and aconitate indicates an altered TCA cycle. TCA cycle is the final metabolic pathway of three major nutrients (protein, fat, and carbohydrates) to generate energy, whose changes represent the energy metabolism disorderly in the body. Thus,

Table 2: List of urinary differential metabolites in cirrhosis patients and among TCM YX, SR Zheng subgroup relative to controls.

Compounds	Liver cirrhosis versus control			YX versus control		SR versus control		SR versus YX	
	VIP[a]	FC[b]	P[c]	FC[d]	P[c]	FC[e]	P[c]	FC[f]	P[c]
				GC-MS					
4-Pyridinecarboxylate	1.855	0.46	$1.53E-02$	0.47	$7.05E-02$	0.38	$9.40E-03$	0.81	$6.54E-01$
Threonine*	1.498	0.64	$5.96E-02$	0.63	$2.98E-02$	0.60	$2.46E-02$	0.96	$8.96E-01$
Proline*	1.474	1.30	$1.79E-01$	1.57	$2.94E-02$	1.79	$3.50E-03$	1.14	$3.97E-01$
Citrate*	1.33	1.50	$8.28E-03$	1.60	$1.39E-02$	1.37	$1.39E-01$	0.85	$3.33E-01$
Aconitate*	1.393	1.36	$1.97E-03$	1.46	$2.30E-03$	1.27	$7.49E-02$	0.87	$2.05E-01$
2-Pentendioate	1.734	1.58	$1.95E-02$	2.14	$2.00E-03$	1.52	$1.57E-01$	0.71	$9.28E-02$
Hippurate*	1.905	0.47	$2.34E-02$	0.57	$1.19E-01$	0.36	$1.33E-02$	0.64	$6.07E-01$
2-Aminobutyrate*	1.954	0.38	$2.04E-02$	0.34	$5.80E-03$	0.30	$4.30E-03$	0.88	$8.64E-01$
Acetyl citrate	1.517	2.75	$2.44E-03$	3.26	$9.30E-03$	3.24	$1.15E-02$	1.00	$9.87E-01$
3,4-Dihydroxyphenylacetate*	2.121	1.88	$2.08E-04$	2.19	<0.0001	1.74	$1.29E-02$	0.80	$1.30E-01$
4-Hydroxy-benzenepropanedioate	1.723	4.29	$6.84E-04$	4.41	$1.65E-02$	5.51	$2.20E-03$	1.25	$4.40E-01$
				UPLC-QTOF-MS					
cis-Aconitate*	2.0	0.75	$6.30E-05$	0.74	<0.0001	0.76	<0.0001	1.03	$6.99E-01$
Pyroglutamate*	2.1	0.69	$7.74E-07$	0.65	<0.0001	0.75	<0.0001	1.15	$1.02E-01$
O-Phosphotyrosine	2.0	0.70	$3.71E-06$	0.72	<0.0001	0.70	<0.0001	0.97	$7.59E-01$
3-Methoxy-4-hydroxyphenylglycol sulfate	2.1	1.70	$3.15E-09$	1.73	<0.0001	1.72	<0.0001	0.99	$9.40E-01$
Alpha-hydroxyisobutyrate*	2.4	0.42	$1.28E-06$	0.46	<0.0001	0.35	<0.0001	0.75	$2.13E-01$
3-Hydroxyisovalerate*	2.4	0.55	$1.84E-10$	0.55	<0.0001	0.54	<0.0001	0.99	$9.57E-01$
Dopaxanthin	1.8	0.23	$7.15E-04$	0.30	$2.00E-04$	0.14	<0.0001	0.46	$3.84E-01$
Alpha-hydroxyhippurate*	2.1	0.35	$8.93E-06$	0.42	<0.0001	0.24	<0.0001	0.57	$1.38E-01$
Canavaninosuccinate	3.1	25.57	$9.19E-21$	25.94	<0.0001	25.79	<0.0001	0.99	$9.58E-01$
L-Aspartyl-4-phosphate	1.6	0.71	$1.41E-04$	0.74	$7.80E-03$	0.60	<0.0001	0.82	$4.96E-02$
Isoxanthopterin	1.6	0.74	$2.66E-03$	0.77	$1.28E-02$	0.71	$1.50E-03$	0.92	$4.96E-01$
Tyrosine-betaxanthin	2.6	0.38	$2.92E-08$	0.41	<0.0001	0.34	<0.0001	0.83	$4.21E-01$
Estrone*	1.4	0.78	$1.70E-03$	0.79	$2.80E-03$	0.78	$1.30E-03$	0.98	$8.48E-01$
Glycocholic acid 3-glucuronide	1.7	5.18	$7.02E-07$	5.37	$5.00E-04$	5.30	$5.00E-04$	0.99	$9.52E-01$
Taurohyocholate*	1.5	119.52	$2.29E-07$	119.94	$2.90E-03$	150.74	$2.00E-04$	1.26	$4.20E-01$
Cortolone-3-glucuronide	2.5	0.36	$2.32E-09$	0.44	<0.0001	0.24	<0.0001	0.54	$2.95E-02$
Tetrahydroaldosterone-3-glucuronide	2.6	0.31	$3.97E-09$	0.37	<0.0001	0.22	<0.0001	0.58	$1.01E-01$
11-Beta-hydroxyandrosterone-3-glucuronide	2.4	0.38	$2.13E-07$	0.44	<0.0001	0.31	<0.0001	0.70	$1.76E-01$
N-Acetyl-leukotriene E4	2.6	0.12	$2.82E-06$	0.13	<0.0001	0.08	<0.0001	0.60	$6.79E-01$
11-Oxo-androsterone glucuronide	2.3	0.25	$3.44E-05$	0.29	<0.0001	0.19	<0.0001	0.67	$4.60E-01$
Glycocholate*	1.9	12.72	$3.61E-10$	12.57	$4.00E-04$	16.45	<0.0001	1.31	$2.15E-01$
Dehydroepiandrosterone 3-glucuronide	2.4	0.29	$1.45E-07$	0.33	<0.0001	0.20	<0.0001	0.60	$2.32E-01$
Androsterone sulfate	2.5	0.01	$1.28E-05$	0.00	<0.0001	0.02	<0.0001	234.20	$9.11E-01$
Testosterone sulfate	2.3	0.21	$4.09E-05$	0.21	<0.0001	0.19	<0.0001	0.90	$8.74E-01$
Glycoursodeoxycholate*	1.3	16.41	$1.30E-04$	9.19	$8.00E-03$	23.03	$2.00E-04$	2.51	$1.57E-02$
Androsterone glucuronide	3.1	0.27	$1.16E-13$	0.31	<0.0001	0.19	<0.0001	0.62	$9.19E-02$
17-hydroxyandrostane-3-glucuronide	2.9	0.27	$2.05E-10$	0.31	<0.0001	0.20	<0.0001	0.67	$2.28E-01$
Glycolithocholate 3-sulfate	2.9	0.04	$3.09E-07$	0.06	<0.0001	0.01	<0.0001	0.12	$6.49E-01$

Note: *Metabolites were verified by reference standards; [a]variable importance in the projection (VIP) was obtained from PLS-DA model with a threshold of 1.0; [b]fold change (FC) was obtained by comparing those metabolites in liver cirrhosis patients to controls; [c]P values were calculated from Wilcoxon-Mann-Whitney test; [d]FC was obtained by comparing those metabolites in liver cirrhosis patients with TCM YX Zheng to controls; [e]FC was obtained by comparing those metabolites in liver cirrhosis patients with TCM SR Zheng to controls; [f]FC was obtained by comparing those metabolites in liver cirrhosis patients with TCM SR Zheng to TCM YX Zheng. FC with a value >1 indicates a relatively higher concentration present in liver cirrhosis patients or liver cirrhosis patients with TCM YX, SR Zheng while a value <1 means a relatively lower concentration as compared to the controls or TCM YX Zheng subgroup.

energy metabolism disorder may well be the biological cause of "soreness and flaccidity of waist and knees" in TCM YX Zheng and is more serious than that of TCM SR Zheng.

On the contrary, the abnormal alteration of hippurate and 4-pyridinecarboxylate was only found in TCM SR subgroup patients, but not in TCM YX subgroup. Decreased hippurate in TCM SR subgroup patients and α-hydroxyhippurate in all cirrhotic subjects were generally produced via gut microbial-human cometabolism [46]. Change of hippurate showed that gut microbiota metabolism in TCM SR subgroup was damaged more significantly than that in TCM YX subgroup. Additionally, 3 urinary metabolites including glycoursodeoxycholate, cortolone-3-glucuronide, and L-aspartyl-4-phosphate (Figure 3) and 3 serum biochemical indices including Alb, TBiL, and APOA-1 (Table 1) were significantly altered between TCM YX subgroup and SR subgroup, suggesting that these metabolites and indices could be potential biomarkers for TCM YX and SR Zheng stratification of the posthepatitis-B cirrhosis patients. L-aspartyl-4-phosphate is a derivative from the interaction between L-aspartate and adenosine triphosphate (ATP). L-aspartate is usually used to improve resistance for fatigue in the body. Reduced levels of L-aspartyl-4-phosphate in cirrhotic patients should be associated with lower tolerance against fatigue. In clinic, the cirrhotic patients with TCM SR Zheng are indeed easier to feel fatigue than those with TCM YX Zheng. Serum TBiL levels have been an important jaundice evidence identifying TCM SR Zheng of many diseases, closely associated with ursodeoxycholic acid (UDCA) [47, 48] and intestinal flora [49]. Glycoursodeoxycholate is the secondary bile acid derived from UDCA conjugated with glycine. Elevated levels of glycoursodeoxycholate in urine of cirrhotic subjects indicated the reduced enterohepatic circulation and the lowered utilization rate of UDCA.

The liver's blood supply mainly comes from the intestine through the portal vein. The liver is vulnerable to exposure of bacterial products translocated from the gut lumen via the portal vein. Disruption of the intestinal barrier in developing liver cirrhosis results in the leaky gut, which contributes to bacterial translocation [50–52]. Increase in intestinal permeability leads to the translocation of intestine-derived bacterial products such as lipopolysaccharide (LPS) and unmethylated CpG containing DNA to the liver via the portal vein. Clinical evidence has demonstrated that elevated LPS level was found in the systemic and portal circulation in cirrhotic patients [53, 54]. Translocated LPS mediates Toll-like receptors (TLRs) activation in the liver, which are expressed on Kupffer cells, endothelial cells, dendritic cells, biliary epithelial cells, hepatic stellate cells, and hepatocytes. TLRs activate these cells to enhance liver inflammation and contribute to acute and chronic liver diseases. Alarmins, the products released from damaged cells or tissues, also trigger TLR signaling and cause inflammation without actual infections, referred to sterile inflammation [55]. Thus, the activation of TLR signaling through intestine-derived microbial products and alarmins may contribute to the progression of liver diseases [50]. And then, cirrhosis-mediated liver dysfunction may decrease the secretion of bile acids that causes bacterial overgrowth and may change bacterial composition in intestine [56, 57]. The analysis of fecal microbiome in patients with hepatitis B and alcoholic liver cirrhosis demonstrated an increase in pathogenic Enterobacteriaceae and Streptococcaceae, while beneficial bifidobacteria and Lachnospiraceae were decreased [58, 59]. For animals with cirrhosis, treatment with probiotics (e.g., *Bifidobacterium*) reduces *Enterobacter*, while it increases *Bifidobacterium* and *Lactobacillus*, resulting in decreased systemic endotoxin levels and improved liver function [60]. In patients with chronic severe hepatitis, the concentration of plasma endotoxin positively correlated with levels of TNF-alpha, IL-1 beta, TBiL, and the number of fecal Enterobacteriaceae and negatively correlated with *Bifidobacterium* [61]. Our results further proved the correlation between intestinal flora, enterohepatic circulation, and liver damage in the posthepatitis B cirrhosis patients. The alteration of urinary metabolites, serum TBiL, Alb, and APOA-1 illustrated that the injury degree of systemic physiopathology in the cirrhotic subjects with TCM SR Zheng was worse than that with TCM YX Zheng. Cirrhosis with TCM SR Zheng could have a poor prognosis of the disease. Moreover, our study well supported the traditional pathogenesis theory of Chinese medicine, which with the accumulation of pathological products, Deficiency Zheng will transform into a preponderant condition of Excess Zheng in chronic diseases, if not treated or if therapy fails [62].

There are some limitations in our study. First, the included participants were restricted to men only because women are easier to suffer from hormone interference, such as menses and early pregnancy, and difficult to judge the pathological or physiological alteration of hormone associated with liver cirrhosis. Second, metabolites of great statistical significance warrant further validation and screening as potential biomarkers for posthepatitis B cirrhosis diagnosis and TCM Zheng stratification in larger group of participants with both genders and other TCM Zhengs.

5. Conclusions

In conclusion, our results suggest that a panel of unique urinary metabolite markers is of clinical potential for the disease diagnosis and patient stratification for liver cirrhosis. These metabolite markers reflect the essence of the patients with posthepatitis B cirrhosis characterized by the disorders of the TCA cycle, amino acid, bile acids, hormones, dopamine, intestinal microbial metabolism, and oxidative stress. Moreover, the energy metabolism disorder is special prominent in cirrhotic patients with TCM YX Zheng, while the abnormality of the dopamine, intestinal microbiota metabolism, and oxidative stress is more serious in those with TCM SR Zheng. Specific urinary metabolites may be used as the biomarkers for TCM Zheng stratification. One of the most remarkable things about this study is that metabonomic profiling, as a powerful approach, partly interprets the biological reasons inducing TCM Zheng manifestation. Cirrhosis with TCM SR Zheng manifests more serious changes in the physiopathology of disease. Enclosing the same cohort of participants, we have obtained more information by integrating two medicine systems, indicating that urinary metabolite variation not only is associated with the pathological progression of cirrhosis

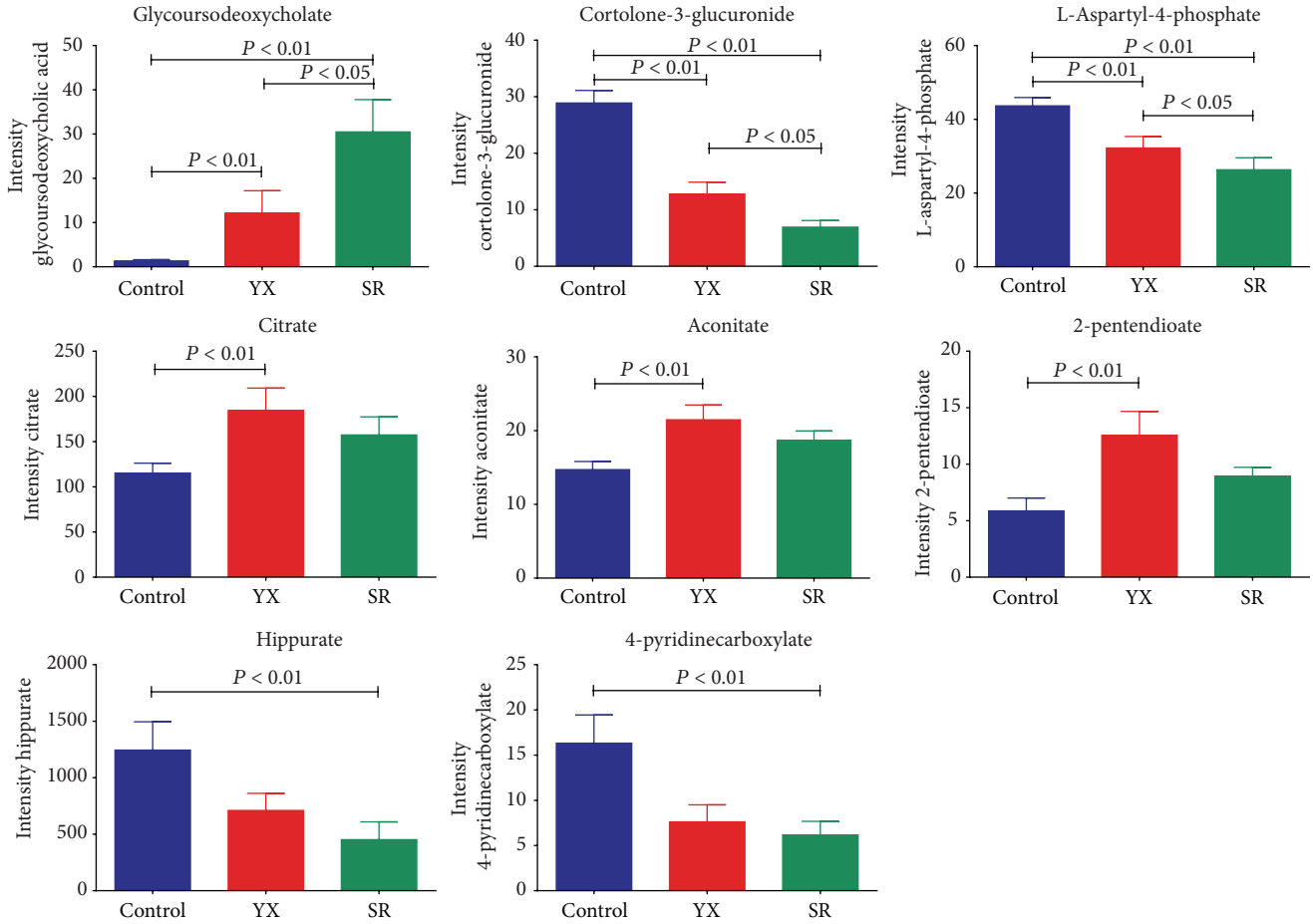

FIGURE 3: Bar charts of eight representative metabolite markers (mean ± SEM.) that are differentially expressed in healthy controls and TCM YX and SR Zheng patients with posthepatitis B cirrhosis.

but also acted as evidence of TCM Zheng stratification, contributing to the personalized diagnosis or treatment.

Disclosure

Xiaoning Wang and Guoxiang Xie are the co-first authors.

Conflict of Interests

The authors declare that there is no conflict of interests.

Acknowledgments

This study was financially supported in part by Program for Outstanding Medical Academic Leader of Shanghai Municipal Health Bureau, China (LJ06023), Budgeted Scientific Research Project of Shanghai Municipal Education Commission, China (I3YZ044, 2010JW027), Natural Science Foundation of Shanghai, China (14ZR1441400), and E-institutes of Shanghai Municipal Education Commission, China (E03008, 085ZY1205).

References

[1] D. Schuppan and N. H. Afdhal, "Liver cirrhosis," *The Lancet*, vol. 371, no. 9615, pp. 838–851, 2008.

[2] G. Garcia-Tsao, S. Friedman, J. Iredale, and M. Pinzani, "Now there are many (stages) where before there was one: in search of a pathophysiological classification of cirrhosis," *Hepatology*, vol. 51, no. 4, pp. 1445–1449, 2010.

[3] R. Testa, U. Valente, D. Risso et al., "Can the MEGX test and serum bile acids improve the prognostic ability of Child-Pugh's score in liver cirrhosis?" *European Journal of Gastroenterology and Hepatology*, vol. 11, no. 5, pp. 559–563, 1999.

[4] M. Oellerich, M. Burdelski, H.-U. Lautz et al., "Assessment of pretransplant prognosis in patients with cirrhosis," *Transplantation*, vol. 51, no. 4, pp. 801–806, 1991.

[5] A. A. Bravo, S. G. Sheth, and S. Chopra, "Liver biopsy," *New England Journal of Medicine*, vol. 344, no. 7, pp. 495–500, 2001.

[6] D. C. Rockey, S. H. Caldwell, Z. D. Goodman, R. C. Nelson, and A. D. Smith, "Liver biopsy," *Hepatology*, vol. 49, no. 3, pp. 1017–1044, 2009.

[7] M. Sebagh, D. Samuel, T. M. Antonini et al., "Twenty-year protocol liver biopsies: invasive but useful for the management of liver recipients," *Journal of Hepatology*, vol. 56, no. 4, pp. 840–847, 2012.

[8] A. Szymczak, K. Simon, M. Inglot, and A. Gladysz, "Safety and effectiveness of blind percutaneous liver biopsy: analysis of 1412 procedures," *Hepatitis Monthly*, vol. 12, no. 1, pp. 32–37, 2012.

[9] L. Castera and M. Pinzani, "Non-invasive assessment of liver fi brosis: are we ready?" *The Lancet*, vol. 375, no. 9724, pp. 1419–1420, 2010.

[10] G. Sebastiani, K. Gkouvatsos, and M. Plebani, "Non-invasive assessment of liver fibrosis: it is time for laboratory medicine," *Clinical Chemistry and Laboratory Medicine*, vol. 49, no. 1, pp. 13–32, 2011.

[11] Y.-F. Liaw, J.-H. Kao, T. Piratvisuth et al., "Asian-Pacific consensus statement on the management of chronic hepatitis B: a 2012 update," *Hepatology International*, vol. 6, no. 3, pp. 531–561, 2012.

[12] K. Yoshioka and S. Hashimoto, "Can non-invasive assessment of liver fibrosis replace liver biopsy?" *Hepatology Research*, vol. 42, no. 3, pp. 233–240, 2012.

[13] C. G. Child and J. G. Turcotte, "Surgery and portal hypertension," *Major problems in clinical surgery*, vol. 1, pp. 1–85, 1964.

[14] R. N. H. Pugh, I. M. Murray Lyon, and J. L. Dawson, "Transection of the oesophagus for bleeding oesophageal varices," *The British Journal of Surgery*, vol. 60, no. 8, pp. 646–649, 1973.

[15] D. L. Kasper, E. Braunwald, A. S. Fauci, S. L. Hauser, and D. L. Longo, *Harrison's Principles of Internal Medicine*, McGRaw-Hill, New York, NY, USA, 16th edition, 2005.

[16] D. Benedeto-Stojanov, A. Nagorni, G. Bjelaković, D. Stojanov, B. Mladenović, and N. Djenić, "The Model for the End-Stage Liver Disease and Child-Pugh score in predicting prognosis in patients with liver cirrhosis and esophageal variceal bleeding," *Vojnosanitetski Pregled*, vol. 66, no. 9, pp. 724–728, 2009.

[17] J. L. Tang, B. Y. Liu, and K. W. Ma, "Traditional Chinese medicine," *The Lancet*, vol. 372, no. 9654, pp. 1938–1940, 2008.

[18] Q. Zhang, P. Liu, H. F. Cheng et al., "Clinical investigation on characteristics of traditional Chinese medical syndrome of hepatocirrhosis," *Journal of Chinese Integrative Medicine*, vol. 1, no. 2, pp. 108–112, 2003.

[19] Q. Zhang, W. T. Zhang, J. J. Wei, X. B. Wang, and P. Liu, "Combined use of factor analysis and cluster analysis in classification of traditional Chinese medical syndromes in patients with posthepatitic cirrhosis," *Journal of Chinese Integrative Medicine*, vol. 3, no. 1, pp. 14–18, 2005.

[20] Q. Zhang, P. Liu, and H. W. Zhang, "Study on the patterns of TCM syndrome differentiation of 900 patients with posthepatitic cirrhosis," *Zhongguo Zhong Xi Yi Jie He Za Zhi*, vol. 26, no. 8, pp. 694–697, 2006.

[21] WHO Regional Office for the Western Pacific, WHO International Standard Terminologies on Traditional Medicine in the Western Pacific Region. : World Health Organization, Geneva, Switzerland, 356, 2007.

[22] Z. Hong-ping, "Clinical study of liver cirrhosis treated by integrated traditional Chinese and western medicine," *Chinese Journal of Integrated Traditional and Western Medicine*, vol. 21, no. 4, pp. 199–201, 2013.

[23] G. Lan-shu and G. Gui-ying, "Clinical observation of triple therapy in integrative chinese and western medicine in treatment of 3266 cases of ascites due to cirrhosis," *World Journal of Integrated Traditional and Western Medicine*, vol. 4, no. 7, pp. 523–525, 2009.

[24] L. Jian, X. Li-kui, D. Xin et al., "Systematic review of therapeutic effects of traditional chinese medicine on post hepatitic cirrhosis at early stage," *Acta Universitatis Traditionis Medicalis Sinensis Pharmacologiaeque Shanghai*, vol. 23, no. 1, pp. 20–23, 2009.

[25] Speciality Committee of Digestive Diseases; Chinese Association of Integrative Medicine, "Consensus on the diagnosis and treatment of liver cirrhosis in integrative medicine practice," *Chinese Journal of Integrated Traditional and Western Medicine*, vol. 19, no. 4, pp. 277–279, 2011.

[26] J. K. Nicholson, J. C. Lindon, and E. Holmes, "'Metabonomics': understanding the metabolic responses of living systems to pathophysiological stimuli via multivariate statistical analysis of biological NMR spectroscopic data," *Xenobiotica*, vol. 29, no. 11, pp. 1181–1189, 1999.

[27] N. J. Waters, C. J. Waterfield, R. D. Farrant, E. Holmes, and J. K. Nicholson, "Metabonomic deconvolution of embedded toxicity: application to thioacetamide hepato- and nephrotoxicity," *Chemical Research in Toxicology*, vol. 18, no. 4, pp. 639–654, 2005.

[28] R. Goodacre, "Metabolomics of a superorganism," *Journal of Nutrition*, vol. 137, no. 1 supplement, pp. 259S–266S, 2007.

[29] W. M. Claudino, A. Quattrone, L. Biganzoli, M. Pestrin, I. Bertini, and A. Di Leo, "Metabolomics: available results, current research projects in breast cancer, and future applications," *Journal of Clinical Oncology*, vol. 25, no. 19, pp. 2840–2846, 2007.

[30] W. R. Wikoff, J. A. Gangoiti, B. A. Barshop, and G. Siuzdak, "Metabolomics identifies perturbations in human disorders of propionate metabolism," *Clinical Chemistry*, vol. 53, no. 12, pp. 2169–2176, 2007.

[31] W. O. Opii, G. Joshi, E. Head et al., "Proteomic identification of brain proteins in the canine model of human aging following a long-term treatment with antioxidants and a program of behavioral enrichment: relevance to Alzheimer's disease," *Neurobiology of Aging*, vol. 29, no. 1, pp. 51–70, 2008.

[32] Y. Qiu, G. Cai, M. Su et al., "Urinary metabonomic study on colorectal cancer," *Journal of Proteome Research*, vol. 9, no. 3, pp. 1627–1634, 2010.

[33] T. Chen, G. Xie, X. Wang et al., "Serum and urine metabolite profiling reveals potential biomarkers of human hepatocellular carcinoma," *Molecular & Cellular Proteomics*, vol. 10, no. 7, 2011.

[34] Y. Cheng, G. Xie, T. Chen et al., "Distinct urinary metabolic profile of human colorectal cancer," *Journal of Proteome Research*, vol. 11, no. 2, pp. 1354–1363, 2012.

[35] X. Wang, X. Wang, G. Xie et al., "Urinary metabolite variation is associated with pathological progression of the post-hepatitis B cirrhosis patients," *Journal of Proteome Research*, vol. 11, no. 7, pp. 3838–3847, 2012.

[36] C. M. A. Chinese Society of Hepatology and C. M. A. Chinese Society of Infectious Diseases, "Guideline on prevention and treatment of chronic hepatitis B in China (2005)," *Chinese Medical Journal*, vol. 120, no. 24, pp. 2159–2173, 2005.

[37] Y. Qiu, M. Su, Y. Liu et al., "Application of ethyl chloroformate derivatization for gas chromatography-mass spectrometry based metabonomic profiling," *Analytica Chimica Acta*, vol. 583, no. 2, pp. 277–283, 2007.

[38] H. Zhang, X. Chen, P. Hu et al., "Metabolomic profiling of rat serum associated with isoproterenol-induced myocardial infarction using ultra-performance liquid chromatography/time-of-flight mass spectrometry and multivariate analysis," *Talanta*, vol. 79, no. 2, pp. 254–259, 2009.

[39] S. W. Schalm, "The diagnosis of cirrhosis: clinical relevance and methodology," *Journal of Hepatology*, vol. 27, no. 6, pp. 1118–1119, 1997.

[40] A. Colli, M. Fraquelli, M. Andreoletti, B. Marino, E. Zuccoli, and D. Conte, "Severe liver fibrosis or cirrhosis: accuracy of US for

detection—analysis of 300 cases," *Radiology*, vol. 227, no. 1, pp. 89–94, 2003.

[41] A. Zipprich, G. Garcia-Tsao, S. Rogowski, W. E. Fleig, T. Seufferlein, and M. M. Dollinger, "Prognostic indicators of survival in patients with compensated and decompensated cirrhosis," *Liver International*, vol. 32, no. 9, pp. 1407–1414, 2012.

[42] G. D'amico, A. Morabito, L. Pagliaro, and E. Marubini, "Survival and prognostic indicators in compensated and decompensated cirrhosis," *Digestive Diseases and Sciences*, vol. 31, no. 5, pp. 468–475, 1986.

[43] A. S. F. Lok and B. J. McMahon, "Chronic hepatitis B," *Hepatology*, vol. 45, no. 2, pp. 507–539, 2007.

[44] Y. Arakawa, M. Moriyama, and Y. Arakawa, "Liver cirrhosis and metabolism (sugar, protein, fat and trace elements)," *Hepatology Research*, vol. 30, pp. S46–S58, 2004.

[45] M. Kato and H. Moriwaki, "Metabolic disorders in patients with liver cirrhosis," *Hepatology Research*, vol. 30, pp. S59–S62, 2004.

[46] J. K. Nicholson, E. Holmes, J. Kinross et al., "Host-gut microbiota metabolic interactions," *Science*, vol. 336, no. 6086, pp. 1262–1267, 2012.

[47] J. N. Thompson, J. Cohen, J. I. Blenkharn, J. S. McConnell, J. Barr, and L. H. Blumgart, "A randomized clinical trial of oral ursodeoxycholic acid in obstructive jaundice," *British Journal of Surgery*, vol. 73, no. 8, pp. 634–636, 1986.

[48] E. M. M. Kuiper, B. E. Hansen, W. Lesterhuis et al., "The long-term effect of ursodeoxycholic acid on laboratory liver parameters in biochemically non-advanced primary biliary cirrhosis," *Clinics and Research in Hepatology and Gastroenterology*, vol. 35, no. 1, pp. 29–33, 2011.

[49] C. Tiribelli and J. D. Ostrow, "Intestinal flora and bilirubin," *Journal of Hepatology*, vol. 42, no. 2, pp. 170–172, 2005.

[50] E. Seki and D. A. Brenner, "Toll-like receptors and adaptor molecules in liver disease: update," *Hepatology*, vol. 48, no. 1, pp. 322–335, 2008.

[51] I. N. Crispe, "The liver as a lymphoid organ," *Annual Review of Immunology*, vol. 27, pp. 147–163, 2009.

[52] J. P. Pradere, J. S. Troeger, D. H. Dapito, A. A. Mencin, and R. F. Schwabe, "Toll-like receptor 4 and hepatic fibrogenesis," *Seminars in Liver Disease*, vol. 30, no. 3, pp. 232–244, 2010.

[53] C. C. Chan, S. J. Hwang, F. Y. Lee et al., "Prognostic value of plasma endotoxin levels in patients with cirrhosis," *Scandinavian Journal of Gastroenterology*, vol. 32, no. 9, pp. 942–946, 1997.

[54] R.-S. Lin, F.-Y. Lee, S.-D. Lee et al., "Endotoxemia in patients with chronic liver diseases: relationship to severity of liver diseases, presence of esophageal varices, and hyperdynamic circulation," *Journal of Hepatology*, vol. 22, no. 2, pp. 165–172, 1995.

[55] G. Y. Chen and G. Nuñez, "Sterile inflammation: sensing and reacting to damage," *Nature Reviews Immunology*, vol. 10, no. 12, pp. 826–837, 2010.

[56] T. A. Miettinen, "Lipid absorption, bile acids, and cholesterol metabolism in patients with chronic liver disease," *Gut*, vol. 13, no. 9, pp. 682–689, 1972.

[57] J. Y. Sung, E. A. Shaffer, and J. W. Costerton, "Antibacterial activity of bile salts against common biliary pathogens: effects of hydrophobicity of the molecule and in the presence of phospholipids," *Digestive Diseases and Sciences*, vol. 38, no. 11, pp. 2104–2112, 1993.

[58] Y. Chen, F. Yang, H. Lu et al., "Characterization of fecal microbial communities in patients with liver cirrhosis," *Hepatology*, vol. 54, no. 2, pp. 562–572, 2011.

[59] H. Lu, Z. Wu, W. Xu, J. Yang, and Y. Chen, "Intestinal microbiota was assessed in cirrhotic patients with hepatitis B virus infection. Intestinal microbiota of HBV cirrhotic patients," *Microbial Ecology*, vol. 61, no. 3, pp. 693–703, 2011.

[60] W. Zhang, Y. Gu, Y. Chen et al., "Intestinal flora imbalance results in altered bacterial translocation and liver function in rats with experimental cirrhosis," *European Journal of Gastroenterology and Hepatology*, vol. 22, no. 12, pp. 1481–1486, 2010.

[61] L. Li, Z. Wu, W. Ma, Y. Yu, and Y. Chen, "Changes in intestinal microflora in patients with chronic severe hepatitis," *Chinese Medical Journal*, vol. 114, no. 8, pp. 869–872, 2001.

[62] C. Hong-xin, *General Introduction to TCM Theory*, Science Press, Beijing, China, 2011.

Hindawi Publishing Corporation
Evidence-Based Complementary and Alternative Medicine
Volume 2015, Article ID 350703, 8 pages
http://dx.doi.org/10.1155/2015/350703

Research Article

A Metabolomics Approach to Stratify Patients Diagnosed with Diabetes Mellitus into Excess or Deficiency Syndromes

Tao Wu,[1,2] Ming Yang,[2] Tao Liu,[2] Lili Yang,[2] and Guang Ji[2]

[1] *Center of Chinese Medicine Therapy and Systems Biology, Shanghai University of Traditional Chinese Medicine, Shanghai 201203, China*
[2] *Institute of Digestive Disease, Longhua Hospital, Shanghai University of Traditional Chinese Medicine, Shanghai 200032, China*

Correspondence should be addressed to Guang Ji; jiliver@vip.sina.com

Received 23 June 2014; Accepted 29 July 2014

Academic Editor: Wei Jia

The prevalence of type 2 diabetes continuously increases globally. The traditional Chinese medicine (TCM) can stratify the diabetic patients based on their different TCM syndromes and, thus, allow a personalized treatment. Metabolomics is able to provide metabolite biomarkers for disease subtypes. In this study, we applied a metabolomics approach using an ultraperformance liquid chromatography (UPLC) coupled with quadruple-time-of-flight (QTOF) mass spectrometry system to characterize the metabolic alterations of different TCM syndromes including excess and deficiency in patients diagnosed with diabetes mellitus (DM). We obtained a snapshot of the distinct metabolic changes of DM patients with different TCM syndromes. DM patients with excess syndrome have higher serum 2-indolecarboxylic acid, hypotaurine, pipecolic acid, and progesterone in comparison to those patients with deficiency syndrome. The excess patients have more oxidative stress as demonstrated by unique metabolite signatures than the deficiency subjects. The results provide an improved understanding of the systemic alteration of metabolites in different syndromes of DM. The identified serum metabolites may be of clinical relevance for subtyping of diabetic patients, leading to a personalized DM treatment.

1. Introduction

Diabetes mellitus (DM) is a chronic disease defined with high blood glucose levels, which may be due either to the progressive failure of pancreatic β-cell function and consequently a lack of insulin production (type 1: T1DM), or to the development of insulin resistance and subsequently the loss of β-cell function (type 2: T2DM). DM affects more than 230 million people worldwide and T2DM is predicted to affect approximately 8% of the population by 2030 [1]. The chronic hyperglycemia of diabetes is associated with significant long-term sequelae, particularly damage and/or dysfunction and failure of various organs, especially the kidneys, eyes, nerves, heart, and blood vessels [2]. Both the macrovascular (coronary artery disease, peripheral artery disease, and stroke) and microvascular (retinopathy, nephropathy, and neuropathy) complications are the major causes of morbidity and mortality of diabetes.

Traditional Chinese medicine (TCM) has a long history and particular advantages in the diagnosis and treatment of diabetes mellitus. Syndrome differentiation is not only the basic unit of TCM theory, but also the bridge to associating disease and formula. TCM can stratify the diabetic patients based on their different TCM syndromes and, thus, allow a personalized treatment. When people suffer from a disease, Yin (things associated with the physical form of an object), Yang (things associated with energetic qualities), Qi (life force that animates the forms of the world), and Xue (dense form of body fluids that have been acted upon and energized by Qi) [3] are in an abnormal state. Similarly, DM could be classified as having deficiency syndrome or excess syndrome, which refers to the insufficiency or excess in Qi, Xue, Yin, and Yang. However, syndromes depend on medical experience, academic origins, and other factors so that the concept of syndromes is vague and broad, which makes clinical application difficult. Hence, it is more important to realize the

syndrome objectification and standardization. Furthermore nowadays although the diagnosis and treatment of manifest diabetes have been thoroughly investigated, the identification of novel pathways or biomarkers indicative of the TCM syndrome differentiation of diabetes is still underway.

With the rapid development of the analytical technology and advanced multivariate statistical and bioinformatic tools, metabolomics has become a promising approach for understanding and elucidating the etiology and mechanisms of human diseases [4–7] and has been extensively applied to life science [8–10]. Metabolomics is also able to provide metabolite biomarkers for disease subtypes. The growing research field of metabolomics has introduced new insights into the pathology of diabetes as well as methods to predict disease onset and has revealed new biomarkers during the last decade. Recent epidemiological studies first used metabolism to predict incident diabetes and revealed branched-chain and aromatic amino acids including isoleucine, leucine, valine, tyrosine, and phenylalanine as highly significant predictors of future diabetes [11, 12]. Our previous work also showed urinary carbohydrate metabolic characterization of DM patients with different traditional Chinese medicine syndromes, including biomarkers different from non-DM patients [13]. Xu et al. found that three TCM syndromes including Qi-deficiency, Qi and Yin-deficiency, and damp heat can be separated using metabolomics technology and such differences can be manifested by plasma fatty acids and lipid parameters [14]. Wei et al. designed an explorative study of 50 prediabetic males, and finally they indicated more disturbances of carbohydrate metabolism and renal function in subtype "Qi-Yin deficiency with stagnation" compared with "Qi-Yin deficiency with dampness" [15]. However, it is still far from clear about the different syndrome of diabetes although so many investigations have been performed [16].

In this study, we applied a metabolomics approach using ultraperformance liquid chromatography (UPLC) coupled with quadruple-time-of-flight (QTOF) mass spectrometry to characterize the metabolic alterations of different TCM syndromes including excess and deficiency in patients diagnosed with DM and discover biomarkers using metabolomics technology to further find the deep connotation of TCM syndromes.

2. Methods

2.1. Study Population. DM patients were prospectively included from the Tianlin Community health center, Shanghai city of China, during August 2009 to May 2010. DM is characterized by a fasting plasma glucose (FPG) of ≥7.0 mmol/L, a post-load plasma glucose (2 h PG) of ≥11.1 mmol/L, or a history of oral hypoglycemic or insulin use, or both, based on the standard formulated by the World Health Organization in 1999 [17]. TCM syndromes, including deficiency and excess syndromes, were differentiated according to the guidelines [18]. Patients suffering from other serious diseases involving major organs or infective diseases were excluded from the study. Patients with deficiency and excess syndrome simultaneously were also excluded. The detailed inclusion and exclusion criteria were shown in previous work [13]. Altogether 295 subjects with T2DM (238 deficiency and 57 excess samples) were recruited to the study. All subjects provided their written informed consent. The ethics committee of the hospital approved the study plan and the study complied with the Declaration of Helsinki.

2.2. Biochemical Analysis. Body mass index (BMI) was calculated as weight (kg) divided by height (m) squared. The waist-hip ratio (WHR) was defined as the waist circumference (cm) divided by the hip circumference (cm). Systolic blood pressure (SBP) and diastolic blood pressure (DBP) were measured using standard mercury sphygmomanometers on the right arm of seated participants. Serum fasting glucose, triglyceride (TG), high density lipoprotein (HDL-C), very low-density lipoprotein cholesterol (VLDL-C), alanine aminotransferase (ALT), and 2 h PG were analyzed using an automatic bioanalyzer (Hitachi7180, Tokyo, Japan). Liver ultrasound examination was carried out on the same equipment (Aloka1700, Japan).

2.3. Chemicals. HPLC grade methanol, acetonitrile, and formic acid were purchased from Merck Chemicals (Darmstadt, Germany). L-chlorophenylalanine was purchased from Sigma-Aldrich (St. Louis, MO). Ultrapure water was produced by a Milli-Q water system (Millipore, Billerica, USA).

2.4. Serum Sample Preparation for UPLC-QTOFMS. Fasting serum samples were obtained and prepared strictly according to the previous work [19]. An aliquot of 100 μL of serum was mixed with 400 μL of a mixture of methanol and acetonitrile [5 : 3, (containing 0.1 mg/mL L-chlorophenylalanine as the internal standard)]. The mixture was then vortexed for 2 min, allowed to stand for 10 min, and centrifuged at 14 500 g for 20 min. The supernatant was used for UPLC-QTOFMS analysis.

2.5. UPLC-QTOFMS Spectral Acquisition of Serum Samples and Data Preprocessing. A Waters ACQUITY ultraperformance liquid chromatography (UPLC) system equipped with a binary solvent manager and a sample manager (Waters Corporation, Milford, MA, USA), coupled to a QTOF mass spectrometry with an electrospray interface (Waters Corporation, Milford, MA), was used throughout the study as aforementioned [19]. All Chromatographic separations were performed with an ACQUITY BEH C18 column (1.7 μm, 100 × 2.1 mm internal dimensions, Waters). The column was maintained at 50°C, and the injection volume of all samples was 5 μL. The LC elution conditions were optimized as follows: linear gradient from 1 to 20% B (0-1 min), 20 to 70% B (1–3 min), 70 to 85% B (3–8 min), 85 to 100% B (8-9 min), and isocratic at 100% B (9–9.5 min) with a flow rate of 0.4 mL/min. (A) Water with 0.1% formic acid and (B) acetonitrile with 0.1% formic acid were used for positive ion mode (ESI+), while (A) water and (B) acetonitrile for negative ion mode (ESI−). The mass spectrometer was operated with source and desolvation temperatures set at 120°C and 300°C, respectively. The desolvation gas was set at a flow rate of

600 L/hr. The capillary voltage was set of 3.2 and 3 kV and the cone voltage of 35 and 50 V, respectively, in the positive and negative ion modes.

The UPLC-MS raw data were processed using MarkerLynx 4.1 (Waters, Manchester, UK) using parameters mentioned in the previous work [20–23]. After removing the ion peaks generated by the internal standard, the data were normalized by dividing the sum of all peak intensities within the sample and then a data matrix consisted of the retention time, m/z value, and the normalized peak area was exported for multivariate statistical analysis using the K-OPLS package (available at http://kopls.sourceforge.net/download.shtml) and Statistics toolbox of the Matlab (version 7.1, Mathwork Inc.) software. Compound annotation was carried out by comparing the retention time, molecular weight, preferred adducts, and in-source fragments based on our in-house reference standard library (−800 mammalian metabolite standards available) and web-based resources, including the Human Metabolome Database (http://www.hmdb.ca/).

2.6. Data Analysis. Data from the common and clinical information were expressed as mean ± standard deviation (S.D.). Differences between the means of groups were analyzed using independent samples t-test for continuous variables and Pearson chi-square tests for categorical variable using the SPSS 17.0 software (SPSS, Chicago, Illinois, USA), with a two-sided P value of <0.05 considered statistically significant.

By applying preprocessing methods, both a synthetic minority oversampling technique (SMOTE) bagging rebalancing method and a genetic algorithm (GA) with kernel-based orthogonal projections to latent structures (K-OPLS), differential metabolites between groups from the UPLC-QTOFMS data were observed. The major protocol was according to our previous work [13, 24] and related literatures [25, 26], as shown in Figure S1 (see Supplementary Material available online at http://dx.doi.org/10.1155/2015/350703).

First, for the reason of the data's unbalance, the SMOTE algorithm was performed to simulate small data and achieve the equilibrium of the whole data set. According to the class of 50% randomly selected samples as training set, the original sample data as test set, and GA-KOPLS algorithm with balanced prediction errors of test set as a fitness function, the nearest neighbor parameters "n" of SMOTE were optimized.

Secondly, under the optimized SMOTE parameter, GA-KOPLS algorithm is applied to modeling and selects the important variables (metabolites) at the same time with the balanced prediction error in test set as the fitness function (minimize error). Evaluation of classifier accuracy during each GA run was performed using a cross-validation [27].

Thirdly, the important variables selected by the GA were applied to a K-OPLS algorithm for classification, and the parameters including the Gaussian kernel function parameter (σ) and the number of Y-orthogonal components (Ao) of the K-OPLS model were optimized with internal tenfold cross-validation of training set. The kernel matrix K was centered to model estimation. The samples from each training set study were taken for classification, in turn, excluding those being classified from the selected samples in the training set. The prediction accuracy of the original data set, AUC, sensitivity, and specificity were used to evaluate the K-OPLS model performance. Details on the model were provided in the previous work [13].

Finally, the frequency of variable significance test was performed by GA, and the P values were calculated based on the binomial probabilities of variables being selected in the 50 independent runs, to identify the metabolites with significant influence in the classification. One has

$$P(x) = \sum_{i=x}^{n} \binom{n}{i} \left(\frac{m}{v}\right)^{i} \left(1 - \frac{m}{v}\right)^{n-i}, \quad (1)$$

where n = number of runs, v = number of variables, and m = mean number of times variables are selected, rounded to an integer. For details, see literature [28]. In addition, these metabolites selected from the model were validated at a univariate level with nonparametric Wilcoxon rank sum test with a critical P value usually set to 0.05.

3. Results

3.1. Clinical Characteristics of Patients. Subjects' clinical characteristics of the three groups were summarized in Table 1. The clinical characteristics of this subset of subjects did not differ significantly between the groups at baseline, except for age, BMI, and the coincidence of fatty liver disease, which were significantly higher in the deficiency group than in the excess group.

3.2. UPLC-QTOFMS Analysis of Serum Metabolite Profiles. The ESI positive ion mode was more efficient with a significantly greater number of serum metabolites detected than the ESI negative ion mode and, therefore, was selected for the full scan detection mode. Among a total of approximately 6680 metabolite features obtained from the UPLC-QTOFMS, 133 metabolites were identified with our in-house reference standard library and further verified by available reference standards. Their peak areas were integrated for further multivariate analysis.

3.3. Classification of the K-OPLS Models. In the present study the nearest neighbor parameter "n" of SMOTE was 3 after optimization, from DM patients with excess or deficiency syndrome. A K-OPLS model was fitted using the Gaussian kernel function with the important variables selected from GA. The parameters of GA including initiate population, K (times of genetic algebra), selective ratio of initiate variable, and probability of simple point crossover were 30, 150, 0.1, and 0.7, respectively (Table 2). Accuracy of classification of cross-validation (ACCV) was calculated for each combination of σ and Ao which were optimized using 10-fold cross-validation. ACCV was the largest when $\sigma = 2.5$ and Ao = 3 for DM patients with excess and deficiency syndrome (Figure 1(a)).

Table 2 showed the R2X, R2Y, Q2Y, AUC, sensitivity, and specificity used in evaluating all the calibration models of the two groups. R2Xcum and R2Ycum represented the cumulative sum of squares of all the X's (metabolic data) and Y's (disease category data) explained by all extracted

Table 1: Clinical characteristics of excess and deficiency syndromes in patients with DM (mean ± SD).

	Patients with DM (n = 295)			
	Total	Excess	Deficiency	P^a
Gender (n, male/female)	295 (107/188)	57 (23/34)	238 (84/154)	0.476
Age (year)	70.69 ± 8.86	67.11 ± 9.49	71.55 ± 8.50	<0.001
BMI (kg/m^2)	25.29 ± 2.90	24.57 ± 2.44	25.46 ± 2.98	0.037
Waist circumference (cm)	90.79 ± 7.92	89.49 ± 6.94	91.1 ± 8.13	0.170
Hip circumference (cm)	101.01 ± 7.39	99.38 ± 6.34	101.41 ± 7.58	0.063
Waist-to-hip ratio (WHR)	0.90 ± 0.06	0.90 ± 0.05	0.90 ± 0.06	0.795
SBP (mmHg)	138.11 ± 14.66	136.53 ± 14.40	138.49 ± 14.73	0.365
DBP (mmHg)	78.41 ± 9.47	79.72 ± 9.62	78.1 ± 9.43	0.247
Obesity (BMI ≥ 25)	51.8% (153/142)	45.6% (26/31)	53.4% (127/111)	0.293
Fatty liver disease	74.9% (221/74)	66.7% (38/19)	76.9% (183/55)	0.045
Hypertension	91.5% (270/25)	87.7% (50/7)	92.4% (220/18)	0.251
Hyperlipidemia	41.0% (121/182)	42.1% (24/33)	39.9% (95/143)	0.762
Coronary heart disease	23.3% (69/226)	29.8% (17/40)	21.8% (52/186)	0.201
Cerebrovascular accident	0.07% (20/275)	0.07% (4/53)	0.07% (16/222)	0.937
Hyperuricemia	0.07% (22/273)	0.07% (4/53)	0.08% (18/220)	0.888
FPG (mmol/L)	7.60 ± 2.12	7.84 ± 2.36	7.55 ± 2.06	0.355
2 h PG (mmol/L)	11.37 ± 3.69	11.51 ± 3.52	11.33 ± 3.74	0.742
TG (mmol/L)	1.55 ± 0.93	1.51 ± 0.84	1.57 ± 0.96	0.675
HDL cholesterol (mmol/L)	1.33 ± 0.36	1.29 ± 0.25	1.34 ± 0.38	0.322
ALT (U/L)	25.26 ± 13.19	26.97 ± 13.84	24.85 ± 13.02	0.276
VLDL cholesterol (mmol/L)	2.57 ± 0.56	2.58 ± 0.59	2.57 ± 0.55	0.935

[a] P value refers to the comparison between excess versus deficiency syndromes within the DM group using independent samples t-test for continuous variables and Pearson chi-square tests for categorical variable with the SPSS 17.0 software (SPSS, Chicago, Illinois, USA). P values < 0.05 were considered significant.

Table 2: Parameters from GA.

GA parameters	Initiate population	K^a	Selective ratio of initiate variable	Probability of simple point crossover
Excess versus deficiency	30	150	0.1	0.7

[a] K means times of genetic algebra.

components. Q2Ycum is an estimate of how well the model predicts the Y's [28]. High coefficient values of R2Y and Q2Y represent good prediction [29]. As displayed by the score plots of K-OPLS (Figure 1(b)), the two sample groups can be separated into distinct clusters to indicate the changes in the metabolic response of serum samples from the DM patients with excess and deficiency syndrome.

The model statistics R2X = 0.425, R2Y = 1.000, and Q2Y = 0.944 in the model suggest a highly predictive and general model (Table 3). Because the nonlinear method was used in the present study, the R2X had less significant meanings. On the contrary, the major indicator is AUC to evaluate the models' accuracy in nonlinear method. AUC = 0.968 (95% confidence interval = 0.950–0.987) predicted that the models had high accuracy (Table 3).

3.4. Representative Differential Metabolites Based on Multivariate and Univariate Analysis. The metabolites contributed for the separation between groups derived from UPLC-QTOFMS analysis were selected in accordance with the criteria of multivariate statistics (GA, $P < 0.001$, Figure 2(a)) and nonparametric univariate statistics (Wilcoxon rank sum test, $P < 0.05$, Figure 2(b)). Four differentially expressed metabolites including 2-indolecarboxylic acid, hypotaurine (HTAU), pipecolic acid, and progesterone between DM patients with excess and deficiency syndrome were found (Figure 3). The serum levels of those four metabolites were higher in DM patients with excess syndrome than those with deficiency syndrome.

4. Discussion

Serum patterns of metabolites reflect the homeostasis of the organism to some extent. Metabolomics, a discipline dedicated to the global study of metabolites, may deepen our understanding of human health and diseases. In the present study, we found that four metabolites can differentiate two different TCM syndromes in DM, which cannot be characterized by the clinical biochemical indicators. The clear separation between two groups by TCM symptoms and metabolic profiles illustrated that excess and deficiency syndrome had their own substance fundaments.

Clinical characteristics of this subset of subjects in Table 1 showed there was no significant difference between the

Table 3: Parameters from KOPLS models.

KOPLS Parameters	Sigma	Ao	ACCV[a]	R2X[b]	R2Y[b]	Q2Y[c]	Total accuracy	Balance accuracy	AUC[d]	AUC 95% confidence interval	sensitivity	specificity
Excess versus Deficency	2.5	3	0.860	0.425	1	0.944	0.949	0.968	0.968	0.950–0.987	1	0.937

[a]Accuracy of classification of cross-validation (ACCV) produced from each combination of σ and Ao parameters after cross-validation. [b]R2Xcum and R2Ycum represent the cumulative sum of squares (SS) of all the X's and Y's explained by all extracted components. [c]Q2Ycum is an estimate of how well the model predicts the Y's. [d]AUC in 0.5~0.7 has lower accuracy, AUC in 0.7~0.9 has certain accuracy (model can be accepted), and AUC in more than 0.9 has high accuracy. When AUC = 0.5, the model has no value.

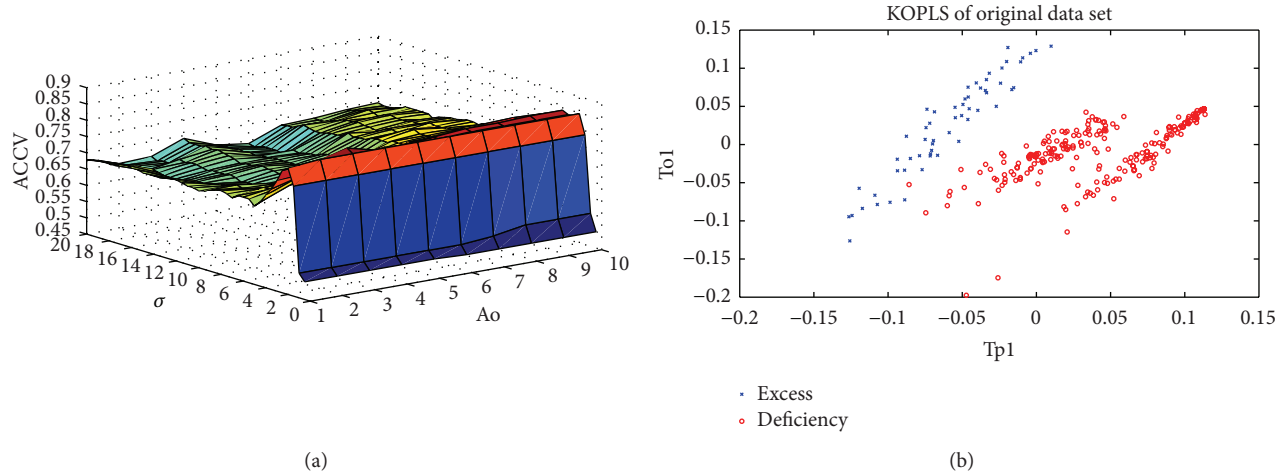

Figure 1: Accuracy of classification of cross-validation (ACCV) (a) and first predictive and Y-orthogonal score components (b) by the K-OPLS model in DM patients with excess and deficiency syndrome.

deficiency and excess groups at baseline, in terms of sex, WC, HC, WHR, DBP, TG, ALT, VLDL, and HDL levels, except for age, BMI, and the coincidence of fatty liver disease, which were significantly higher in the deficiency group than in the excess group. The higher age in deficiency group is in accordance with clinical TCM theory that Qi, Xue, Yin, and Yang are more insufficient in older than in younger persons. This result shows that the clinical biochemical indicators are difficult to differentiate the TCM syndromes. Hence novel approaches for differentiating syndromes are urgently needed. The nontarget metabolomics provides a global view of the organism and also provides an opportunity to stratify the different TCM syndromes like we performed before [13].

In the present study, we performed UPLC-QTOFMS-based serum metabolic profiling combined with GA-KOPLS analysis on DM patients with different syndromes and four metabolites were eventually found between the two TCM syndromes. In order to exclude the effect of age and BMI, we separated two subsets with the cutoff of 70 in age, 25 in BMI. We found that there was no significant difference of the four differential metabolites between groups with Mann-Whitney Test Analysis ($P > 0.05$, Supplementary Table S1). Furthermore, we performed the KOPLS model based on the same parameters. It was shown that no matter the age >70 or ≤70 ($n = 161$ versus 134), deficiency group and excess group could be distinctly separated on the classification (Supplementary Figure S2). Similar results were also found in BMI ≥25 or <25 ($n = 153$ versus 142) (Supplementary Figure S3). Those results prompt that the age and BMI with significant difference between deficiency and excess groups do not affect our final metabolomics results.

2-Indolecarboxylic acid similar to melatonin is a strong inhibitor of lipid peroxidation. Štětinová et al. performed an in vitro study with a standard lipid peroxidation assay, and they finally found that tested drugs inhibited lipid peroxidation in the order of tryptamine (59%) > 2-indolecarboxylic acid (38%) > indomethacin (26%) > melatonin and indole-3-carboxylic acid (13%) [30].

HTAU is a product of enzyme cysteamine dioxygenase in taurine and hypotaurine metabolic pathway. It may function as an antioxidant and a protective agent under physiological conditions [31, 32], and it results in the prevention of peroxynitrite-induced tyrosine nitration to 3-nitrotyrosine and oxidation to dityrosine. Nitration and oxidation of tyrosine residues in proteins have been detected in several conditions of oxidative stress that involve the overproduction of NO^+ and oxygen radicals. Hence, it is tempting to postulate that the protection afforded by HTAU on tyrosine modification may have important physiological significance. Gossai and Lau-Cam compared taurine, aminomethanesulfonic acid, homotaurine, and HTAU for the ability to modify indices of oxidative stress and membrane damage

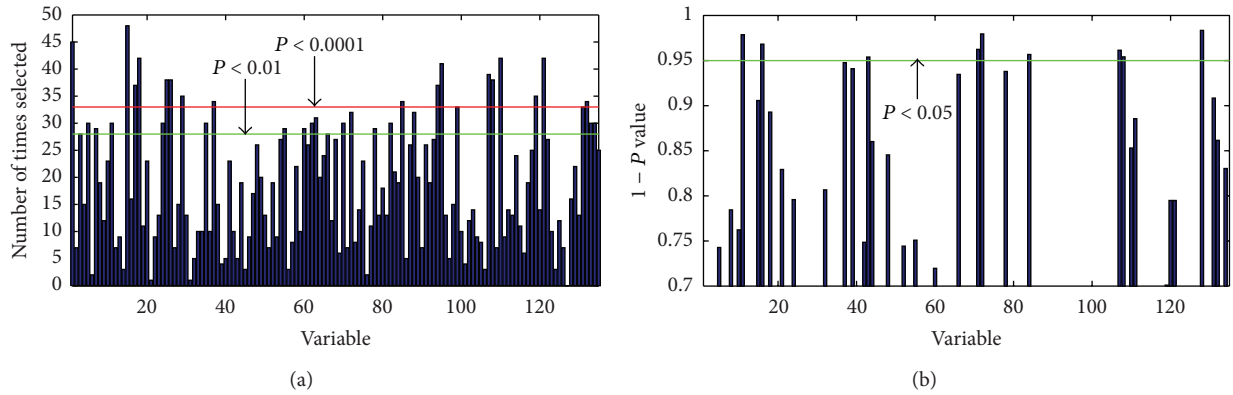

Figure 2: GA runs (a) and Wilcoxon rank sum test (b) in DM patients with excess and deficiency syndrome. (a) X-axis presents 135 metabolites as variables; Y-axis presents the number of selected times of the variables from GA. (b) X-axis presents 135 metabolites as variables; Y-axis presents the value of $1 - P$ from Wilcoxon rank sum test.

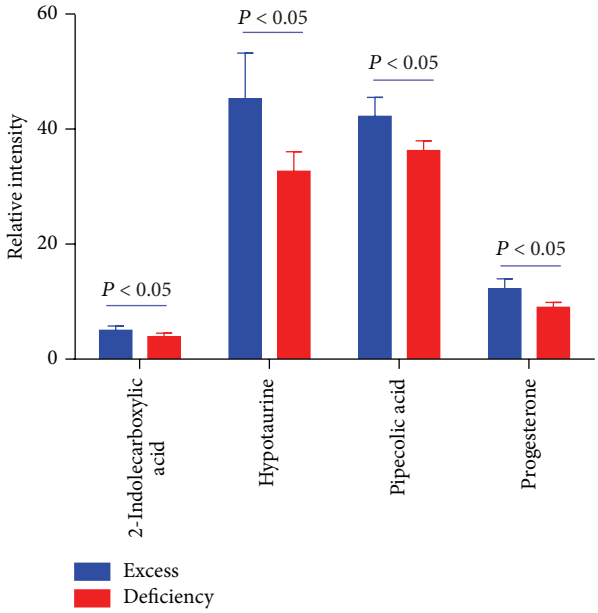

Figure 3: Differentially expressed metabolites between groups in DM patients with excess and deficiency syndrome combined with GA runs and Wilcoxon rank sum test.

associated with T2DM. Relative to control values, taurine and its congeners had equiproctective roles in reducing membrane damage, the formation of intracellular malondialdehyde and oxidized glutathione, and the decreases in reduced glutathione and antioxidative enzyme activities in diabetic erythrocytes [33].

Pipecolic acid (piperidine-2-carboxylic acid), the carboxylic acid of piperidine, is a small organic molecule which accumulates in pipecolic acidemia. It is a metabolite of lysine found in human physiological fluids such as urine and serum. However, it is uncertain whether pipecolic acid originates directly from food intake or from mammalian or intestinal bacterial enzyme metabolism.

Progesterone, converted from pregnenolone, serves as an intermediate in the biosynthesis of gonadal steroid hormones and adrenal corticosteroids. Progesterone was observed to have antioxidant properties, reducing the concentration of oxygen free radicals [34]. Recently, a crosstalk between progesterone and melatonin has been observed in various preclinical studies. The melatonin is reported to increase progesterone level and expression of progesterone receptors in reproductive tissues [35].

Interestingly, the above four metabolites are all related to oxidative stress. We suggest that diabetic patients with excess syndrome may have more severe systemic oxidative stress than those with deficiency syndrome. Understanding syndromes is a core research to develop more efficient therapeutic strategies, classification, and diagnostic criteria for patients. It will contribute to TCM syndrome objectification and standardization to the better diagnosis and therapy of disease. Further investigations with larger sample sizes are needed to confirm our findings.

5. Conclusion

The present study provides an improved understanding of the systemic alteration of metabolites in different syndromes of DM. It also presents that metabolomics method would be helpful in establishing a suitable model for reasonably evaluating disease syndrome, exploring pathological mechanism of syndrome, and clarifying the relationships between the syndrome and related diseases. Furthermore, the identified serum metabolites may be of clinical relevance for subtyping of diabetic patients, leading to a personalized DM treatment.

Conflict of Interests

The authors declare that there is no conflict of interests.

Acknowledgments

The authors are indebted to all the patients who participated in this study. This study was supported by the National Natural Science Foundation of China (81202979), the Leading Academic Discipline Project and Innovative Research

Team in Universities from Shanghai Municipal Education Commission (J50305), E-institutes of Shanghai Municipal Education Commission China (E03008), and the Natural Science Foundation of Shanghai (11ZR1436900).

References

[1] G. C. Farrell, "The liver and the waistline: fifty years of growth," *Journal of Gastroenterology and Hepatology*, vol. 24, supplement 3, pp. S105–S118, 2009.

[2] B. S. Nayak and L. Roberts, "Relationship between inflammatory markers, metabolic and anthropometric variables in the Caribbean type 2 diabetic patients with and without microvascular complications," *Journal of Inflammation*, vol. 3, article 17, 2006.

[3] L. M. Wang, X. Zhao, X. L. Wu, Y. Li, and D. H. Yi, "Diagnosis analysis of 4 TCM patterns in suboptimal health status: a structural equation modelling approach," *Evidence-Based Complementary and Alternative Medicine*, vol. 2012, Article ID 970985, 6 pages, 2012.

[4] P. N. Kirke, J. L. Mills, and J. M. Scott, "Homocysteine metabolism in pregnancies complicated by neural tube defects," *Nutrition*, vol. 13, no. 11-12, pp. 994–995, 1997.

[5] Y. Ni, M. Su, Y. Qiu et al., "Metabolic profiling using combined GC-MS and LC-MS provides a systems understanding of aristolochic acid-induced nephrotoxicity in rat," *FEBS Letters*, vol. 581, no. 4, pp. 707–711, 2007.

[6] X. Wang, X. Wang, G. Xie et al., "Urinary metabolite variation is associated with pathological progression of the post-hepatitis B cirrhosis patients," *Journal of Proteome Research*, vol. 11, no. 7, pp. 3838–3847, 2012.

[7] A. Craig, J. Sidaway, E. Holmes et al., "Systems toxicology: integrated genomic, proteomic and metabonomic analysis of methapyrilene induced hepatotoxicity in the rat," *Journal of Proteome Research*, vol. 5, no. 7, pp. 1586–1601, 2006.

[8] N. N. Kaderbhai, D. I. Broadhurst, D. I. Ellis, R. Goodacre, and D. B. Kell, "Functional genomics via metabolic footprinting: monitoring metabolite secretion by *Escherichia coli* tryptophan metabolism mutants using FT-IR and direct injection electrospray mass spectrometry," *Comparative and Functional Genomics*, vol. 4, no. 4, pp. 376–391, 2003.

[9] S. S. Heinzmann, C. A. Merrifield, S. Rezzi et al., "Stability and robustness of human metabolic phenotypes in response to sequential food challenges," *Journal of Proteome Research*, vol. 11, no. 2, pp. 643–655, 2012.

[10] K. Suhre, C. Meisinger, A. Döring et al., "Metabolic footprint of diabetes: a multiplatform metabolomics study in an epidemiological setting," *PLoS ONE*, vol. 5, no. 11, Article ID e13953, 2010.

[11] K. Suhre, "Metabolic profiling in diabetes," *Journal of Endocrinology*, vol. 221, no. 3, pp. R75–R85, 2014.

[12] N. Friedrich, "Metabolomics in diabetes research," *Journal of Endocrinology*, vol. 225, no. 3, pp. 29–42, 2012.

[13] T. Wu, M. Yang, H.-F. Wei, S.-H. He, S.-C. Wang, and G. Ji, "Application of metabolomics in traditional chinese medicine differentiation of deficiency and excess syndromes in patients with diabetes mellitus," *Evidence-based Complementary and Alternative Medicine*, vol. 2012, Article ID 968083, 11 pages, 2012.

[14] W. Xu, L. Zhang, Y. Huang, Q. Yang, H. Xiao, and D. Zhang, "Discrimination of type 2 diabetes mellitus corresponding to different traditional Chinese medicine syndromes based on plasma fatty acid profiles and chemometric methods," *Journal of Ethnopharmacology*, vol. 143, no. 2, pp. 463–468, 2012.

[15] H. Wei, W. Pasman, C. Rubingh et al., "Urine metabolomics combined with the personalized diagnosis guided by Chinese medicine reveals subtypes of pre-diabetes," *Molecular BioSystems*, vol. 8, no. 5, pp. 1482–1491, 2012.

[16] H. L. Jiang, J. J. Niu, W. F. Zhang et al., "The role of central nervous system on hypoglycemia and the feasibility of the brain theory in traditional Chinese medicine on treatment of diabetes mellitus," *Journal of Integrative Medicine*, vol. 12, no. 1, pp. 1–6, 2014.

[17] "Definition, diagnosis, and classification of diabetes mellitus and its complications," Report of a WHO consultation , World Health Organisation, Geneva, Switzerland, 1999.

[18] Y. Y. Zheng, *Guiding Principle of Clinical Research on New Drugs of Traditional Chinese Medicine*, The Publishing House of Chinese Medicine Science, Beijing, China, 2002.

[19] Y. Qiu, G. Cai, M. Su et al., "Serum metabolite profiling of human colorectal cancer using GC-TOFMS and UPLC-QTOFMS," *Journal of Proteome Research*, vol. 8, no. 10, pp. 4844–4850, 2009.

[20] G. Xie, R. Plumb, M. Su et al., "Ultra-performance LC/TOF MS analysis of medicinal Panax herbs for metabolomic research," *Journal of Separation Science*, vol. 31, no. 6-7, pp. 1015–1026, 2008.

[21] G. Xie, M. Ye, Y. Wang et al., "Characterization of pu-erh tea using chemical and metabolic profiling approaches," *Journal of Agricultural and Food Chemistry*, vol. 57, no. 8, pp. 3046–3054, 2009.

[22] G. Xie, X. Zheng, X. Qi et al., "Metabonomic evaluation of melamine-induced acute renal toxicity in rats," *Journal of Proteome Research*, vol. 9, no. 1, pp. 125–133, 2010.

[23] T. Chen, G. Xie, X. Wang et al., "Serum and urine metabolite profiling reveals potential biomarkers of human hepatocellular carcinoma," *Molecular & Cellular Proteomics*, vol. 10, no. 7, 2011.

[24] M. Yang, J. Chen, X. Shi, and H. Niu, "Rapid determination of aesculin, aesculetin and fraxetin in Cortex Fraxini extract solutions based on ultraviolet spectroscopy," *E-Journal of Chemistry*, vol. 8, no. 1, pp. S225–S236, 2011.

[25] P. Filzmoser, B. Liebmann, and K. Varmuza, "Repeated double cross validation," *Journal of Chemometrics*, vol. 23, no. 4, pp. 160–171, 2009.

[26] M. Rantalainen, M. Bylesjö, O. Cloarec, J. K. Nicholson, E. Holmes, and J. Trygg, "Kernel-based orthogonal projections to latent structures (K-OPLS)," *Journal of Chemometrics*, vol. 21, no. 7–9, pp. 376–385, 2007.

[27] R. Cavill, H. C. Keun, E. Holmes, J. C. Lindon, J. K. Nicholson, and T. M. D. Ebbels, "Genetic algorithms for simultaneous variable and sample selection in metabonomics," *Bioinformatics*, vol. 25, no. 1, pp. 112–118, 2009.

[28] K. Yuan, H. Kong, Y. Guan, J. Yang, and G. Xu, "A GC-based metabonomics investigation of type 2 diabetes by organic acids metabolic profile," *Journal of Chromatography B: Analytical Technologies in the Biomedical and Life Sciences*, vol. 850, no. 1-2, pp. 236–240, 2007.

[29] J. Girard, "Contribution of free fatty acids to impairment of insulin secretion and action. mechanism of beta-cell lipotoxicity," *Medical Science*, vol. 21, pp. 19–25, 2005.

[30] V. Štětinová, L. Smetanová, V. Grossmann, and P. Anzenbacher, "In vitro and in vivo assessment of the antioxidant activity of melatonin and related indole derivatives," *General Physiology and Biophysics*, vol. 21, no. 2, pp. 153–162, 2002.

[31] M. Fontana, L. Pecci, S. Duprè, and D. Cavallini, "Antioxidant properties of sulfinates: protective effect of hypotaurine on peroxynitrite-dependent damage," *Neurochemical Research*, vol. 29, no. 1, pp. 111–116, 2004.

[32] M. Fontana, F. Giovannitti, and L. Pecci, "The protective effect of hypotaurine and cysteine sulphinic acid on peroxynitrite-mediated oxidative reactions," *Free Radical Research*, vol. 42, no. 4, pp. 320–330, 2008.

[33] D. Gossai and C. A. Lau-Cam, "The effects of taurine, taurine homologs and hypotaurine on cell and membrane antioxidative system alterations caused by type 2 diabetes in rat erythrocytes," *Advances in Experimental Medicine and Biology*, vol. 643, pp. 359–368, 2009.

[34] D. G. Stein, "Progesterone exerts neuroprotective effects after brain injury," *Brain Research Reviews*, vol. 57, no. 2, pp. 386–397, 2008.

[35] J. Sehajpal, T. Kaur, R. Bhatti, and A. P. Singh, "Role of progesterone in melatonin-mediated protection against acute kidney injury," *Journal of Surgical Research*, 2014.

Hindawi Publishing Corporation
Evidence-Based Complementary and Alternative Medicine
Volume 2014, Article ID 204797, 7 pages
http://dx.doi.org/10.1155/2014/204797

Research Article

Diarylheptanoids from *Alpinia officinarum* Cause Distinct but Overlapping Effects on the Translatome of B Lymphoblastoid Cells

Tomohito Kakegawa,[1] Saeko Takase,[1] Eri Masubuchi,[1] and Ken Yasukawa[2]

[1] *Faculty of Pharmaceutical Sciences, Josai International University, 1 Gumyo, Togane, Chiba 283-8555, Japan*
[2] *School of Pharmacy, Nihon University, 7-7-1 Narashinodai, Funabashi, Chiba 274-8555, Japan*

Correspondence should be addressed to Tomohito Kakegawa; tomohito@jiu.ac.jp

Received 16 May 2014; Revised 25 July 2014; Accepted 25 July 2014; Published 31 August 2014

Academic Editor: Wei Jia

Diarylheptanoids (AO-0001, AO-0002, and AO-0003) isolated from *Alpinia officinarum* inhibit proinflammatory mediators and exhibit cytotoxic and antiviral activity. However, the precise mechanisms of action of these diarylheptanoids are unknown as are their effects on expression of specific genes. Here, we used a translatome analysis to investigate the mechanisms and modes of action of these three diarylheptanoids. Polysome-associated messenger RNAs (mRNAs) were prepared from diarylheptanoids-treated and control cells from a human B lymphoblastoid cell line; these mRNA samples were then used for microarray analysis. Microarray Data Analysis Tool version 3.2 was used to analyze the microarray data analysis; this software uses pathway information of the WikiPathways for gene ontology analysis. Each of the diarylheptanoids caused upregulation or downregulation of the same 37 and 286 genes, respectively. Among the 37 upregulated genes, 16 were related to mRNA processing based on the WikiPathways analysis. Our findings provided new insights into the mode of action of diarylheptanoids from *A. officinarum*.

1. Introduction

Alpinia officinarum belongs to the family Zingiberaceae and is known as lesser galangal. *A. officinarum* rhizomes have been used in many Asian cuisines and as traditional medicine; these rhizomes have been used as antiemetics, stomachics, and analgesics in Asia since ancient times. In a series of studies on bioactive compounds from natural sources, we found that a methanol extract from the rhizome of *A. officinarum* is effective in inhibiting 12-O-tetradecanoylphorbol-13-acetate- (TPA-) induced tumor promotion in skin of mice [1]. Diarylheptanoids isolated from *A. officinarum* have many reported effects; they inhibit the melanogenesis caused by B16 melanoma cells [2]; induce apoptosis, S-phase arrest, and differentiation of human neuroblastoma cells [3]; exhibit cytotoxic activity [4]; suppress inducible nitric oxide synthase expression [5]; inhibit biosynthesis of prostaglandin and leukotrienes [6, 7]; and inhibit proinflammatory mediators [8]. Additionally, diarylheptanoids reportedly have antiviral activity against influenza virus [9, 10], respiratory syncytial virus, poliovirus, measles virus, herpes simplex virus, and type 1 poliovirus [11, 12]. However, the precise mechanisms of action of these diarylheptanoids are undefined as are any effects they have on the expression of specific genes.

Over the last 10 years, translatome analyses of eukaryotic cells or tissues have been increasingly used by researchers. The polysome microarray approach, which was originally reported by Zong et al., is the most commonly used method for translatome analysis [13]. With this approach, mRNAs associated with several ribosomes (usually >3) are separated from mRNAs associated with fewer ribosomes; these polysome-associated mRNAs are then used to label probes on microarrays [14]. As genetic information transforms from DNA to protein, the cellular abundance of proteins is predominantly controlled at the level of translation [15]; observed correlations between mRNA levels and respective protein levels are low [16]. Analysis of the translatome,

an intermediate level between the transcriptome and the proteome represented by polysome-associated mRNAs, has provided substantial and somewhat surprising new information [17].

In this study, we used this microarray-based approach to comprehensively identify the polysome-associated mRNAs in a human B lymphoblastoid cell line (BJAB) and to examine changes to this mRNA profile caused by each of the three *A. officinarum* diarylheptanoids.

2. Materials and Methods

2.1. Chemicals. Chemicals were purchased from Wako Pure Chemical Industries, Ltd., Osaka, Japan. AO-0001: (5*R*)-7-(4″-hydroxy-3″-methoxyphenyl)-5-methoxy-1-phenyl-3-heptanone, AO-0002: (5*R*)-5-hydroxy-7-(4″-hydroxy-3″-methoxyphenyl)-1-phenyl-3-heptanone, and AO-0003 : 7-(4″-hydroxy-3″-methxoyphenyl)-1-phenyl-4*E*-hepten-3-one (Figure 1) were isolated from the rhizome of *A. officinarum* as described previously [4]; each was stored as 40 mM stock solution in 100% dimethyl sulfoxide (DMSO) (final concentration of DMSO 0.1%).

2.2. Cell Culture. BJAB cells were grown in Roswell Park Memorial Institute (RPMI) 1640 medium (Sigma), 10% fetal bovine serum (Sigma), 5 μg/mL amphotericin B (Bristol-Myers), and 10 μg/mL gentamicin (Sigma). The cells were maintained at 37°C with 5% CO_2 in a humid environment [18]. Proliferation of the BJAB B-lymphoblastoid cell line is rapidly and almost completely suppressed by picomolar concentrations of the immunosuppressive macrolide rapamycin [19]. This hypersensitivity to rapamycin of BJAB cells might indicate that the canonical translation system in BJAB is highly dependent on mTOR (mammalian target of rapamycin) and is highly activated. Thus, we used BJAB cells.

2.3. Cellular Fractionation and RNA Preparation. Polysome analysis was performed as described previously [18] with slight modifications. Briefly, 40 mL of exponentially growing BJAB cells (0.5×10^6cells/mL) was untreated or was treated with DMSO-only, 40 μM AO-0001, 40 μM AO-0002, or 40 μM AO-0003 for 3 hours. The concentration of each diarylheptanoid used for treatment was determined based on previous findings [2–5]. To prepare cytoplasmic extract for ribosomal fractionation, cells were washed with ice-cold RPMI 1640 medium containing 0.1 mg/mL cycloheximide and collected by centrifugation; each resulting pellet was homogenized with a Teflon pestle in an Eppendorf tube in ice-cold 0.375 mL of low salt buffer (LSB) (0.1 M NaCl, 3 mM $MgCl_2$, 20 mM Tris-HCl [pH 7.6], and 1 mM dithiothreitol). Next, 100 μL of lysis buffer (LSB with 0.2 M sucrose, 1.2% Triton N-101), 15 μL of 5 M NaCl, and 50 μL of 10 mg/mL heparin-Na in LSB were added to each homogenate; each mixture was centrifuged at 10,000 ×g for 5 min to clear the resultant supernatant of nuclei, mitochondria, and debris. Lysate (<0.4 mL) was layered over a 4.5 mL linear sucrose gradient solution (0.5–1.5 M in LSB, prepared by Gradient Master 107, Biocomp) in a 5 mL tube and centrifuged at

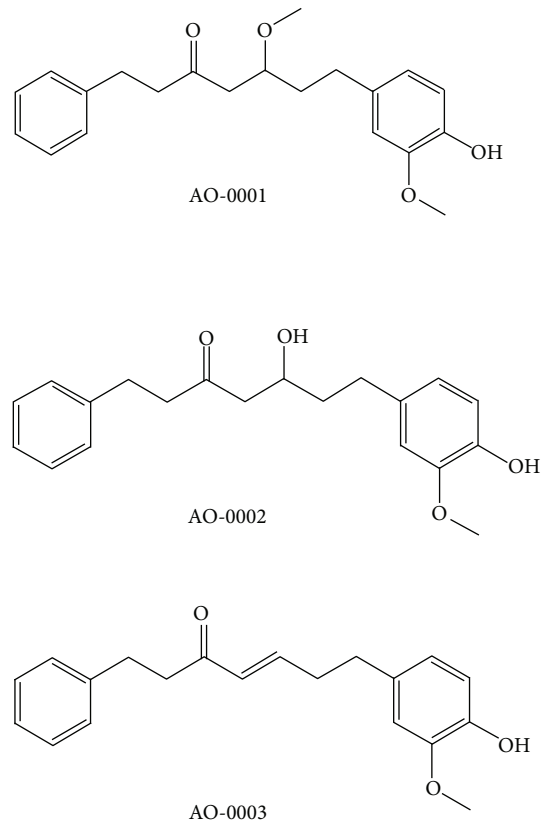

Figure 1: The chemical structures of AO-0001, AO-0002, and AO-0003.

47,000 rpm for 70 minutes at 4°C in Hitachi RPS 55ST rotor. Each gradient was fractioned at a rate of 0.5 mL per minute by upward displacement via a Piston Gradient Fractionator (Biocomp), which was equipped with an absorbance monitor (BioLogic DuoFlow and BioLogic Optics Module II OM-1). Resulting profiles of absorbance at 254 nm are shown in Figure 2. Each fraction was stored at −30°C until use for total RNA extractions [18].

2.4. RNA Preparation for CodeLink Human Whole Genome Bioarray Analysis. The microarray analysis was performed as a trust analysis service at Filgen Incorporation (Nagoya, Japan). The Agilent Bioanalyzer 2100 RNA Nano LabChip (Agilent Technologies) analysis system was used to assess the RNA quality of each experimental sample. Under standard conditions, processing of RNAs used with the CodeLink Human Whole Genome Bioarray (Applied Microarrays, Inc.) was in accordance with methods described in the manufacturer's instructions, as subsequently detailed. MessageAmp II-Biotin Enhanced Kits (Ambion) were used to synthesize 10 μg of biotin-labeled RNA from each experimental sample.

2.5. Microarray Hybridization, Scanning, Normalization, and Annotation. Hybridization was carried out according the instructions supplies with the CodeLink Controls and Buffer Kit (Applied Microarrays, Inc.). For each experimental sample, 10 μg of biotin-labeled material was the nominal

Table 1: Number of transcripts exhibiting altered polysomal loading in BJAB cells following treated with AO-0001, AO-0002, or AO-0003.

	AO-0001		AO-0002		AO-0003		Common Gene
	Probe*	Gene	Probe*	Gene	Probe*	Gene	
Downregulated (ratio ≦ 0.5)	965	634	950	663	900	585	37
Upregulated (ratio ≧ 2)	1308	994	1960	1349	1574	1222	286
Total altered	**2273**	**1628**	**2910**	**2012**	**2474**	**1807**	**323**

*Total of 54359 probes were used.

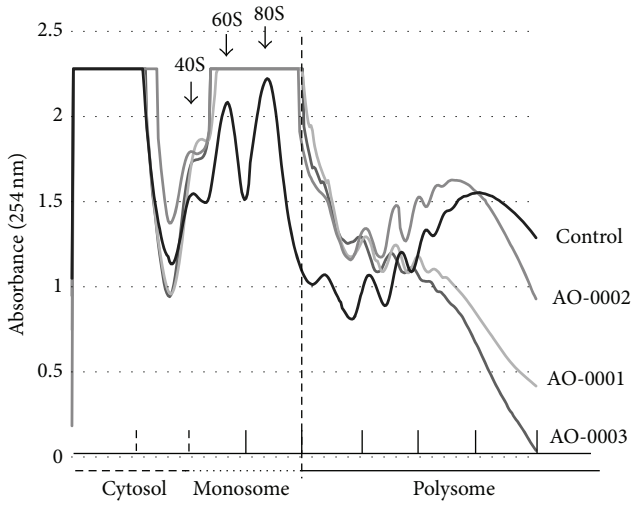

Figure 2: Polysome sedimentation profiles of fractions isolated from control BJAB cells and BJAB cells treated with AO-0001, AO-0002, or AO-0003. The cytosol fraction was layered onto a 0.5 M–1.5 M linear sucrose gradient (prepared by Gradient Master 107, Biocomp) in LSB (20 mM Tris-HCl pH 7.0, 10 mM NaCl, 3 mM $MgCl_2$); the gradient tube was centrifuged at 47,000 rpm in a Hitachi SW55Ti rotor for 70 minutes. A Piston Gradient Fractionator (Biocomp) equipped with an absorbance monitor (254 nm) was used to separate each gradient into nine fractions (0.5 mL/fraction). The absorbance of each 9th fraction (0.5 mL) could not be measured because, in each case, the 9th fraction was retained at the bottom of the ultracentrifuge tube. Positions of ribosomal 40S and 60S subunits and 80S monosomes are indicated by arrows.

amount of material used on the CodeLink Bioarrays. The arrays and labeled material were incubated together at a constant temperature of 37°C overnight. GenePix 4400A (Molecular Devices, Inc.) was used to scan each labeled array. CodeLink Expression Analysis v5.0 (Applied Microarrays, Inc.) software was used for the data analysis. Net intensity was calculated by withdrawing surrounding background of the spot from row intensity. Normalization is performed by adjusting the median of all the read microarray data with a fixed value. Microarray Data Analysis Tool version 3.2 (Filgen, Inc.) was used as described in the manufacturer's instruction for all subsequent data analysis. This software uses pathway information and data from either GenMAPP (http://www.genmapp.org/) or WikiPathways. We used data from the WikiPathways database because it is an open, collaborative platform dedicated to curating biological pathways (http://www.wikipathways.org/index.php/WikiPathways).

3. Results

3.1. Translatome Analysis of Diarylheptanoid-Treated BJAB Cells. To catalogue ribosome loading onto BJAB mRNAs in the presence or absence of diarylheptanoids isolated from *A. officinarum* (Figure 1), we generated polysomal profiles of BJAB cells under each of four conditions (Figure 2). Treatment with AO-0001 or AO-0003 decreased ribosome loading onto mRNAs in BJAB cells. We quantified the fraction of all mRNAs that bound more than 2 ribosomes; we then labeled these polysome-associated mRNAs with biotin and used the labeled mRNAs to label CodeLink Bioarrays. After normalizing net intensity for each probe, sample versus control ratios were calculated for each probe. Probes indicating more than 2-fold upregulation (ratio ≥ 2) or 2-fold downregulation (ratio ≤ 0.5) of the respective transcript or gene are listed in Table 1. The microarray analysis indicated that each of AO-0001, AO-0002, and AO-0003 altered (downregulated or upregulated) polysomal loading of more than 3,000 transcripts/genes (Table 1). Treatment versus control net intensity values were plotted for any transcript that exhibited a normalized net intensity value greater than 40 and that was upregulated (ratio ≥ 2) or downregulated (ratio ≤ 0.5) (Figure 3(a)). Total mRNA isolated from monosome fractions of AO-0003 treated BJAB cells was also used for DNA microarray analysis; these data were processed and are plotted in Figure 3(a). Each of AO-0001, AO-0002, and AO-0003 caused downregulation of 37 genes and upregulation of 286 genes in the treatment versus control normalized net intensity values which were plotted for each of these transcripts. The plots of AO-0001-affected transcripts and AO-0003-affected transcripts were very similar. Each of AO-0001 and AO-0002 caused downregulation of multiple genes encoding proinflammatory mediators [8, 20]; AO-0001 downregulated interleukin 8 (ratio of net intensity; 0.409), interleukin 18 (IL-18) (0.489), macrophage inflammatory protein-1α (0.241), and epidermal growth factor receptor (0.439); AO-0002 downregulated IL-18 (0.487) and macrophage inflammatory protein-1α (0.330). Each of AO-0001, AO-0002, and AO-0003 caused downregulation of the transcription factor notch-1 with the following net intensities, 0.244, 0.450, and 0.418, respectively.

3.2. WikiPathways Analysis. The Microarray Data Analysis Tool version 3.2 (Filgen, Inc.) was used for follow-up pathway analysis. This software uses pathway information that can be taken from either of GenMAPP (http://www.genmapp.org/) or WikiPathways. We chose to use the WikiPathways (http://www.wikipathways.org/index.php/WikiPathways) because it

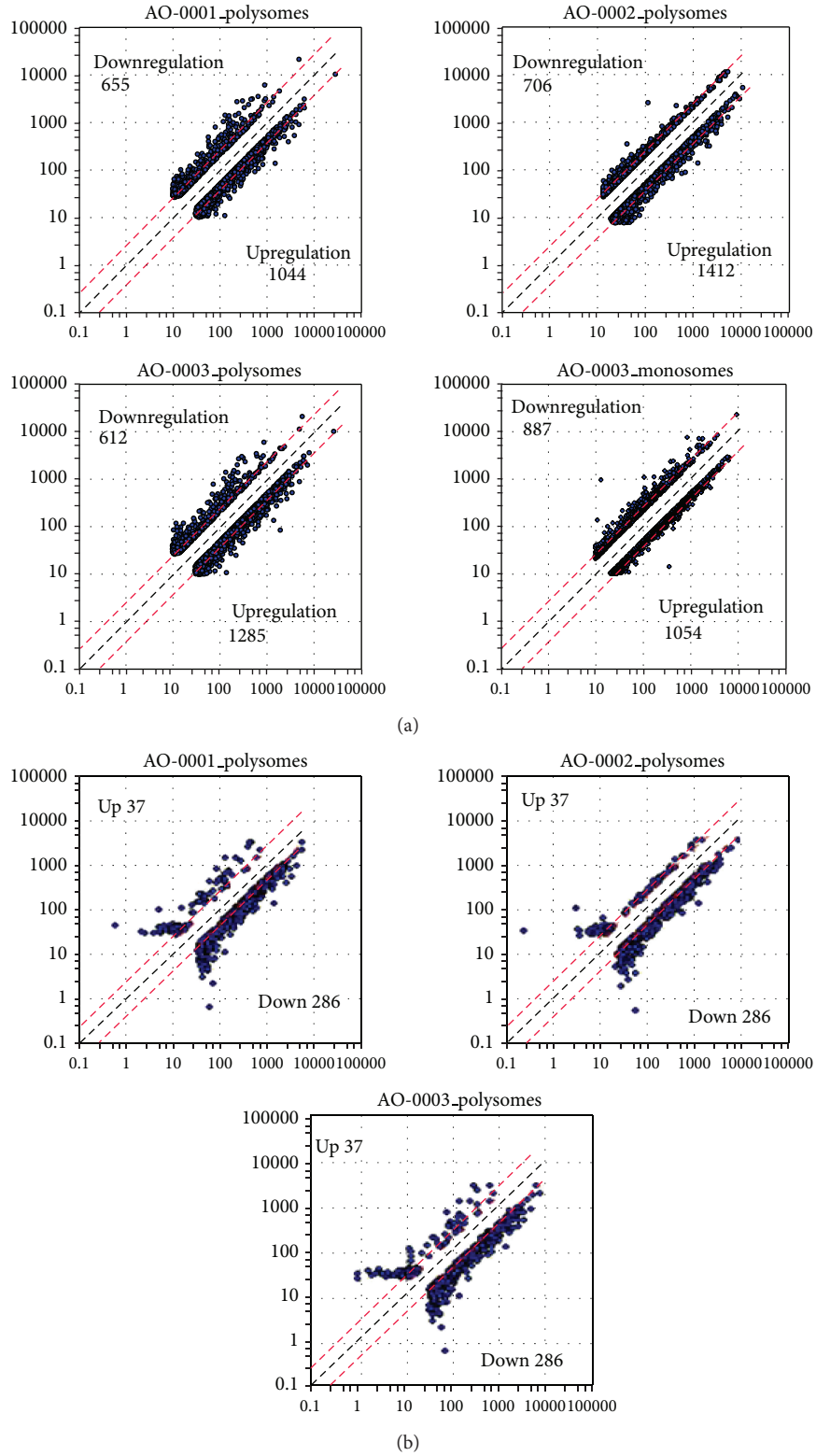

Figure 3: Scatter plot of normalized intensities versus control intensities (a) and of normalized intensities of genes affected by each diarylheptanoid (b). (a) Net intensity for each spot: the net intensity was calculated by subtracting surrounding background intensity, which was derived from row intensity, from the intensity of the respective spot. Normalization was performed by adjusting the median of all the read microarray data relative to a fixed value. After the net intensity of each probe was normalized, a sample versus control ratio was calculated. For those probes with 2-fold upregulation (Ratio ≥ 2) or downregulation (Ratio ≤ 0.5) in treated cells and that exhibited a normalized net intensity of more than 40, the net intensity values were plotted. (b) Normalized net intensity values of genes that were regulated by each diarylheptanoid were potted versus control normalized net intensity values.

Table 2: Number of WikiPathways transcripts that exhibited altered polysomal loading following AO-0001, AO-0002, or AO-0003.

WikiPathways	Total gene no.	AO-0001		AO-0002		AO-0003	
Pathway name		z score	Altered gene number	z score	Altered gene number	z score	Altered gene number
Alanine and aspartate metabolism WP106 41117	12	2.73	4			3.33	5
Apoptosis WP254 41184	79	−2.18	2			−2.45	2
Calcium regulation in the cardiac cell WP536 41204	145					−2.19	8
Cell cycle WP179 45137	72					2.93	16
Diurnally regulated genes with circadian orthologs WP410 41104	42	2.52	9				
DNA replication WP466 41036[*1]	38	3.95	11				13
Glycolysis and gluconeogenesis WP534 41077	45	3.29	11				14
GPCRs, class A rhodopsin-like WP455 41121[*2]	227	−3.40	7	−2.67	13	−3.05	11
MAPK signaling pathway WP382 41048[*3]	153					−2.10	9
mRNA processing WP411 45374[*4]	110	7.40	34	5.54	31	9.80	45
Proteasome degradation WP183 45274	52			3.09	13		
Translation factors WP107 41026	42			3.02	11	3.05	11

WikiPathways transcripts with a P value < 0.5 are listed.
[*1]DNA: deoxyribonucleic acids
[*2]GPCRs: G protein-coupled receptors
[*3]MAPK: mitogen-activated protein kinases
[*4]The following 16 transcripts were each upregulated after treatment with each diarylheptanoid (AO-0001, AO-0002, or AO-0003). CSTF1: cleavage stimulation factor, 3′ pre-RNA, subunit 1, 50 kDa; CSTF3: cleavage stimulation factor, 3′ pre-RNA, subunit 3, 77 kDa; DDX1: DEAD (Asp-Glu-Ala-Asp) box helicase 1; FUS: fused in sarcoma; HNRNPAB: heterogeneous nuclear ribonucleoprotein A/B; HNRNPC: heterogeneous nuclear ribonucleoprotein C (C1/C2); HNRNPK: heterogeneous nuclear ribonucleoprotein K; NONO: non-POU domain containing, octamer-binding; PTBP1: polypyrimidine tract binding protein 1; PRPF40A: PRP40 pre-mRNA processing factor 40 homolog A (S. cerevisiae); PRPF6: PRP6 pre-mRNA processing factor 6 homolog (*S. cerevisiae*); SRSF7: serine/arginine-rich splicing factor 7; SNRNP70: small nuclear ribonucleoprotein 70 kDa (U1); SF3A3: splicing factor 3a, subunit 3, 60 kDa; SF3B2: splicing factor 3b, subunit 2, 145 kDa; U2AF2: U2 small nuclear RNA auxiliary factor 2.

Table 3: Features of 5′ UTRs in transcripts for which AO-0001, AO-0002, and AO-0003 each caused altered polysomal loading.

	Upstream open reading frame		In-frame stop codon		Other features	
	Number of transcripts	% of total	Number of transcripts	% of total	Number of transcripts	% of total
Downregulated (Ratio ≦ 0.5)	5	14%	16	43%	16	43%
Upregulated (Ratio ≧ 2)	41	14%	156	53%	95	33%

is publically available. AO-0001, AO-0002, and AO-0003 altered 7, 4, and 10 (resp.) of the pathways curated in WikiPathways database (Table 2). AO-0001 treatment of BJAB cells altered regulation of diurnally regulated genes with circadian orthologs. AO-0002 altered regulation of genes involved in proteasome degradation. AO-0003 altered regulation of genes involved in calcium regulation in the cardiac cell, cell cycle, mitogen-activated protein kinases (MAPK) signaling, or some combination thereof.

Notably, each diarylheptanoid altered class A rhodopsin-like GPCRs and the mRNA processing pathway (Table 2). Based on the WikiPathways analysis, AO-0001, AO-0002, and AO-0003 affected 35, 34, and 46 (resp.) mRNA processing-related genes; moreover, 16 of these transcripts were upregulated by all three diarylheptanoids.

3.3. Features of 5′ UTRs of Transcripts Regulated by Each Diarylheptanoid, AO-0001, AO-0002, and AO-0003. Different types of *cis*-acting elements encoded in mRNA 5′ untranslated region (5′ UTR) sequences can mediate regulation of translational initiation; such elements include (1) secondary structure that can block a scanning ribosome and thereby inhibit recognition of an AUG initiation codon, (2) IRESs that stimulate cap-independent translation, (3) protein binding sites that either repress or promote translation in response via transacting factors, and (4) upstream AUG codons, in some cases, associated with upstream open reading frames (uORFs) [21]. We analyzed in-frame uORF and terminator codons of the 5′UTR of 329 transcripts that were each regulated by each of the diarylheptanoids, AO-0001, AO-0002, and AO-0003 (Table 3). Of these transcripts, 49 (14%) contained a uORF, and uORFs were present in both down-regulated and upregulated transcripts. Additionally, 53% of the upregulated transcripts each contained an in-frame terminator codons.

Interactions between RNA binding proteins and RNA elements control mRNA translation [22]. To date, at least 25 cellular IRES-containing mRNAs have been identified [23–28]. Among these cellular IRES-containing mRNAs, AO-0001 upregulated the mRNA encoding the insulin receptor

(ratio of net intensity: 2.582), and AO-0002 downregulated the human inhibitor of apoptosis 2 protein transcript (0.448).

4. Discussion

Recently, Tebaldi et al. showed that the analysis of the translatome, an intermediate between the transcriptome and the proteome comprising polysome-associated mRNAs, can provide substantial and somewhat surprising information [17]. Translatome analyses can identify gene ontology (GO) terms within gene sets that represent the transcriptome, translatome, or proteome and then compare between sets with regard to GO term; this approach parses information about cellular components, molecular functions, and biological processes subject to differential regulation at different levels of gene expression [29]. Translatome analysis renders detection of "stress response" and "translation" related genes compared with transcriptome analysis. In this study, 16 transcripts that relate to mRNA processing were identified from the WikiPathways database (Table 2).

Each of AO-0001, AO-0002, and AO-0003 has anti-inflammatory effects and inhibits tumor progression [1, 2]. The dose (μmol/ear) of 50% inhibitory dose of TPA-induced inflammation was AO-0001 < AO-0002 < AO-0003. Notably, the number of downregulated inflammatory related transcripts was greatest with AO-0001; it was fewer with AO-0002 and fewest with AO-0003. Future examination of the relationships between the anti-inflammatory effect of each diarylheptanoid and the resulting corresponding levels of IL-8, IL-18, macrophage inflammatory protein-1 α, notch-1, and epidermal growth factor in vivo is important.

AO-0001 has lower cytotoxic effects on IMR-32 cells than does AO-0003 [3]. AO-0003 had larger effects on the BJAB translatome than did AO-0002, which had a smaller effect at the same concentration (40 μM); however, AO-0002 caused higher upregulation of genes encoding class A rhodopsin-like GPCRs, mRNA processing proteins, and proteasome-related proteins than did AO-0003 (Figure 2, Table 2). Each of AO-0001, AO-0002, and AO-0003 exhibits antimeasles virus activity; however, AO-0001 and AO-0003 do not exhibit anti-respiratory syncytial virus (-RSV) activity [11]. It is possible that some host factors such as splicing factors or heterogeneous nuclear ribonucleoproteins (hnRNPs) listed in Table 2 might affect virus structure and/or replication cycle. Among the proteins encoded by these transcripts, heterogeneous nuclear ribonucleoprotein C (C1/C2), heterogeneous nuclear ribonucleoprotein K, human 55 kDa nuclear matrix protein/octamer-binding non-POU domain containing, and PTB 1 are each identified as an IRES-transacting factor [21]. Overall, our findings provided new insights into the mode of action of diarylheptanoids from *A. officinarum* with regard to anti-inflammatory, antitumor promotion, and antiviral effects.

5. Conclusions

This translatome analysis identified genes that were upregulated or downregulated by 2 h exposure to each of three diarylheptanoids from *A. officinarum*. Notably, genes related to mRNA processing and class A rhodopsin-like GPCRs were upregulated or downregulated by each of the three diarylheptanoids. Based on these findings, we propose that the biological effects of *A. officinarum* diarylheptanoids are mediated via control of expression of specific genes. Translatome analysis might be useful for advancing our understanding of molecular effects of complementary and alternative medicines.

Abbreviations

5′ UTR:	5′ untranslated region
BJAB:	Human B-lymphoblastoma cell line
DMSO:	Dimethyl sulfoxide
DNA:	Deoxyribonucleic acids
GO:	Gene ontology
GPCRs:	G protein-coupled receptors
hnRNPs:	Heterogeneous nuclear ribonucleoproteins
IL-18:	Interleukin 18
IRES:	Internal ribosome entry site
LSB:	Low salt buffer
MAPK:	Mitogen-activated protein kinases
mRNA:	Messenger ribonucleic acid
RPMI medium:	Roswell Park Memorial Institute medium
RSV:	Respiratory syncytial virus
TPA:	12-O-Tetradecanoylphorbol-13-acetate
uORF:	Upstream open reading frame.

Conflict of Interests

The authors declare no financial conflict of interests.

References

[1] K. Yasukawa, Y. Sun, S. Kitanaka, N. Tomizawa, M. Miura, and S. Motohashi, "Inhibitory effect of the rhizomes of *Alpinia officinarum* on TPA-induced inflammation and tumor promotion in two-stage carcinogenesis in mouse skin," *Journal of Natural Medicines*, vol. 62, no. 3, pp. 374–378, 2008.

[2] H. Matsuda, S. Nakashima, Y. Oda, S. Nakamura, and M. Yoshikawa, "Melanogenesis inhibitors from the rhizomes of *Alpinia officinarum* in B16 melanoma cells," *Bioorganic and Medicinal Chemistry*, vol. 17, no. 16, pp. 6048–6053, 2009.

[3] K. Tabata, U. Yamazaki, M. Okada et al., "Diarylheptanoids derived from alpinia officinarum induce apoptosis, S-phase arrest and differentiation in human neuroblastoma cells," *Anticancer Research*, vol. 29, no. 12, pp. 4981–4988, 2009.

[4] Y. Sun, K. Tabata, H. Matsubara, S. Kitanaka, T. Suzuki, and K. Yasukawa, "New cytotoxic diarylheptanoids from the rhizomes of *Alpinia officinarum*," *Planta Medica*, vol. 74, no. 4, pp. 427–431, 2008.

[5] H. J. Lee, J. S. Kim, and J.-H. Ryu, "Suppression of inducible nitric oxide synthase expression by diarylheptanoids from *Alpinia officinarum*," *Planta Medica*, vol. 72, no. 1, pp. 68–71, 2006.

[6] F. Kiuchi, M. Shibuya, and U. Sankawa, "Inhibitors of prostaglandin biosynthesis from *Alpinia officinarum*," *Chemical and Pharmaceutical Bulletin*, vol. 30, no. 6, pp. 2279–2282, 1982.

[7] F. Kiuchi, S. Iwakami, M. Shibuya, F. Hanaoka, and U. Sankawa, "Inhibition of prostaglandin and leukotriene biosynthesis by gingerols and diarylheptanoids," *Chemical and Pharmaceutical Bulletin*, vol. 40, no. 2, pp. 387–391, 1992.

[8] P. N. Yadav, Z. Liu, and M. M. Rafi, "A diarylheptanoid from lesser galangal (*Alpinia officinarum*) inhibits proinflammatory mediators via inhibition of mitogen-activated protein kinase, p44/42, and transcription factor nuclear factor-κB," *The Journal of Pharmacology and Experimental Therapeutics*, vol. 305, no. 3, pp. 925–931, 2003.

[9] R. Sawamura, Y. Sun, K. Yasukawa, T. Shimizu, W. Watanabe, and M. Kurokawa, "Antiviral activities of diarylheptanoids against influenza virus *in vitro*," *Journal of Natural Medicines*, vol. 64, no. 1, pp. 117–120, 2010.

[10] R. Sawamura, T. Shimizu, Y. Sun et al., "*In vitro* and *in vivo* anti-influenza virus activity of diarylheptanoids isolated from *Alpinia officinarum*," *Antiviral Chemistry and Chemotherapy*, vol. 21, no. 1, pp. 33–41, 2010.

[11] K. Konno, R. Sawamura, Y. Sun et al., "Antiviral activities of diarylheptanoids isolated from *Alpinia officinarum* against respiratory syncytial virus, poliovirus, measles virus, and herpes simplex virus type 1 *in vitro*," *Natural Product Communications*, vol. 6, no. 12, pp. 1881–1884, 2011.

[12] K. Konno, M. Miura, M. Toriyama et al., "Antiviral activity of diarylheptanoid stereoisomers against respiratory syncytial virus *in vitro* and *in vivo*," *Journal of Natural Medicines*, vol. 67, no. 4, pp. 773–781, 2013.

[13] Q. Zong, M. Schummer, L. Hood, and D. R. Morris, "Messenger RNA translation state: the second dimension of high-throughput expression screening," *Proceedings of the National Academy of Sciences of the United States of America*, vol. 96, no. 19, pp. 10632–10636, 1999.

[14] O. Larsson, N. Sonenberg, and R. Nadon, "Identification of differential translation in genome wide studies," *Proceedings of the National Academy of Sciences of the United States of America*, vol. 107, no. 50, pp. 21487–21492, 2010.

[15] B. Schwanhüusser, D. Busse, N. Li et al., "Global quantification of mammalian gene expression control," *Nature*, vol. 473, no. 7347, pp. 337–342, 2011.

[16] C. Vogel and E. M. Marcotte, "Insights into the regulation of protein abundance from proteomic and transcriptomic analyses," *Nature Reviews Genetics*, vol. 13, no. 4, pp. 227–232, 2012.

[17] T. Tebaldi, A. Re, G. Viero et al., "Widespread uncoupling between transcriptome and translatome variations after a stimulus in mammalian cells," *BMC Genomics*, vol. 13, no. 1, article 220, 2012.

[18] T. Kakegawa, N. Ohuchi, A. Hayakawa et al., "Identification of AUF1 as a rapamycin-responsive binding protein to the 5′-terminal oligopyrimidine element of mRNAs," *Archives of Biochemistry and Biophysics*, vol. 465, no. 1, pp. 274–281, 2007.

[19] J. E. Kay, M. C. Smith, V. Frost, and G. Y. Morgan, "Hypersensitivity to rapamycin of BJAB B lymphoblastoid cells," *Immunology*, vol. 87, no. 3, pp. 390–395, 1996.

[20] S. Shishodia, "Molecular mechanisms of curcumin action: gene expression," *BioFactors*, vol. 39, no. 1, pp. 37–55, 2013.

[21] C. Barbosa, I. Peixeiro, and L. Romão, "Gene expression regulation by upstream open reading frames and human disease," *PLoS Genetics*, vol. 9, no. 8, Article ID e1003529, 2013.

[22] X. Pichon, L. A. Wilson, M. Stoneley et al., "RNA binding protein/RNA element interactions and the control of translation," *Current Protein and Peptide Science*, vol. 13, no. 4, pp. 294–304, 2012.

[23] C. P. Chan, K. H. Kok, H. V. Tang, C. M. Wong, and D. Y. Jin, "Internal ribosome entry site-mediated translational regulation of ATF4 splice variant in mammalian unfolded protein response," *Biochimica et Biophysica Acta*, vol. 1833, no. 10, pp. 2165–2175, 2013.

[24] K. W. Sherrill, M. P. Byrd, M. E. van Eden, and R. E. Lloyd, "BCL-2 translation is mediated via internal ribosome entry during cell stress," *The Journal of Biological Chemistry*, vol. 279, no. 28, pp. 29066–29074, 2004.

[25] D. Warnakulasuriyarachchi, S. Cerquozzi, H. H. Cheung, and M. Holcík, "Translational induction of the inhibitor of apoptosis protein HIAP2 during endoplasmic reticulum stress attenuates cell death and is mediated via an inducible internal ribosome entry site element," *The Journal of Biological Chemistry*, vol. 279, no. 17, pp. 17148–17157, 2004.

[26] K. A. Spriggs, L. C. Cobbold, S. H. Ridley et al., "The human insulin receptor mRNA contains a functional internal ribosome entry segment," *Nucleic Acids Research*, vol. 37, no. 17, pp. 5881–5893, 2009.

[27] S. Vagner, M. C. Gensac, A. Maret et al., "Alternative translation of human fibroblast growth factor 2 mRNA occurs by internal entry of ribosomes," *Molecular and Cellular Biology*, vol. 15, no. 1, pp. 35–44, 1995.

[28] K. J. D. Lang, A. Kappel, and G. J. Goodall, "Hypoxia-inducible factor-1α mRNA contains an internal ribosome entry site that allows efficient translation during normoxia and hypoxia," *Molecular Biology of the Cell*, vol. 13, no. 5, pp. 1792–1801, 2002.

[29] T. Tebaldi, E. Dassi, G. Kostoska, G. Viero, and I. A. Quattrone, "tRanslatome: an R/Bioconductor package to portray translational control," *Bioinformatics*, vol. 30, no. 2, pp. 289–291, 2014.

Hindawi Publishing Corporation
Evidence-Based Complementary and Alternative Medicine
Volume 2014, Article ID 769515, 9 pages
http://dx.doi.org/10.1155/2014/769515

Research Article

Apocynum Tablet Protects against Cardiac Hypertrophy via Inhibiting AKT and ERK1/2 Phosphorylation after Pressure Overload

Jianyong Qi,[1] Qin Liu,[1] Kaizheng Gong,[2] Juan Yu,[3] Lei Wang,[1] Liheng Guo,[1] Miao Zhou,[4] Jiashin Wu,[5] and Minzhou Zhang[1]

[1] *Intensive Care Laboratory, Guangdong Province Hospital of Chinese Medicine, 2nd Affiliated Hospital of Guangzhou University of Chinese Medicine, 101 Dade Road, Yuexiu District, Guangzhou 510120, China*
[2] *Department of Cardiology, The Second Clinical Medical School, Yangzhou University, Yangzhou 225001, China*
[3] *Animal Laboratory, Guangdong Province Hospital of Chinese Medicine, 2nd Affiliated Hospital of Guangzhou University of Chinese Medicine, Guangzhou 510120, China*
[4] *Department of Oral and Maxillary Surgery, Stomatology Hospital of Guangzhou Medical University, Guangzhou 510140, China*
[5] *Department of Pharmaceutical Sciences, College of Pharmacy, Northeast Ohio Medical University, Rootstown, OH 44272, USA*

Correspondence should be addressed to Minzhou Zhang; minzhouzhang8@163.com

Received 10 April 2014; Revised 28 May 2014; Accepted 4 June 2014; Published 29 June 2014

Academic Editor: Ping Liu

Background. Cardiac hypertrophy occurs in many cardiovascular diseases. Apocynum tablet (AT), a traditional Chinese medicine, has been widely used in China to treat patients with hypertension. However, the underlying molecular mechanisms of AT on the hypertension-induced cardiac hypertrophy remain elusive. The current study evaluated the effect and mechanisms of AT on cardiac hypertrophy. *Methods*. We created a mouse model of cardiac hypertrophy by inducing pressure overload with surgery of transverse aortic constriction (TAC) and then explored the effect of AT on the development of cardiac hypertrophy using 46 mice in 4 study groups (combinations of AT and TAC). In addition, we evaluated the signaling pathway of phosphorylation of ERK1/2, AKT, and protein expression of GATA4 in the cardioprotective effects of AT using Western blot. *Results*. AT inhibited the phosphorylation of Thr202/Tyr204 sites of ERK1/2, Ser473 site of AKT, and protein expression of GATA4 and significantly inhibited cardiac hypertrophy and cardiac fibrosis at 2 weeks after TAC surgery ($P < 0.05$). *Conclusions*. We experimentally demonstrated that AT inhibits cardiac hypertrophy via suppressing phosphorylation of ERK1/2 and AKT.

1. Introduction

Cardiac hypertrophy occurs in many heart diseases (e.g., essential hypertension, myocardial infarction, and valvular diseases). Characterized by an increase in the size of cardiac myocytes and whole heart enlargement, cardiac hypertrophy is an adaptive reaction in response to increased pressure overload. Sustained after-overload usually induces an initial compensatory hypertrophy, which can progress to pathologic cardiac hypertrophy and finally to congestive heart failure [1]. Overpressure is a major initiative stimulus triggering protein synthesis, gene expression reprogramming, and activation of various signaling molecules, such as protein kinase C (PKC) pathway, the mitogen-activated protein kinases (MAPK) pathway, and the phosphatidylinositol 3-kinase (PI3-K)/Akt pathway, and, thus, subsequently modifies transcriptional regulatory factors (GATA4) and resulting in cardiac hypertrophy [2–4].

Apocynum tablet (AT, Guangdong Peace Pharmaceutical Corp, Guangdong, China), a traditional Chinese medicine formulated mainly with following herbs: *Apocynum, Chrysanthemum,* and *Fangchi*, has been widely used in China to treat patients with hypertension [5]. Clinical trials demonstrated that apocynum tablet is effective and safe for treating hypertension [6, 7]. However, the underlying molecular mechanisms of AT on the hypertension-induced

cardiac hypertrophy remain elusive. The current study evaluated a hypothesis that AT can protect hypertension patients from cardiac hypertrophy by inhibiting phosphorylation of ERK1/2 and AKT. To evaluate this hypothesis, we compared cardiac hypertrophy and phosphorylation of ERK1/2 and AKT between mouse models of hypertension with and without pretreatment of AT.

2. Methods

2.1. Animals and Reagents. This study was performed in accordance with the guidelines and with approval from the Institutional Animal Care and Use Committee of Guangdong Province Hospital of Chinese Medicine, Guangzhou University of Traditional Chinese Medicine, and with the Guide for the Care and Use of Laboratory Animals published by the National Academy of Sciences (8th edition, Washington, DC, 2011).

2.2. Transverse Aortic Constriction. To explore the effects of AT in cardiac hypertrophy, we constructed a cardiac hypertrophy model by using transverse aortic constriction (TAC) surgery to impose pressure overload in mice using similar protocol as was published previously [8, 9]. In brief, increased pressure in the transverse thoracic aorta was induced by means of TAC (Figures 1(a) and 1(b)). Male mice (C57BL/6J, 8 to 10 weeks old, 25 ± 5 g body weight, from the Experimental Animal Center of Guangdong Province) were anesthetized with pentobarbital sodium (60 mg/kg IP, Sigma-Aldrich Corp). The mice were orally intubated with 20-gauge tubing and ventilated (Harvard Apparatus Rodent Ventilator, model 687) at 110 breaths per minute (0.2 mL tidal volume). A 3 mm center thoracotomy was created. The transverse aortic arch was ligated (7–0 Prolene) between the innominate and left common carotid arteries with an overlying 28-gauge needle, and then the needle was removed, leaving a discrete region of stenosis. The chest was closed, and the pneumothorax was evacuated. Some mice were subjected to a sham operation in which the aortic arch was visualized but not banded.

2.3. Protocol. Based on literature, clinical usage (a 70 Kg person taking 2 AT pills each time, three times a day, each tablet weighs 0.6 g), and the Meeh-Rubner equation of dose conversion between humans and mice, human dosage of AT (0.51 g/kg/day) equals 0.67 g/kg/day for mouse. We choose 0.6 g/kg dosage for mice by intragastric administration (i.g) daily. Mice were assigned to four groups: NS-SHAM group, NS-TAC group, AT-SHAM group, and AT-TAC group. Mice in NS-SHAM received saline i.g and all the surgery except constricting the aorta; mice in NS-TAC were subjected to saline i.g and TAC surgery; AT-SHAM mice received AT i.g and all the surgery except constricting the aorta; AT-TAC mice received AT i.g and TAC surgery.

2.4. HW Assessment and Histological Examination. At the completion of the experiment, animals were euthanized and their hearts were removed, the left ventricle was quickly separated from the atria and right ventricular free wall, and their heart [left ventricle + right ventricle] weights (HW) and body weights (BW) were determined. Then, left ventricles were fixed overnight in 4% paraformaldehyde before embedding in paraffin. Sections of 5 μm were prepared and stained with hematoxylin-eosin (HE) or Sirius red for evaluation of myocyte hypertrophy and collagen content, respectively.

Cardiomyocytes from LV cross sections were stained with hematoxylin-eosin, and mean values from each mouse were calculated by measurements from 60 to 80 cells from an individual mouse using light microscopy at ×400 magnification. Sirus-stained sections were quantitatively analyzed using light microscopy at ×40 magnification to evaluate myocardial fibrosis using the difference in color (red fibrotic area as opposed to yellow myocardium). Digital photographs were obtained by using a color image analyzer (QWin Colour Binary 1, LEICA).

2.5. Western Blot Analysis. Western blot was performed as previously described [10]. Briefly, samples were lysed in 100 μL buffer containing 20 mM Tris-HCl (pH 7.4), 100 mM NaCl, 10 mM sodium pyrophosphate, 5 mM EDTA, 50 mM NaF, 1 mM sodium vanadate, 0.1% SDS, 10% glycerol, 1% Triton X-100, 1% sodium deoxycholate, 1 mM leupeptin, 0.1 mM aprotinin, and 1 mM PMSF. Protein concentration was determined with a BCA protein assay kit (Pierce Biotechnology, Inc, Rockford, IL, USA), and proteins were separated on a 10% SDS-polyacrylamide gel and then electrophoretically transferred to nitrocellulose membranes (Pall Corporation, East Hill, NY, USA). Results are expressed as the changes over control (Con) or sham (SHAM of TAC group). Following antibodies were used in this study: anti-phospho-ERK1/2 (Thr202/Tyr204, Cell Signaling Technology, Beverly, MA, USA), anti-phospho-PKB (Ser473, Cell Signaling Technology), anti-ERK1/2 (Santa Cruz Technology, Delaware, CA, USA), and anti-GATA4 (Selleckchem Technology, Houston, TX, USA). The sheets were analyzed with antibodies according to the supplier's protocol and visualized peroxidase using an enhanced-chemiluminescence system (ECL kit, Pierce Biotechnology, Inc.). Bands were visualized by use of a super western sensitivity chemiluminescence detection system (Pierce, IL). Autoradiographs were quantitated by a densitometry Science Imaging system (Bio-Rad, Hercules, CA).

2.6. Statistical Analysis. Data are presented as mean ± SEM. Statistical analysis was performed by one-way analysis of variance followed by Turkey's method or unpaired two-tailed Student's t-tests. Results were considered statistically significant at $P < 0.05$.

3. Results

3.1. AT Inhibited Cardiac Hypertrophy in Response to Pressure Overload. There were no significant differences in body weight among the four groups of mice ($P > 0.05$, Table 1). At the end of 2 weeks after surgery, cardiomyocytes were much bigger in NS-TAC than NS-SHAM mice (377.8 ± 29.2 μm^2

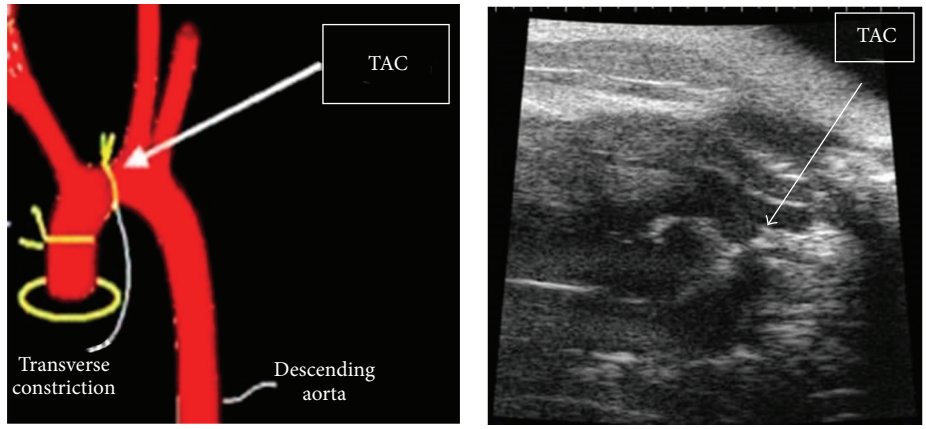

Figure 1: Schematic diagram (a) and echocardiography (b) of TAC surgery.

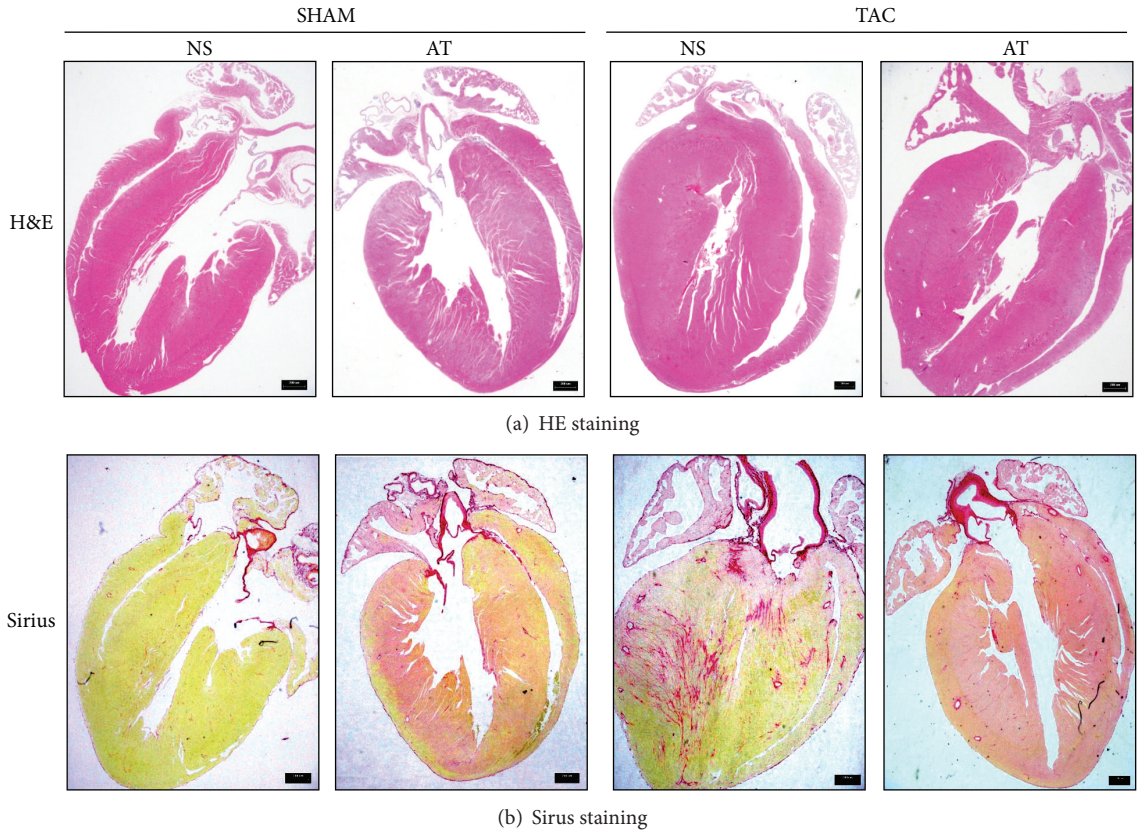

Figure 2: Dye-stained hypertrophic heart sections. (a) H&E-stained (upper) and (b) Sirius red-stained (lower) sections of representative hearts from NS and AT mice 14 days after either SHAM or TAC surgery. Scale at bottom is in mm.

versus $170.8 \pm 7.8\,\mu m^2$, $P < 0.001$, Figures 2(a), 3(a) and 3(b)). Also cardiac fibrosis formed much more in the NS-TAC mice than in the NS-SHAM mice ($9.84 \pm 0.42\%$ versus $2.10 \pm 0.82\%$, $P < 0.001$, Figures 2(b) and 3(c)). Heart weights (HW) were significantly heavier in the NS-TAC mice than NS-SHAM mice (HW, 151.2 ± 5.7 mg versus 128.6 ± 3.7 mg, $P < 0.001$, Figure 4(a)). The ratio of left ventricular weight (LVW) to tibal length (TL) was higher in the NS-TAC mice than in the NS-SHAM mice (6.1 ± 0.5 versus 4.5 ± 0.2, $P < 0.01$, Figure 4(c)). However, the ratios of lung weight to body weight (BW) differed insignificantly among the four groups ($P > 0.05$, Figure 4(d)). Therefore, these results showed that compensate pathological cardiac hypertrophy, but not decompensate heart failure, was formed after TAC surgery. Subsequently, we compared the effects between NS-TAC mice and AT-TAC mice. As shown in Figure 4, HW and LVW/TL

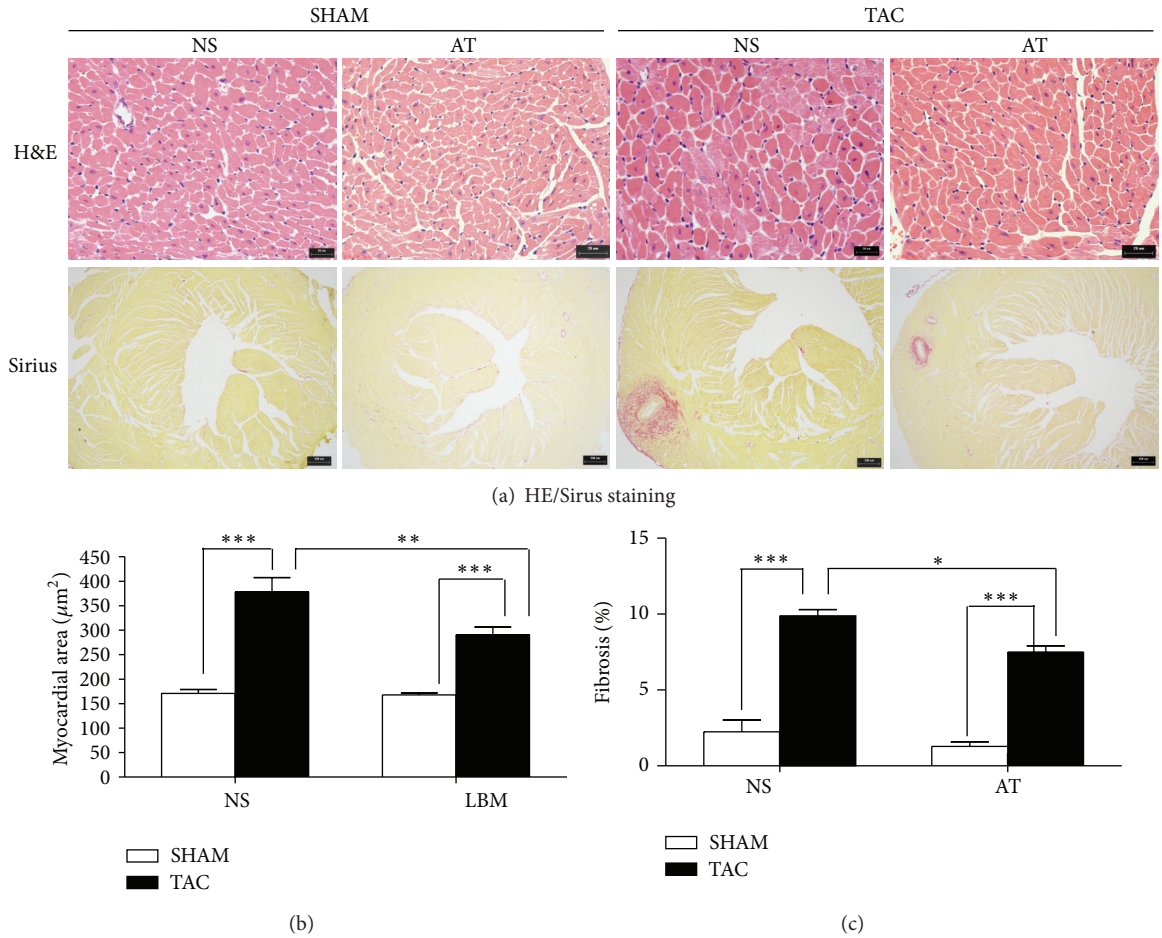

FIGURE 3: Histological sections of the left ventricular (LV) wall (Groups: NS-SHAM, NS-TAC, AT-SHAN and AT-TAC mice). (a) The LV cross sections of the four groups stained with H&E (×400 magnification, Scale bar, 20 μm) and Sirius red (red staining, ×40 magnifications, Scale bar, 200 μm). (b) Mean cross-sectional area of cardiomyocytes and (c) the fraction of fibrotic area. $^{*}P < 0.05$, $^{**}P < 0.01$, and $^{***}P < 0.001$, comparison among the groups.

TABLE 1: Anatomical data of the four groups.

Group	NS-SHAM ($n = 6$)	NS-TAC ($n = 15$)	LBM-SHAM ($n = 9$)	LBM-TAC ($n = 16$)
BW, g	23 ± 0.3	23 ± 0.4	22 ± 0.3	23 ± 0.2
HW, mg	116.5 ± 3.8	151.2 ± 5.7***	106.6 ± 4.0	128.6 ± 3.7$^{*\#\#}$
LVW, mg	78.7 ± 3.9	104.5 ± 8.9**	57.7 ± 9.5	92.4 ± 2.9$^{**\#}$
Lung, mg	135.7 ± 3.2	147.9 ± 8.7	167.7 ± 10.4	154.6 ± 5.8
Liver, mg	876.0 ± 17.5	1054.6 ± 47.1	948.5 ± 51.7	980.4 ± 33.5
TL, mm	17.4 ± 0.2	17.3 ± 0.1	17.1 ± 0.1	17.1 ± 0.1
HW/BW	5.1 ± 0.2	6.5 ± 0.3**	4.8 ± 0.1	5.6 ± 0.1$^{\#}$
HW/TL	6.7 ± 0.2	8.8 ± 0.3***	6.2 ± 0.2	7.5 ± 0.2$^{*\#\#}$
LVW/TL	4.5 ± 0.2	6.1 ± 0.5**	3.4 ± 0.6	5.4 ± 0.2$^{**\#}$
Lung/BW	5.9 ± 0.1	6.4 ± 0.5	7.6 ± 0.6	6.7 ± 0.3
Liver/BW	38.4 ± 0.6	48.9 ± 2.4	42.3 ± 1.7	42.5 ± 1.5

NS: saline; AT: apocynum tablets; TAC: transverse aortic constriction; BW: body weight; HW: heart weight; LVW: left ventricular weight; TL: tibial length; $^{*}P < 0.05$, $^{**}P < 0.01$, and $^{***}P < 0.001$ compared to NS-SHAM or AT-SHAM from the same group. $^{\#}P < 0.05$, $^{\#\#}P < 0.01$, compared to AT-TAC from NS-TAC group.

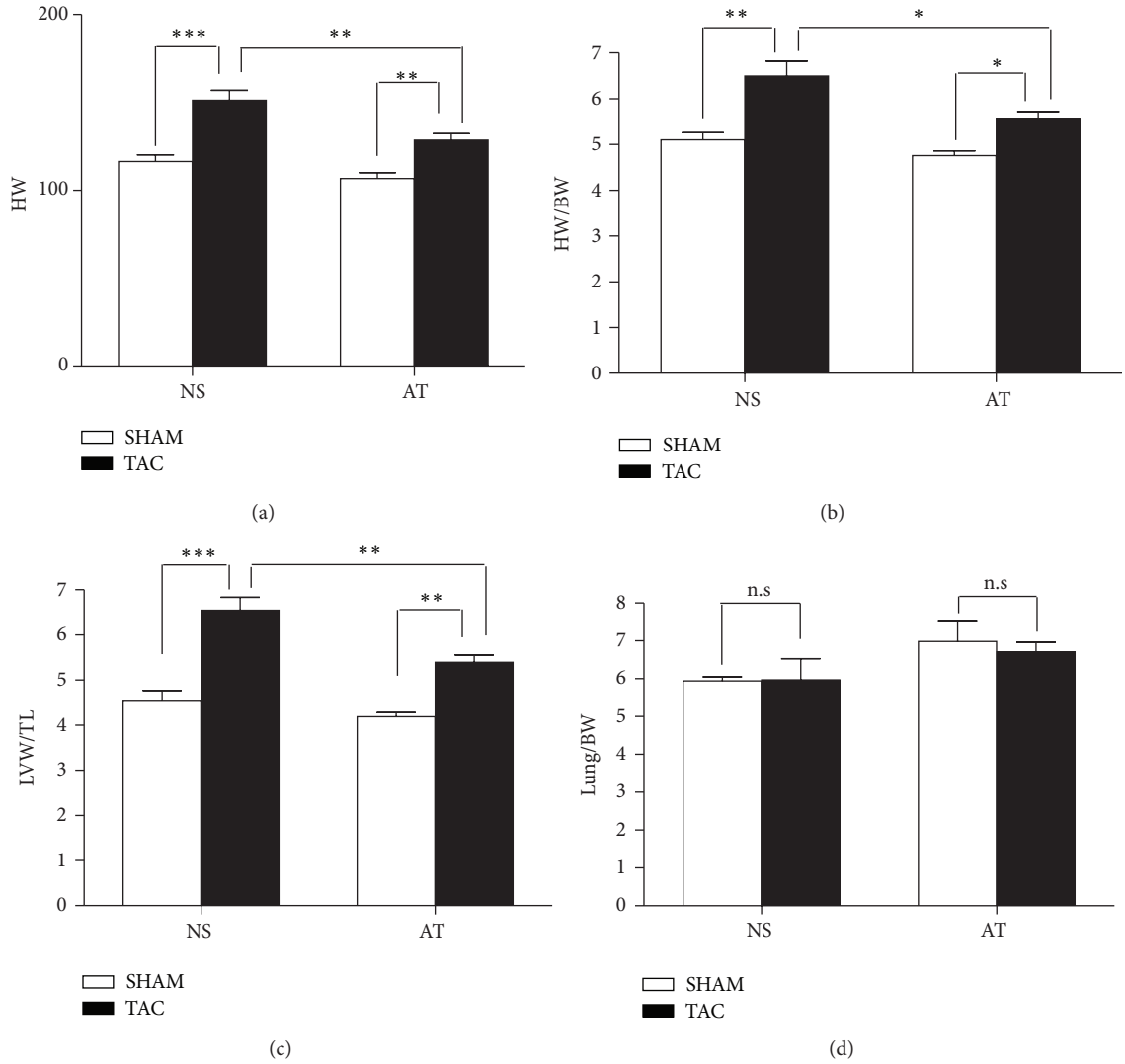

Figure 4: Differences among the four groups. (a) HW, (b) HW/BW, (c) LVW/TL, (d) Lung/BW were compared among the four groups (NS-SHAM, NS-TAC, AT-SHAN, and AT-TAC mice). $^{*}P < 0.05$, $^{**}P < 0.01$, and $^{***}P < 0.001$; n.s.: no significance.

were significantly lower in AT-TAC (HW, 128.6 ± 3.7 mg; LVW/TL, 5.4 ± 0.2, resp.) than NS-TAC mice (HW, 151.2 ± 5.7 mg, $P < 0.001$; LVW/TL, 6.1 ± 0.5, $P < 0.001$, resp., Figure 4(c)). Together, these date demonstrated that AT could inhibit cardiac hypertrophy in response to pressure overload.

3.2. AT Decreased the Mortality in Response to Pressure Overload. Recent clinical data have demonstrated that AT drastically improved cardiac function, structure, and quality of life in hypertension patients [11]. One critical question arising from the observation that AT prevented hypertrophy in the TAC mice is whether it has a beneficial or harmful impact on animal survival. To investigate this, we evaluated the effects of AT on post-TAC survival by analyzing Kaplan-Meier curves in the four groups of mice. We found that the survival rate was significantly higher in the AT-TAC mice than the NS-TAC mice (Figure 5). AT-TAC mice displayed a significantly improved survival compared to NS-TAC mice (Figure 5), whereas NS-TAC mice had 87% survival ($n = 31$) 2 weeks after TAC, AT-TAC mice had 96% survival ($n = 28$; $P < 0.001$). AT-SHAM and NS-SHAM mice that underwent sham surgery, which included thoracotomy but no constriction of the aorta, had 100% survival for both AT-SHAM and NS-SHAM groups (Figure 5). Thus, AT significantly improved mice survival after TAC surgery in response to pressure overload.

3.3. Phosphorylation of ERK1/2 and AKT Were Inhibited after AT Stimulation. To investigate the mechanisms of AT inhibition on cardiac hypertrophy in response to pressure overload, we focused on MAPK and AKT, which are two main signal transduction pathways involved in cardiac hypertrophy [12]. By using Western blot analysis, we found that the ERK1/2 phosphorylations of threonines at 202th and 204th sites were enhanced in NS-TAC group, compared with NS-SHAM group ($P < 0.05$, Figures 6(a) and 6(c)). Interestingly,

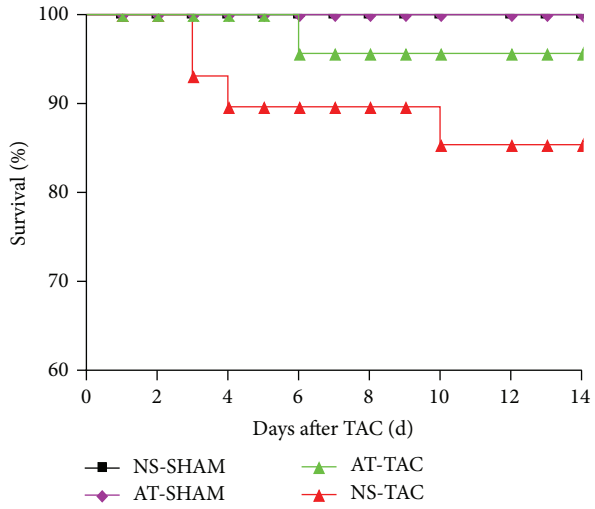

Figure 5: Kaplan-Meier survival curves of NS-SHAM, AT-SHAM, AT-TAC, and NS-TAC mice.

the phosphorylations of threonines at 202th and 204th sites were reduced after AT stimulation in AT-TAC group, compared with NS-TAC group. Thus, these data revealed that AT reversed TAC-induced cardiac hypertrophy through the ERK1/2 phosphorylations of threonines at 202th and 204th sites. Moreover, we detected that the AKT phosphorylation of tyrosine at 473th site, which was increased in NS-TAC group ($P < 0.05$, versus NS-SHAM groups, Figures 6(b) and 6(d)), but decreased after AT stimulation in AT-TAC group. Together, these data revealed that AT reversed TAC-induced cardiac hypertrophy via suppressing the ERK1/2 phosphorylations of threonines at 202th and 204th sites and AKT phosphorylation of tyrosine at 473th site.

3.4. The Protein Expression of GATA4 Was Reduced after AT Treatment in Mice. To further investigate the potential role of the ERK1/2 and AKT pathway in the hypertrophic-inhibiting effect of AT in TAC, we analyzed a typical downstream target, GATA4. GATA4 is a zinc finger, containing transcription factor that plays key roles in promoting heart growth and regulating cardiac hypertrophy [13, 14], and is associated with multiple hypertrophic signaling pathways, such as ERK1/2 [15], p38, Akt [16], and CnA/NFATc3 [17]. As shown in Figure 7, protein expression of GATA4 in the NS-TAC group was significantly increased compared with NS-SHAM group ($P < 0.05$), in consistence with literature [18, 19]. However, after AT stimulation, the protein expression of GATA4 was reduced in AT-TAC mice, compared with NS-TAC group ($P < 0.05$, Figures 7(a) and 7(b)), which was also consistent with the changes in ERK and AKT. Thus, these data revealed that AT reversed TAC-induced cardiac hypertrophy through the protein expression of GATA4.

We formulated a working model based on the observations of this study (Figure 8). Stress overload of TAC could activate the phosphorylation of the protein kinases of ERK1/2 and AKT, enhance the expression of GATA4, promote the transcription of hypertrophic gene, and result in cardiac hypertrophy and fibrosis. AT could inhibit the phosphorylation of ERK1/2 and AKT, reduce GATA4, and inhibit pathological development of cardiac hypertrophy.

4. Discussion

This study illustrated the mechanism of AT protection against pathological cardiac hypertrophy in mice. Our results can be summarized as follows: (1) AT could attenuate cardiac hypertrophy and cardiac fibrosis in response to pressure overload in vivo; (2) the effects of AT could be mediated by mitogen-activated protein kinase 1/2 signaling pathway; (3) AKT signaling pathway also participated in the protective role of AT on pathological cardiac hypertrophy; and (4) GATA4 was also reduced after AT stimulation in response to TAC. To our knowledge, this is the first study to demonstrate the effectiveness and mechanism of AT in reducing pathological cardiac hypertrophy in response to pressure overload in mice.

Clinical studies revealed that systolic and diastolic blood pressure in hypertension patients were reduced more significantly by treatments with apocynum tablets than with nifedipine alone. Apocynum tablet in combination with nifedipine had a stable antihypertensive effect [6, 7]. Apocynum leaves, which are a major ingredient of apocynum tablets, contain three main active compounds: quercetin, flavonoids, and carbohydrates [5]. Quercetin could enhance capillary resistance, reduce capillary fragility, lower blood pressure, dilate coronary artery, and enhance coronary blood flow [20]. Another major ingredient of AT, chrysanthemum, could increase cardiac output and stroke volume and slowly and persistently decrease blood pressure [21]. The current study further advanced our knowledge by demonstrating AT treatment could prevent the development of pathological cardiac hypertrophy.

Cardiac hypertrophy is regulated by a network of signaling pathways, including beta-adrenergic receptor signaling and associated kinases, PKC-alpha, Ca^{2+}/calmodulin-dependent kinase II signaling, Phosphodiesterase 5, MAPKs, HDAC, PI3-K/AKT, and GATA4 [22]. Previous studies demonstrated that cardiac hypertrophy is mediated by a PI3-K/AKT and ERK1/2 pathway, which can be pharmacological targets for cardioprotection [23, 24]. Considering there is still no effective Chinese medicine to treat cardiac hypertrophy, we did not set the positive control of Chinese medicine and different AT dosages. The present study demonstrated that AT significantly decreased cardiac hypertrophy and suppressed the increases of phosphorylation of Akt and ERK1/2 following the TAC surgery in mice.

The zinc-finger containing transcription factor GATA4 has been ascribed to a number of critical functions in the heart, spanning from the specification and differentiation of cardiac myocytes early in development to the regulation of the cardiac hypertrophic response in the adult. GATA4 mediates these processes through directly binding to the promoters of the ANF, BNP, alpha-MHC, and beta-MHC genes, thereby controlling their expression in the heart [25]. Overexpression of GATA4 by adenoviral gene transfer

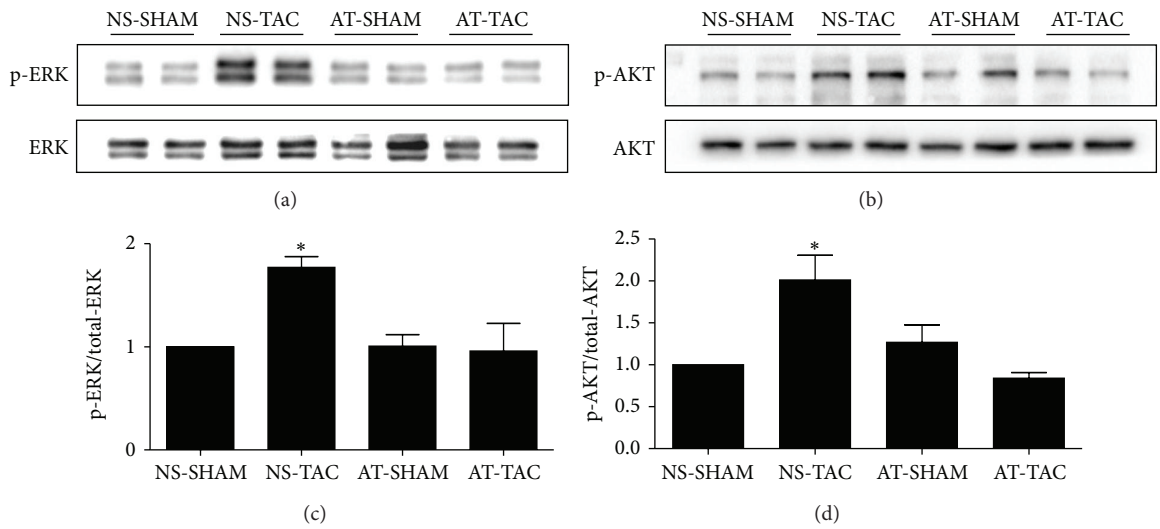

Figure 6: AT inhibited the phosphorylation of ERK1/2 and AKT in response to TAC. (a) Phosphorylated (p)-Thr202/204 extracellular signal-regulated kinase (ERK) 1/2 and (b) p-Ser473 protein kinase B (AKT), and quantified data for (c) p-ERK1/2 and for (d) p-AKT. Data (mean ± SEM, $n = 3$) were expressed as fold changes from total protein (ERK1/2, AKT) and control (NS-SHAM). $^{*}P < 0.05$ study group versus NS-SHAM group.

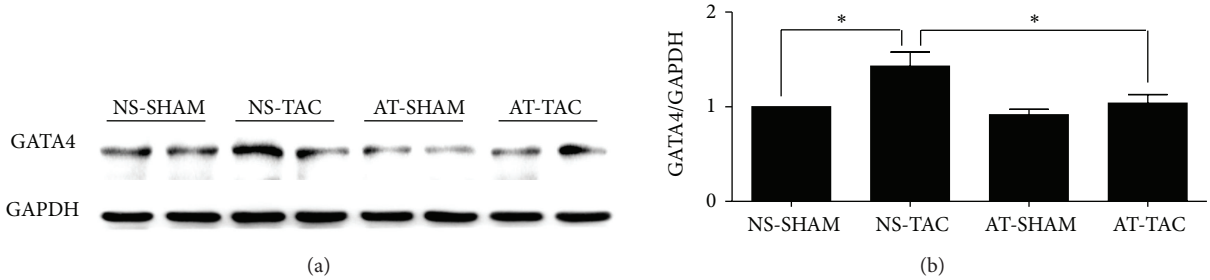

Figure 7: The protein expression of GATA4 was reduced after AT treatment in mice. (a) Western blot bands of the protein expression of GATA4 and GAPDH and (b) their fold changes in the four groups (NS-SHAM, NS-TAC, AT-SHAM, and AT-TAC). Data are mean ± SEM ($n = 7$). $^{*}P < 0.05$ NS-TAC versus NS-SHAM and AT-TAC groups.

induced cardiomyocyte hypertrophy [26]. Cardiac specific knockout of GATA4 in adult mouse renders the heart less able to hypertrophy with agonist or pressure overload stimulation, as well as more likely to succumb to heart failure [27]. Both ERK1/2 and AKT activity were necessary for the increase in GATA4 DNA binding from hearts underwent acute wall stretching [28]. Here we demonstrated that GATA4 expression was reduced after AT treatment in response to pressure overload. Together, our findings contribute to further understanding the molecular mechanisms of cardiac protection of AT.

Although there are several cardioprotective drugs for treating heart failure and cardiac hypertrophy, such as beta-adrenergic receptor blocker, ACE inhibitor, and calcium channel blockers, the mobility and mortality of heart failure and cardiac hypertrophy were still high in the United States [29]. These inadequate results could be due to the presence of multiple mechanistic pathways of cardiac hypertrophy and the lack of therapies targeting these pathways simultaneously. Increasing evidences demonstrated that there are several bioactive ingredients contributing to AT's cardioprotection effects against cardiac hypertrophy, such as apocynum leaves and wild chrysanthemum [30, 31]. The complex profile of active ingredients in AT could act on multiple signaling pathways, which might possibly overcome the deficiencies of these single-target drugs in protecting against cardiac hypertrophy.

We used 28 G needle to construct the TAC model in the current study. This method reliably produced a model of cardiac hypertrophy 2 weeks after TAC surgery (Figure 2). Our preliminary study showed that we produced stable aortic pressure gradient (AoPg) waved in 70–90 mmHg after TAC surgery for 1 week (data not shown), in consistence with a report from Vatner's laboratory [9].

In conclusion, the present results enhanced our understanding of the role of AT on cardiac hypertrophy. We demonstrated that selective ERK1/2 and AKT modulation for cardioprotection is feasible, suggesting their possibilities to be therapeutic targets. These data experimentally provided evidences that AT inhibits cardiac hypertrophy from pressure

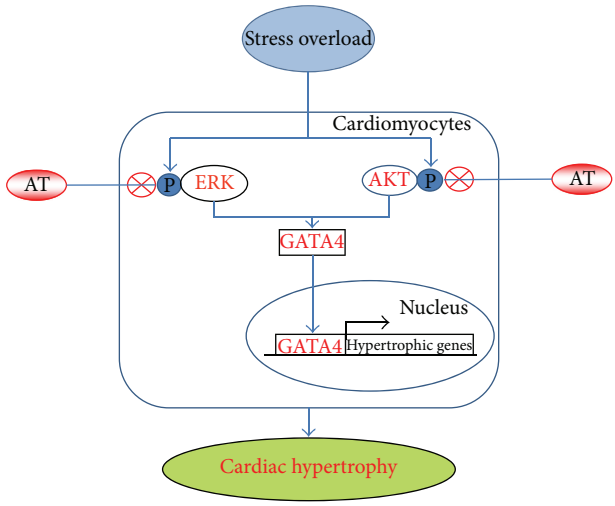

FIGURE 8: A model of pathways in the cardioprotection of AT in response to pressure stress overload. TAC (stress overload) could activate phosphorylation of the protein kinases of ERK1/2 and AKT, enhance the expression of GATA4, promote the transcription of hypertrophic gene, and result in cardiac hypertrophy and cardiac fibrosis. AT could inhibit the phosphorylation of ERK1/2 and AKT, reduce GATA4, and inhibit pathological development of cardiac hypertrophy. ⊗ denotes inhibition of protein kinase by AT treatment.

overload and elucidated the mechanisms of the effective AT treatment in patients with cardiac hypertrophy.

Conflict of Interests

No conflict of interests, financial or otherwise, is declared by the authors.

Authors' Contribution

Jianyong Qi and Qin Liu contributed to the work equally.

Acknowledgments

This study was supported by National Natural Science Foundation of Guangdong S20120410008010 (to Jianyong Qi), Guangdong Province Medical Research Foundation A2013235 (to Jianyong Qi), National Natural Science Foundation of China 81173439 (to Minzhou Zhang), and 81202782 (to Lei Wang), Specialized Research Fund for the Doctoral Program of Higher Education of China 20134425110001 (to Minzhou Zhang).

References

[1] J. H. van Berlo, M. Maillet, and J. D. Molkentin, "Signaling effectors underlying pathologic growth and remodeling of the heart," *Journal of Clinical Investigation*, vol. 123, no. 1, pp. 37–45, 2013.

[2] V. Kandalam, R. Basu, L. Moore et al., "Lack of tissue inhibitor of metalloproteinases 2 leads to exacerbated left ventricular dysfunction and adverse extracellular matrix remodeling in response to biomechanical stress," *Circulation*, vol. 124, no. 19, pp. 2094–2105, 2011.

[3] Y. Hu, S. J. Matkovich, P. A. Hecker, Y. Zhang, J. R. Edwards, and G. W. Dorn II, "Epitranscriptional orchestration of genetic reprogramming is an emergent property of stress-regulated cardiac microRNAs," *Proceedings of the National Academy of Sciences of the United States of America*, vol. 109, no. 48, pp. 19864–19869, 2012.

[4] M. G. Dionyssiou, N. B. Nowacki, S. Hashemi et al., "Cross-talk between glycogen synthase kinase 3β (GSK3β) and p38MAPK regulates myocyte enhancer factor 2 (MEF2) activity in skeletal and cardiac muscle," *Journal of Molecular and Cellular Cardiology*, vol. 54, no. 1, pp. 35–44, 2013.

[5] H. Q. Liu, "Determination of isoquercitrin of compound kendir leaves tablets HPLC," *Traditional Chinese Medicine*, vol. 26, pp. 3–4, 2004.

[6] Y. Xu, "Clinical observation of Apocynum tablets combined with nifedipine for treating 77 patients of essential hypertension," *Journal of Cardiovascular and Pulmonary Diseases*, vol. 10, pp. 1479–1480, 2010.

[7] S. H. Wang, "Nifedipine combined with apocynum tablets for treating essential hypertension," *Asia Pacific Traditional Medicine*, vol. 7, pp. 56–57, 2011.

[8] J. Y. Qi, M. Xu, Z. Z. Lu, and Y. Y. Zhang, "Differential expression of 14-3-3ε during physiological, pathological cardiac hypertrophy and chronic heart failure in mice," *Gene Therapy and Molecular Biology*, vol. 13, no. 1, pp. 71–81, 2009.

[9] H. Qiu, P. Lizano, L. Laure et al., "H11 kinase/heat shock protein 22 deletion impairs both nuclear and mitochondrial functions of stat3 and accelerates the transition into heart failure on cardiac overload," *Circulation*, vol. 124, no. 4, pp. 406–415, 2011.

[10] J.-Y. Qi, M. Xu, Z.-Z. Lu, and Y.-Y. Zhang, "14-3-3 inhibits insulin-like growth factor-I-induced proliferation of cardiac fibroblasts via a phosphatidylinositol 3-kinase-dependent pathway," *Clinical and Experimental Pharmacology and Physiology*, vol. 37, no. 3, pp. 296–302, 2010.

[11] P. P. Li, L. S. Zhao, and S. X. Cui, "Influence of Apocynum tablet on ambulatory blood pressure in elderly patients with hypertension," *Chinese Journal of Gerontology*, vol. 16, pp. 3153–3154, 2011.

[12] R. Meng, Z. Pei, A. Zhang et al., "AMPK activation enhances PPARα activity to inhibit cardiac hypertrophy via ERK1/2 MAPK signaling pathway," *Archives of Biochemistry and Biophysics*, vol. 511, no. 1-2, pp. 1–7, 2011.

[13] M. Xin, E. N. Olson, and R. Bassel-Duby, "Mending broken hearts: cardiac development as a basis for adult heart regeneration and repair," *Nature Reviews Molecular Cell Biology*, vol. 14, no. 8, pp. 529–541, 2013.

[14] J. H. Van Berlo, J. W. Elrod, B. J. Aronow, W. T. Pu, and J. D. Molkentin, "Serine 105 phosphorylation of transcription factor GATA4 is necessary for stress-induced cardiac hypertrophy in vivo," *Proceedings of the National Academy of Sciences of the United States of America*, vol. 108, no. 30, pp. 12331–12336, 2011.

[15] I. Kehat, J. Davis, M. Tiburcy et al., "Extracellular signal-regulated kinases 1 and 2 regulate the balance between eccentric and concentric cardiac growth," *Circulation Research*, vol. 108, no. 2, pp. 176–183, 2011.

[16] G. Y. Oudit and J. M. Penninger, "Cardiac regulation by phosphoinositide 3-kinases and PTEN," *Cardiovascular Research*, vol. 82, no. 2, pp. 250–260, 2009.

[17] K. Wang, B. Long, J. Zhou, and P. Li, "miR-9 and NFATc3 regulate myocardin in cardiac hypertrophy," *The Journal of Biological Chemistry*, vol. 285, no. 16, pp. 11903–11912, 2010.

[18] J. H. van Berlo, B. J. Aronow, and J. D. Molkentin, "Parsing the roles of the transcription factors GATA-4 and GATA-6 in the adult cardiac hypertrophic response," *PLoS ONE*, vol. 8, no. 12, Article ID e84591, 2013.

[19] S. Kobayashi, K. Mao, H. Zheng et al., "Diminished GATA4 protein levels contribute to hyperglycemia-induced cardiomyocyte injury," *The Journal of Biological Chemistry*, vol. 282, no. 30, pp. 21945–21952, 2007.

[20] C. Kwan, W. Zhang, S. Nishibe, and S. Seo, "A novel in vitro endothelium-dependent vascular relaxant effect of *Apocynum venetum* leaf extract," *Clinical and Experimental Pharmacology and Physiology*, vol. 32, no. 9, pp. 789–795, 2005.

[21] D. H. Wu, L. W. Yang, and W. W. Su, "The progress in chemical constituents and pharmacological studies of wild chrysanthemum," *Chinese Herbal Medicine*, vol. 27, pp. 142–144, 2004.

[22] J. S. Burchfield, M. Xie, and J. A. Hill, "Pathological ventricular remodeling: mechanisms: part 1 of 2," *Circulation*, vol. 128, no. 4, pp. 388–400, 2013.

[23] V. B. Pillai, N. R. Sundaresan, and M. P. Gupta, "Regulation of Akt signaling by sirtuins: its implication in cardiac hypertrophy and aging," *Circulation Research*, vol. 114, no. 2, pp. 368–378, 2014.

[24] S. Ulm, W. Liu, M. Zi et al., "Targeted deletion of ERK2 in cardiomyocytes attenuates hypertrophic response but provokes pathological stress induced cardiac dysfunction," *Journal of Molecular and Cellular Cardiology*, vol. 72, pp. 104–116, 2014.

[25] J. D. Molkentin, "The zinc finger-containing transcription factors GATA-4, -5, and -6: ubiquitously expressed regulators of tissue-specific gene expression," *The Journal of Biological Chemistry*, vol. 275, no. 50, pp. 38949–38952, 2000.

[26] Q. Liang, L. J. de Windt, S. A. Witt, T. R. Kimball, B. E. Markham, and J. D. Molkentin, "The transcription factors GATA4 and GATA6 regulate cardiomyocyte hypertrophy *in vitro* and *in vivo*," *The Journal of Biological Chemistry*, vol. 276, no. 32, pp. 30245–30253, 2001.

[27] T. Oka, M. Maillet, A. J. Watt et al., "Cardiac-specific deletion of gata4 reveals its requirement for hypertrophy, compensation, and myocyte viability," *Circulation Research*, vol. 98, no. 6, pp. 837–845, 2006.

[28] O. Tenhunen, B. Sármán, R. Kerkelä et al., "Mitogen-activated protein kinases p38 and ERK 1/2 mediate the wall stress-induced activation of GATA-4 binding in adult heart," *The Journal of Biological Chemistry*, vol. 279, no. 23, pp. 24852–24860, 2004.

[29] A. S. Go, D. Mozaffarian, V. L. Roger et al., "Heart disease and stroke statistics—2014 update: a report from the American Heart Association," *Circulation*, vol. 129, no. 3, pp. e28–e292, 2014.

[30] H. Yang, F. Xie, Y. Yang, and Y. Luo, "Preparation and in vitro release characteristics of pulsed-release tablets of *Apocynum venetum*," *Zhongguo Zhong Yao Za Zhi*, vol. 36, no. 11, pp. 1427–1430, 2011.

[31] Q. Wu, C. X. Chen, W. L. Gu, J. P. Gao, Y. Wan, and J. Lv, "Effect of Chrysanthemum indicum on ventricular remodeling in rats," *Zhong Yao Cai*, vol. 33, no. 7, pp. 1112–1115, 2010.

Hindawi Publishing Corporation
Evidence-Based Complementary and Alternative Medicine
Volume 2014, Article ID 796518, 7 pages
http://dx.doi.org/10.1155/2014/796518

Research Article

Effects of Inhalation of Essential Oil of *Citrus aurantium* L. var. *amara* on Menopausal Symptoms, Stress, and Estrogen in Postmenopausal Women: A Randomized Controlled Trial

Seo Yeon Choi, Purum Kang, Hui Su Lee, and Geun Hee Seol

Department of Basic Nursing Science, School of Nursing, Korea University, 145 Anam-ro, Seongbuk-gu, Seoul 136-701, Republic of Korea

Correspondence should be addressed to Geun Hee Seol; ghseol@korea.ac.kr

Received 29 April 2014; Revised 20 May 2014; Accepted 30 May 2014; Published 12 June 2014

Academic Editor: Ping Liu

This study aimed to investigate the effects of inhalation of the essential oil of *Citrus aurantium* L. var. *amara* (neroli oil) on menopausal symptoms, stress, and estrogen in postmenopausal women. Sixty-three healthy postmenopausal women were randomized to inhale 0.1% or 0.5% neroli oil or almond oil (control) for 5 minutes twice daily for 5 days. Menopause-related symptoms, as determined by the Menopause-Specific Quality of Life Questionnaire (MENQOL); sexual desire visual analog scale (VAS); serum cortisol and estrogen concentrations, blood pressure, pulse, and stress VAS, were measured before and after inhalation. Compared with the control group, the two neroli oil groups showed significant improvements in the physical domain score of the MENQOL and in sexual desire. Systolic blood pressure was significantly lower in the group inhaling 0.5% neroli oil than in the control group. Compared with the control group, the two neroli oil groups showed significantly lower diastolic blood pressure and tended to improve pulse rate and serum cortisol and estrogen concentrations. These findings indicate that inhalation of neroli oil helps relieve menopausal symptoms, increase sexual desire, and reduce blood pressure in postmenopausal women. Neroli oil may have potential as an effective intervention to reduce stress and improve the endocrine system.

1. Introduction

The World Health Organization (WHO) defines menopause as permanent cessation of menstruation caused by the loss of ovarian follicular activity. Menopause is a natural process of female aging and accompanies diverse physiological changes in women. One of the most prominent changes is a decrease in female sex hormones, resulting in vasomotor symptoms such as hot flushes and palpitations [1]. In addition, psychological changes, including depression, anxiety, restlessness, and sleep disorders may occur during the menopausal transition. Climacteric women may experience other symptoms, including decreased sexual desire and increased muscle pains, and carry higher risks of cardiovascular diseases. Menopausal symptoms have also been reported to have a negative impact on women's daily lives and even degrade their quality of life [2].

As vasomotor symptoms including hot flushes are primarily caused by a decrease in estrogen [3], hormone replacement therapy (HRT) has been regarded as an effective remedy [1]. Despite its positive effects, HRT has various potential side effects, including thromboembolism, gallstones, breast cancer, and stroke [4]. Moreover, HRT was found to improve quality of life only when applied for a short time [5]. Lifestyle modifications, regular exercise, and use of antidepressants have therefore been recommended in tandem with HRT [6, 7], with several recent studies analyzing the ability of complementary and alternative medicines to relieve menopausal symptoms [8].

The essential oil of *Citrus aurantium* L. var. *amara*, also known as neroli oil, has been reported to have antianxiety effects by regulating 5-HT receptors in rats [9] and to have antidepressant effects through the monoaminergic system in mice [10]. Neroli oil has also been reported to have sedative, antianxiety, and antidepressant effects on mice [11]. In addition, limonene, one of the major chemical components in the essential oil of *Citrus aurantium* L. var. *amara*, has been shown to have antianxiety [12] and motor relaxant effects,

indicating sedative activity [13] in mice. Moreover, a study in rats reported that olfactory stimulation with grapefruit oil, which is rich in limonene, stimulated sympathetic nerves by activating histamine H1 receptors and that limonene treatment induced similar responses [14]. Limonene-rich bergamot essential oil also demonstrated direct vasorelaxant effects [15].

Taken together, these findings in rodents indicate that neroli oil can be effective in relieving not only psychological climacteric symptoms, such as stress, depression, and anxiety, but also physiological symptoms, such as those related to vasomotor effects and blood pressure. To date, however, no clinical study has tested the effects of neroli oil on postmenopausal women. This study therefore evaluated the effects of neroli oil inhalation on physiological and psychological symptoms in postmenopausal women and assessed the potential of neroli oil inhalation as a nursing intervention.

2. Materials and Methods

2.1. Study Design and Participants. This double-blinded, randomized controlled trial was designed to assess the effects of inhalation of several concentrations of neroli oil on menopausal symptoms, stress, and estrogen levels in healthy postmenopausal women. Ninety-two women aged ≤65 years with natural menopause living in Seoul, South Korea, were recruited for the study between November 2013 and March 2014; of these women, 11 did not meet the eligibility criteria or withdrew their consent to participate. The remaining 81 participants were told the purpose and protocol of the experiment. The detailed inclusion criteria included (1) age ≤65 years with natural menopause, (2) no experience of HRT or aromatherapy in the previous six weeks, (3) no history of psychiatric illness, (4) no current medication for anxiety or depression, (5) no disturbance of olfactory acuity, and (6) being free of allergies related to aromatherapy. Eighteen participants were excluded, including 11 who missed two or more treatments with neroli or almond oil, five who were not assessed after treatment, and two who used drugs such as antibiotics during the treatment period. The study design and protocol were approved by the Ethical Review Committee of the Chung-Ang University (code: 1041078-201310-HR-0072-03), and all participants provided written informed consent.

2.2. Intervention. Neroli oil and almond oil were obtained from Aromarant Co. Ltd. (Rottingen, Germany). Neroli oil was dissolved in almond oil that has no smell and no deleterious effects, at concentrations of 0.1% and 0.5% (v/v). The participants were assigned by a random number table to groups receiving 0.1% or 0.5% (v/v) neroli oil dissolved in almond oil, or almond oil (control). Only the compounder was aware of subject assignment. Neither the participants nor the investigators knew the allocation. Subjects in the three groups received 10 bottles, each containing 1 mL of neroli oil in almond oil or almond oil; all bottles had the same shape and color. Each subject was self-treated for 10 sessions, performed at 10 AM and 10 PM for 5 consecutive days. Each subject was instructed to decant the contents of one bottle onto a fragrance pad, sit in a stable and comfortable place, position the pad 30 cm away from her nose, and inhale the fragrance for five minutes with normal breathing.

2.3. Outcome Measurements and Data Collection. Pretrial surveys and measurements were performed on the day before day 1 of the 5-day intervention, while posttrial surveys and measurements were performed on day 6. The pretrial survey included general characteristics, self-reported menopause-specific qualify of life questionnaire (MENQOL), and stress and sexual visual analog scale (VAS), while pretrial measurements included systolic blood pressure (SBP), diastolic blood pressure (DBP), pulse rate, and serum cortisol and estrogen levels. Posttrial survey and measurements included all of the above parameters, except for general characteristics. To minimize the effect of data collection time, all surveys and measurements were conducted between 9 AM and 10 AM.

2.3.1. MENQOL. The MENQOL is a self-reported survey, composed of 29 assessment items, including 16 in the physical domain, 7 in the psychosocial domain, 3 in the vasomotor domain, and 3 in the sexual functioning domain. For each item, the respondent selects whether or not she experienced that symptom over the previous four weeks; if yes, she rates it on a scale from 2, corresponding to "not bothered at all," to 8, corresponding to "extremely bothered" [16]. Mean total MENQOL score and mean score on each domain were determined. A factor analysis verified the reliability of the MENQOL and showed that five questions were redundant [17]. This study therefore excluded the five redundant questions and assessed the remaining 24 questions. The present study used a Korean translation of the original MENQOL, which has been used in previous research after an expert review [18].

2.3.2. Sexual Desire Scale and Stress Scale. The sexual desire of each participant was measured by VAS [19], a 10 cm line oriented horizontally. Each participant marked on the scale by crossing the line at the point that corresponded to the intensity of sexual desire, with 0 indicating no sexual desire and 10 indicating extremely strong desire. The same VAS was used for subjective measurement of stress level. Each participant marked the intensity of stress, where 0 corresponded to no stress and 10 to extreme stress.

2.3.3. Blood Pressure and Pulse Rate. The SBP and DBP of each participant were measured with a sphygmomanometer on the left arm after 15 minutes of rest in a sitting position. Both before and after the intervention, SBP and DBP were measured twice and their averages were calculated. Pulse rate per minute was measured twice with a stop watch before and after the intervention after 15 minutes of rest in a sitting position, and the averages were calculated.

2.3.4. Serum Cortisol and Estrogen Concentrations. Blood samples (3 mL each) were obtained before and after the intervention from each subject between 9 and 10 AM. Serum was obtained by centrifugation and was immediately frozen and stored at −70°C. Serum cortisol (Enzo Life Sciences, NY,

USA) and estrogen (CUSABIO, Wuhan, China) concentrations were measured by ELISA, with the results read in a microplate reader at a wavelength of 450 nm.

2.4. Statistical Analysis. All data are reported as mean ± standard deviation, with all statistical analyses performed using SPSS version 20.0 (SPSS Inc., Chicago, IL, USA). Intergroup comparisons of any normally distributed variable were performed using one-way analysis of variance (ANOVA), followed by least significant difference Scheffe's posthoc analysis. Nonnormally distributed variables were compared using the Kruskal-Wallis test, with posthoc analysis by the Mann-Whitney test and Bonferroni's method for significance threshold adjustment. Within group, comparisons of normally and nonnormally distributed variables were assessed using paired t-tests and Wilcoxon signed rank tests, respectively. A P value <0.05 was defined as statistically significant.

3. Results

3.1. General Characteristics of the Participants and Test of Homogeneity. Of the 92 women assessed for eligibility, seven did not meet the eligibility criteria and four refused to participate. Of the remaining 81 women, 18 dropped out during the study period, including 11 who missed two or more treatment sessions, 5 who did not attend posttreatment measurements, and 2 who were on medication during the intervention. Thus, data were collected and analyzed for 63 women, including 22 who received almond oil, 22 who received 0.1% neroli oil, and 19 who received 0.5% neroli oil (Figure 1). The mean age of the study population was 55.81 years and their mean BMI was 22.97 kg/m^2. There were no significant differences among the three groups in general characteristics, including age and BMI, or in any of the baseline outcome measures (Table 1).

3.2. Effect of Neroli Oil on Menopausal Symptoms, Sexual Desire, and Stress. After the 5 days of intervention, the total MENQOL score significantly decreased from the baseline in the 0.1% ($P < 0.001$) and 0.5% ($P = 0.03$) neroli oil groups but did not decrease significantly in the control group (Table 2).

The three groups showed significant differences in mean change of the physical domain of the MENQOL ($P = 0.04$, Table 2). A posthoc analysis showed a significant difference between the 0.1% neroli oil and control groups ($P = 0.008$). The mean changes in the other domains did not differ significantly among the groups but tended to be more pronounced in the two neroli oil groups than in the almond oil group. The 0.1% neroli oil group showed a significant change in mean physical domain ($P < 0.001$) and vasomotor domain ($P = 0.002$) scores.

Although the sexual desire VAS score of the control group decreased significantly ($P = 0.013$) after the intervention, the sexual desire VAS scores of the 0.1% ($P = 0.049$) and 0.5% ($P = 0.001$) neroli oil groups increased significantly, with the three groups differing significantly in mean change ($P < 0.001$). A posthoc analysis based on the Mann-Whitney test showed that both the 0.1% ($P = 0.001$) and 0.5% ($P < 0.001$) neroli oil groups had significantly higher sexual desire VAS scores after treatment than the control group.

Stress level, as assessed by stress VAS measurement, decreased in all three groups but did not differ significantly among the groups.

3.3. Effect of Neroli Oil on Blood Pressure and Pulse Rate. After the 5-day intervention, the SBP of the control group increased 6.68 ± 16.23 mmHg, whereas the SBPs of the 0.1% and 0.5% neroli oil groups decreased 2.89 ± 13.89 mmHg and 5.92 ± 12.90 mmHg, respectively, with the difference in mean changes among the groups being statistically significant ($P = 0.03$, Figure 2(a)). A posthoc analysis showed a significant difference between the 0.5% neroli oil and control groups ($P = 0.03$).

In addition, DBP of the control group increased 7.34 ± 12.78 mmHg, whereas the DPBs of the 0.1% and 0.5% neroli groups decreased 2.43 ± 7.47 mmHg and 3.18 ± 5.97 mmHg, respectively, with the difference in mean changes among the groups being statistically significant ($P = 0.001$, Figure 2(b)).

Pulse rate increased in the control (0.09 ± 6.80 beats/min) and 0.1% neroli oil (0.26 ± 5.80 beats/min) groups but decreased −1.92 ± 8.93 beats/min in the 0.5% neroli oil group, with none of these differences being statistically significant (Figure 2(c)).

3.4. Effect of Neroli Oil on Serum Cortisol and Estrogen Levels. After the 5-day treatment period, serum cortisol concentrations decreased in all three groups, but none of the differences was statistically significant (Table 3). Similarly, there were no differences in serum estrogen concentrations within or among the three groups (Table 4).

4. Discussion

This study was designed to investigate the effects of neroli oil inhalation on menopausal symptoms, stress, and serum estrogen level among postmenopausal women. Postmenopausal women aged ≤65 years inhaled neroli oil or almond oil twice daily for five days, and the effects on MENQOL, sexual desire and stress VAS, blood pressure, pulse rate, and serum cortisol and estrogen concentrations were measured.

The MENQOL measures the quality of life related to climacteric symptoms among women in menopausal transition. This study showed that inhalation of neroli oil, at concentrations of 0.1% and 0.5%, significantly altered total MENQOL score and significantly enhanced sexual desire, as measured by a VAS, compared with the inhalation of almond oil alone. In contrast, the sexual domain of the MENQOL was not improved significantly in the neroli oil groups. A previous study of the MENQOL reported that the four domains—vasomotor, physical, psychosocial, and sexual functioning—have correlations among themselves [20]. In addition, the sexual functioning domain of the MENQOL assessed functional aspects such as vaginal dryness, as well as subjective aspects. The sexual desire VAS measured only subjective aspects. Therefore, the significant improvements

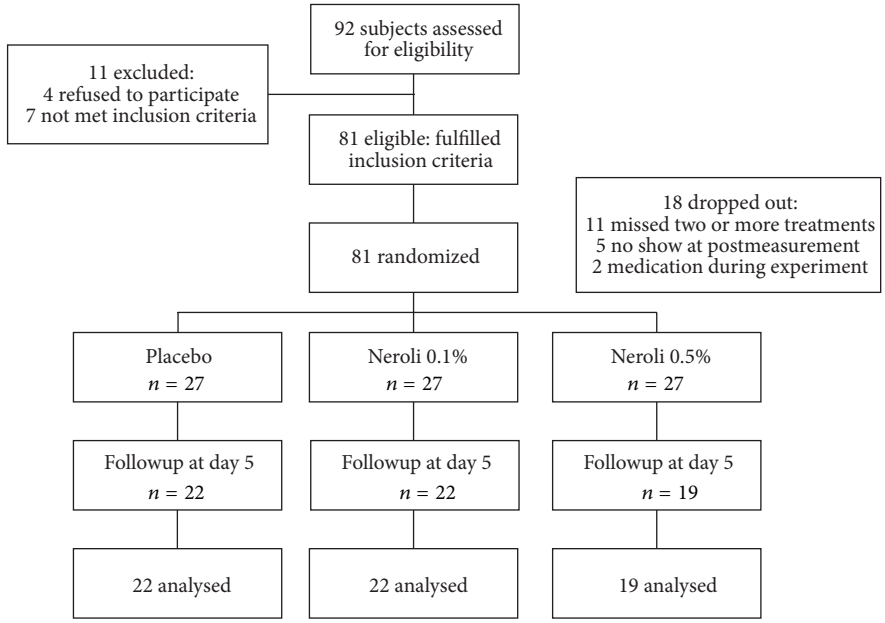

Figure 1: Study flow diagram.

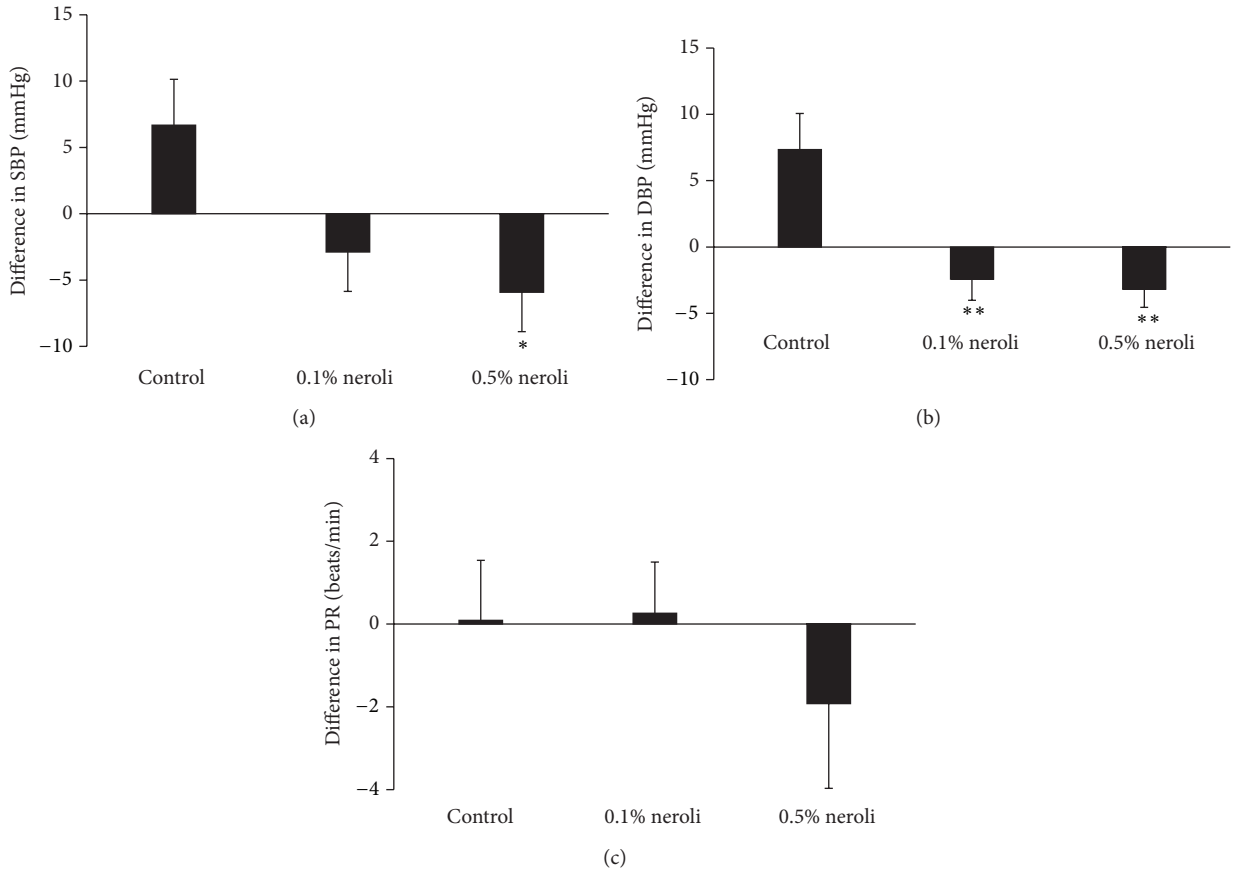

Figure 2: Effects of neroli oil inhalation on (a) systolic blood pressure, (b) diastolic blood pressure, and (c) pulse rate. Values are expressed as mean ± SEM. $^{*}P < 0.05$, $^{**}P < 0.01$ compared with the control group. SBP, systolic blood pressure; DBP, diastolic blood pressure; PR, pulse rate.

Table 1: Homogeneity test for general characteristics and measurement variables.

Characteristics or variables	Control ($n = 22$)	0.1% neroli oil ($n = 22$)	0.5% neroli oil ($n = 19$)	Total ($N = 63$)	P value
Age (years)	55.73 (2.35)	56.46 (2.26)	55.16 (2.99)	55.81 (2.55)	0.27
BMI (kg/m^2)	22.75 (2.48)	22.74 (1.78)	23.49 (1.91)	22.97 (2.08)	0.43
Age at menarche (years)	15.90 (1.38)	15.59 (1.79)	15.19 (1.42)	15.57 (1.55)	0.31
Age at menopause (years)	50.05 (10.24)	52.27 (2.45)	51.53 (2.09)	51.27 (6.30)	0.50
Frequency of lifetime pregnancy	2.82 (0.85)	3.00 (1.31)	2.95 (0.85)	2.92 (1.02)	0.85[a]
Number of children	1.86 (0.47)	2.05 (0.79)	1.95 (0.52)	1.95 (0.61)	0.46[a]
Number of family members	3.32 (1.04)	3.32 (1.13)	3.37 (1.30)	3.33 (1.14)	0.94[a]
Duration of physical exercise (min/week)	188.18 (223.39)	213.75 (191.84)	255.26 (329.99)	217.34 (248.45)	0.63[a]
Frequency of physical exercise (times/week)	3.00 (3.19)	3.73 (3.01)	3.81 (2.09)	3.5 (2.81)	0.22[a]
Frequency of sexual intercourse (times/6 months)	9.87 (10.18)	8.36 (7.82)	7.87 (11.67)	8.74 (9.80)	0.54[a]
MENQOL (score)					
Overall	2.66 (0.95)	2.53 (0.91)	2.63 (1.04)	2.61 (0.95)	0.91
Physical	2.58 (1.07)	2.44 (0.29)	2.66 (1.27)	2.55 (1.06)	0.97[a]
Psychological	2.45 (1.49)	1.90 (1.01)	2.24 (1.26)	2.22 (1.27)	0.40[a]
Sexual	3.80 (1.62)	4.02 (2.27)	3.46 (1.87)	3.77 (1.93)	0.70[a]
Vasomotor	2.20 (1.69)	2.52 (1.66)	2.16 (1.59)	2.30 (1.63)	0.53[a]
Sexual desire VAS (cm)	3.61 (2.69)	2.98 (2.05)	2.74 (1.79)	3.13 (2.22)	0.62[a]
Stress VAS (cm)	4.64 (1.53)	3.86 (2.26)	4.72 (2.04)	4.39 (1.97)	0.30[a]
SBP (mmHg)	122.48 (15.65)	122.59 (11.57)	117.32 (12.89)	120.96 (13.51)	0.38
DBP (mmHg)	78.52 (9.31)	78.11 (8.35)	72.76 (8.04)	76.64 (8.85)	0.07
PR (beats/min)	71.23 (6.87)	72.04 (8.73)	72.05 (7.61)	71.76 (7.66)	0.92
Serum cortisol (ng/mL)	7.80 (4.90)	6.22 (3.85)	11.53 (15.64)	8.38 (9.43)	0.45[a]
Serum estrogen (ng/mL)	139.76 (27.92)	135.25 (21.82)	143.78 (26.64)	139.40 (25.37)	0.69[a]

BMI, body mass index; MENQOL, Menopause-Specific Qualify of Life Questionnaire; VAS, visual analog scale; SBP, systolic blood pressure; DBP, diastolic blood pressure; PR, pulse rate.
Data reported as mean (standard deviation).
One-way ANOVA, [a]Kruskal-Wallis test.

Table 2: Effect of neroli oil on menopausal symptoms, sexual desire, and stress ($N = 63$).

Variables	Control ($n = 22$)	0.1% neroli oil ($n = 22$)	0.5% neroli oil ($n = 19$)	P value
MENQOL (score)				
Overall	−0.19 ± 0.80	−0.71 ± 0.61	−0.52 ± 0.88	0.27
Physical[a]	−0.02 ± 0.81	−0.64 ± 0.57	−0.40 ± 0.97	0.04*
Psychological[a]	−0.28 ± 1.65	−0.28 ± 0.97	−0.43 ± 1.24	0.76
Sexual[a]	−0.74 ± 1.56	−1.50 ± 1.83	−1.39 ± 1.61	0.45
Vasomotor[a]	−0.20 ± 1.30	−0.92 ± 1.13	−0.35 ± 1.34	0.06
Sexual desire VAS[a] (cm)	−1.82 ± 3.03	0.81 ± 1.84	3.10 ± 3.10	<0.01***
Stress VAS[a] (cm)	−1.52 ± 2.30	−1.08 ± 1.98	−2.28 ± 2.49	0.24

MENQOL, Menopause-Specific Qualify of Life Questionnaire; VAS, visual analog scale.
One-way ANOVA, [a]Kruskal-Wallis test.
Data presented as mean ± standard deviation.
*$P < 0.05$, ***$P < 0.001$ compared with the control group.

Table 3: Effect of neroli oil on serum cortisol levels ($N = 63$).

	Before (ng/mL)	After (ng/mL)	P value	Difference (ng/mL)	P value
Control	7.80 ± 4.90	7.52 ± 8.77	0.76	−0.28 ± 6.85	0.571
0.1% neroli oil	6.22 ± 3.85	6.08 ± 2.93	0.73	−0.14 ± 4.61	
0.5% neroli oil	11.53 ± 15.64	8.41 ± 7.32	0.38	−3.12 ± 9.40	

Data presented as mean ± standard deviation.

Table 4: Effect of neroli oil on serum estrogen levels ($N = 63$).

	Before (ng/mL)	After (ng/mL)	P value	Difference (ng/mL)	P value
Control	139.76 ± 27.92	135.92 ± 24.00	0.49	−3.84 ± 18.60	
0.1% neroli oil	135.25 ± 21.82	131.70 ± 24.37	0.43	−3.55 ± 24.11	0.270
0.5% neroli oil	143.78 ± 26.64	148.33 ± 34.67	0.94	4.55 ± 25.78	

Data presented as mean ± standard deviation.

in the physical and vasomotor domains in the two neroli oil groups presumably affected sexual desire VAS, although the sexual domain of the MENQOL itself did not change significantly.

Women in menopausal transition frequently experience both vasomotor and psychological symptoms, but both have different underlying factors. Psychological symptoms are associated with subject lifestyle and behavioral factors, whereas vasomotor symptoms show much stronger correlations with menopausal stages than with lifestyle and environmental elements [21]. In addition, decreased estrogen is an important factor in the complex mechanism of hot flushes [22]. The present study showed that vasomotor symptoms improved significantly after treatment with 0.1% neroli oil. Neurotransmitters such as 5-HT are involved in regulating body temperature; using the same mechanism, HRT activates noradrenaline or neurotransmitters like 5-HT to treat vasomotor symptoms [22]. The significant improvements in vasomotor symptoms observed in subjects who inhaled neroli oil were likely due to the activation of 5-HT neurotransmitters, a mechanism similar to the antianxiety effects of neroli oil in animal models [9].

Stress poses significant risks in cardiovascular diseases, and an increased level of stress can cause physiological responses by the cardiovascular system, including increases in blood pressure and pulse rate [23]. Although the present study did not show a significant change in subjective stress VAS among the three groups, neroli oil inhalation significantly reduced both SBP and DBP, suggesting that neroli oil relieves cardiovascular responses to stress. In addition, although the concentration of serum cortisol, a physiological indicator of stress, did not decrease in either of the neroli oil groups, the decrease was greater in the 0.5% neroli oil group than in the 0.1% neroli oil and control groups. This result is in agreement with findings showing that neroli oil had sedative and relaxant effects in animals [13] and that essential oil from bergamot, another member of the citrus family, not only lowered blood pressure but also relaxed blood vessels in animals [15, 24]. Although serum cortisol levels did not differ among the three groups, the results presented here suggest that neroli oil reduces physiological responses to stress.

Neroli oil may also reduce blood pressure by acting on the autonomic nervous system. Olfactory stimulation with limonene, which is abundant in neroli essential oil, was found to elevate sympathetic nerve activity by activating H1 receptors in an animal model [14]. Moreover, neroli oil has been reported to contain adrenergic amines such as synephrine, octopamine, and tyramine [25]. These results suggest that neroli oil treatment modulates autonomic nerves to reduce blood pressure.

Herbal remedies for treatment of climacteric symptoms include black cohosh, hops, wild yam, and ginseng [8]. Terpenes, composed of isoprene as a building block, can be found in most of these herbs, as well as in neroli oil. Although serum estrogen levels did not increase significantly after neroli oil treatment, serum estrogen slightly increased in the 0.5% neroli oil group while slightly decreasing in the other two groups. Similar to other herbs, neroli oil may affect the endocrine system in alleviating menopausal symptoms.

5. Conclusion

In summary, the present randomized controlled trial showed that inhalation of neroli oil by postmenopausal women improved their quality of life related to menopausal symptoms, increased sexual desire, and reduced blood pressure. In addition, inhalation of neroli oil may reduce stress levels and stimulate the endocrine system. These findings indicate that neroli oil can be used to relieve various symptoms related to menopause.

Conflict of Interests

The authors declare that there is no conflict of interests regarding the publication of this paper.

Acknowledgments

This work was supported by a National Research Foundation of Korea (NRF) Grant funded by the Korean government (MEST) (no. 2012R1A2A2A02007145) and the Institute of Nursing Research, Korea University Grant.

References

[1] H. C. Fantasia and M. A. Sutherland, "Hormone therapy for the management of menopause symptoms," *Journal of Obstetric, Gynecologic, & Neonatal Nursing*, vol. 43, no. 2, pp. 226–235, 2014.

[2] N. E. Avis, A. Colvin, J. T. Bromberger et al., "Change in health-related quality of life over the menopausal transition in a multiethnic cohort of middle-aged women: study of Women's Health Across the Nation," *Menopause*, vol. 16, no. 5, pp. 860–869, 2009.

[3] W. G. Rossmanith and W. Ruebberdt, "What causes hot flushes? the neuroendocrine origin of vasomotor symptoms in the menopause," *Gynecological Endocrinology*, vol. 25, no. 5, pp. 303–314, 2009.

[4] O. Ortmann and C. Lattrich, "The treatment of climacteric symptoms," *Deutsches Arzteblatt*, vol. 109, no. 17, pp. 316–324, 2012.

[5] N. F. Col, G. Weber, A. Stiggelbout, J. Chuo, R. D'Agostino, and P. Corso, "Short-term menopausal hormone therapy for symptom relief: an updated decision model," *Archives of Internal Medicine*, vol. 164, no. 15, pp. 1634–1640, 2004.

[6] A. Daley, H. Stokes-Lampard, and C. Macarthur, "Exercise for vasomotor menopausal symptoms," *Cochrane Database of Systematic Reviews*, no. 5, Article ID CD006108, 2011.

[7] G. M. Dickson, "Menopause management: how you can do better," *Journal of Family Practice*, vol. 61, no. 3, pp. 138–145, 2012.

[8] F. Borrelli and E. Ernst, "Alternative and complementary therapies for the menopause," *Maturitas*, vol. 66, no. 4, pp. 333–343, 2010.

[9] C. A. R. A. Costa, T. C. Cury, B. O. Cassettari, R. K. Takahira, J. C. Flório, and M. Costa, "Citrus aurantium L. essential oil exhibits anxiolytic-like activity mediated by 5-HT1A-receptors and reduces cholesterol after repeated oral treatment," *BMC Complementary and Alternative Medicine*, vol. 13, article 42, 2013.

[10] L.-T. Yi, H.-L. Xu, J. Feng, X. Zhan, L.-P. Zhou, and C.-C. Cui, "Involvement of monoaminergic systems in the antidepressant-like effect of nobiletin," *Physiology and Behavior*, vol. 102, no. 1, pp. 1–6, 2011.

[11] L. M. Lopes Campêlo, C. Gonçalves e Sá, A. A. C. de Almeida et al., "Sedative, anxiolytic and antidepressant activities of Citrus limon (Burn) essential oil in mice," *Pharmazie*, vol. 66, no. 8, pp. 623–627, 2011.

[12] A. A. C. de Almeida, J. P. Costa, R. B. F. de Carvalho, D. P. de Sousa, and R. M. de Freitas, "Evaluation of acute toxicity of a natural compound (+)-limonene epoxide and its anxiolytic-like action," *Brain Research*, vol. 1448, pp. 56–62, 2012.

[13] T. G. do Vale, E. C. Furtado, J. G. Santos Jr., and G. S. B. Viana, "Central effects of citral, myrcene and limonene, constituents of essential oil chemotypes from Lippia alba (mill.) N.E. Brown," *Phytomedicine*, vol. 9, no. 8, pp. 709–714, 2002.

[14] J. Shen, A. Niijima, M. Tanida, Y. Horii, K. Maeda, and K. Nagai, "Olfactory stimulation with scent of grapefruit oil affects autonomic nerves, lipolysis and appetite in rats," *Neuroscience Letters*, vol. 380, no. 3, pp. 289–294, 2005.

[15] P. Kang, S. H. Suh, S. S. Min, and G. H. Seol, "The essential oil of Citrus bergamia Risso induces vasorelaxation of the mouse aorta by activating K + channels and inhibiting Ca 2+ influx," *Journal of Pharmacy and Pharmacology*, vol. 65, no. 5, pp. 745–749, 2013.

[16] J. R. Hilditch, J. Lewis, A. Peter et al., "A menopause-specific quality of life questionnaire: development and psychometric properties," *Maturitas*, vol. 24, no. 3, pp. 161–175, 1996.

[17] K. B. van Dole, R. F. Devellis, R. D. Brown, M. L. Jonsson Funk, B. N. Gaynes, and R. E. Williams, "Evaluation of the menopause-specific quality of life questionnaire: a factor-analytic approach," *Menopause*, vol. 19, no. 2, pp. 211–215, 2012.

[18] O. Lee, J. Kim, H. Lee, and R. Choue, "Nutritional status, quality of diet and quality of life in postmenopausal women with mild climacteric symptoms based on food group intake patterns," *Korean Journal of Community*, vol. 17, no. 1, pp. 69–80, 2012.

[19] M. E. Cline, J. Herman, E. R. Shaw, and R. D. Morton, "Standardization of the visual analogue scale," *Nursing Research*, vol. 41, no. 6, pp. 378–380, 1992.

[20] A. Bener, D. E. Rizk, H. Shaheen, R. Micallef, N. Osman, and E. V. Dunn, "Measurement-specific quality-of-life satisfaction during the menopause in an arabian gulf country," *Climacteric*, vol. 3, no. 1, pp. 43–49, 2000.

[21] R. Hardy and D. Kuh, "Change in psychological and vasomotor symptom reporting during the menopause," *Social Science and Medicine*, vol. 55, no. 11, pp. 1975–1988, 2002.

[22] D. C. Deecher, "Physiology of thermoregulatory dysfunction and current approaches to the treatment of vasomotor symptoms," *Expert Opinion on Investigational Drugs*, vol. 14, no. 4, pp. 435–448, 2005.

[23] C. J. Huang, H. E. Webb, M. C. Zourdos, and E. O. Acevedo, "Cardiovascular reactivity, stress, and physical activity," *Frontiers in Physiology*, vol. 4, p. 314, 2013.

[24] K.-M. Chang and C.-W. Shen, "Aromatherapy benefits autonomic nervous system regulation for elementary school faculty in Taiwan," *Evidence-Based Complementary and Alternative Medicine*, vol. 2011, Article ID 946537, 7 pages, 2011.

[25] F. Pellati, S. Benvenuti, M. Melegari, and F. Firenzuoli, "Determination of adrenergic agonists from extracts and herbal products of *Citrus aurantium* L. var. *amara* by LC," *Journal of Pharmaceutical and Biomedical Analysis*, vol. 29, no. 6, pp. 1113–1119, 2002.

Hindawi Publishing Corporation
Evidence-Based Complementary and Alternative Medicine
Volume 2014, Article ID 326107, 11 pages
http://dx.doi.org/10.1155/2014/326107

Review Article

A Review of Botanical Characteristics, Traditional Usage, Chemical Components, Pharmacological Activities, and Safety of *Pereskia bleo* (Kunth) DC

Sogand Zareisedehizadeh,[1] Chay-Hoon Tan,[2] and Hwee-Ling Koh[1]

[1] *Department of Pharmacy, Faculty of Science, National University of Singapore, 18 Science Drive 4, Singapore 117543*
[2] *Department of Pharmacology, Yong Loo Lin School of Medicine, National University of Singapore, Singapore 117597*

Correspondence should be addressed to Hwee-Ling Koh; phakohhl@nus.edu.sg

Received 19 February 2014; Accepted 2 May 2014; Published 3 June 2014

Academic Editor: Wei Jia

Pereskia bleo, a leafy cactus, is a medicinal plant native to West and South America and distributed in tropical and subtropical areas. It is traditionally used as a dietary vegetable, barrier hedge, water purifier, and insect repellant and for maintaining health, detoxification, prevention of cancer, and/or treatment of cancer, hypertension, diabetes, stomach ache, muscle pain, and inflammatory diseases such as dermatitis and rheumatism. The aim of this paper was to provide an up-to-date and comprehensive review of the botanical characteristics, traditional usage, phytochemistry, pharmacological activities, and safety of *P. bleo*. A literature search using MEDLINE (via PubMed), Science direct, Scopus and Google scholar and China Academic Journals Full-Text Database (CNKI) and available eBooks and books in the National University of Singapore libraries in English and Chinese was conducted. The following keywords were used: *Pereskia bleo, Pereskia panamensis, Pereskia corrugata, Rhodocacus corrugatus, Rhodocacus bleo, Cactus panamensis, Cactus bleo*, Spinach cactus, wax rose, Perescia, and Chinese rose. This review revealed the association between the traditional usage of *P. bleo* and reported pharmacological properties in the literature. Further investigation on the pharmacological properties and phytoconstituents of *P. bleo* is warranted to further exploit its potentials as a source of novel therapeutic agents or lead compounds.

1. Introduction

Pereskia bleo is a medicinal plant of the family Cactaceae. Cacti are well-known desert plants and widely recognized by their specialized growth form of the stems and leaves. This family consists of 100 genera and about 2000 species [1, 2]. The genus *Pereskia* consists of 17 species with regular leaf development and function. They are generally representative of the "ancestral cactus." This genus does not look much like other types of cacti because of having substantial leaves and thin stems [3–5]. The plants in the genus *Pereskia* originate from the region between Brazil and Mexico and South America and Central America [6–8] and are cultivated in many tropical and subtropical countries including India, Malaysia, Singapore, and Indonesia [1]. They also generally resemble other types of plants such as roses [3, 8]. *Pereskia* species are divided into Clades A and B [9] (Table 1). The two clades of *Pereskia* differ in their geographical distribution. Clade A is found around the Gulf of Mexico and the Caribbean Sea whereas Clade B is found in the south of the Amazon Basin. The stems of the species of *Pereskia* within Clade A begin to form bark early in the life of the plant like most non-cacti. In contrast, *Pereskia* species within Clade B typically delay forming bark, thus giving the stem the potential to become a major organ for photosynthesis [4].

Among them, *Pereskia aculeata* Mill (*P. aculeate*), *Pereskia grandifolia* Haw (*P. grandifolia*), and *Pereskia bleo* (Kunth) DC. (*P. bleo*) are listed to be found in Singapore and Malaysia [7, 10, 11]. *P. bleo and P. grandifolia* are used for medicinal purposes in these areas [1, 11]. Hence, more information on these three species is presented below.

Table 1: Clades of the genus *Pereskia* [9].

Clade A	Clade B
	Pereskia aculeata Mill.
Pereskia aureiflora F.Ritter	*Pereskia bahiensis* Gürke
Pereskia bleo (Kunth) DC	*Pereskia diaz-romeroana*
Pereskia guamacho F.A.C.Weber	Cárdenas
Pereskia lychnidiflora DC	*Pereskia grandifolia* Haw.
Pereskia marcanoi Areces	*Pereskia horrida* DC
Pereskia portulacifolia (L.) DC	*Pereskia nemorosa* Rojas Acosta
Pereskia quisqueyana Alain	*Pereskia sacharosa* Griseb.
Pereskia zinniiflora DC	*Pereskia stenantha* F.Ritter
	Pereskia weberiana K.Schum.

1.1. Pereskia aculeata Mill. Its common names are Barbados gooseberry or lemon vine [12, 13] and it is native to tropical America [14]. This plant is a scrambling vine growing to the height of 10 m to a tree. The stems reach 2-3 cm in diameter. Younger stems have hooked thorns and older stems have clusters of woody spines. The leaves are 4–11 cm long and 1.5–4 cm wide, simple, and deciduous in the dry season. The flowers are white, cream, or pinkish with 2.5–5 cm diameter and strongly scented. This plant has translucent rounded white to pink berries which turn to yellow or orange with the diameter of 2 cm upon ripening. The fruits are edible and containing numerous small seeds. They somewhat resemble the gooseberry in appearance and are of excellent flavor [15, 16]. The leaves are also edible and are a popular vegetable in parts of the Brazilian state of Minas Gerais under the name of ora-pro-nóbis [14].

1.2. Pereskia grandifolia Haw. It is also known as rose cactus or *Rhodocactus grandifolia*. This plant is native to the Northeastern Brazil restingas and is cultivated in tropical and subtropical areas [7]. It is a shrub or small tree, 2–5 m high, with a grayish-brown trunk up to 20 cm in diameter. The spines range from black to brown and their number at each areole gradually increases with age. The new twigs may be spineless while the trunk may have up to 90 spines in areoles, each 2–6.5 cm long. The leaves vary in size from 9 to 23 cm long and the shapes range from elliptic to ovate and obovate-lanceolate. Usually 10–15 flowers of dense inflorescence develop at the ends of stems, but sometimes there are 30 or more. The flowers are pink-purple and look like rose with 3–5 cm diameter [12]. The leaves of *P. grandifolia* are edible [11].

1.3. Pereskia bleo (Kunth) DC. *P. bleo* is also known as *Cactus bleo* and has been commonly used for a variety of medicinal and non-medicinal purposes in different countries [1, 2]. However, to the best of our knowledge, a comprehensive review of *P. bleo* is not available. The objective of this paper is to provide a comprehensive review of the botanical characteristics, traditional usage, phytoconstituents, pharmacological activities, and safety of *P. bleo*. Such information will serve as a useful resource for the proper usage of this plant and for future research.

2. Method

Internet sources including MEDLINE (via Pubmed), Science direct, Scopus and Google scholar, and China Journals Full-Text Database (via CNKI) were searched for publications on this plant. The following keywords were used: *Pereskia bleo, Pereskia panamensis, Pereskia corrugata, Rhodocactus corrugatus, Rhodocactus bleo, Cactus panamensis, Cactus bleo*, Spinach cactus, wax rose, Perescia, and Chinese rose. No restriction on the language and date of publication was implemented. In addition, available books and eBooks in the National University of Singapore (NUS) libraries were manually searched for the relevant information.

3. Results and Discussion

3.1. Botanical Characteristics. *P. bleo* belongs to the order of *Caryophyllales Juss. ex Bercht. & J. Presl*, superorder of *Caryophyllanae Takht* and subclass of *Magnoliidae Novák ex Takht*. It is in the Cactaceae family, *Peresioideae* subfamily, and *Pereskia* Mill genus [44, 45]. In the International Plant Nomenclature Index (IPNI) [46], its ID code is 273592-2 and its basionym is *Cactus bleo* (Kunth). Basionym name is defined as "previously published legitimate name-bringing or epithet-bringing synonym from which a new name is formed for a taxon of different rank or position taxon of different rank or position" [17]. The scientific and common names of *P. bleo* are listed in Table 2. This plant is also known as "Pokok Jarum Tujuh Bilah" in Malay and "Cak Sing Cam" or "Qi Xing Zhen (七星针)" in Chinese [8, 40]. Its Chinese name literally means "seven stars needle" [7].

P. bleo originates from Mesoamerica (Panama), Western South America (Columbia) [1, 2, 6, 12] and is distributed in tropical and subtropical regions [1, 2]. It is a deciduous, shrubby, tree-like plant with a height of 0.6–8 m. The trunk reaches 10 cm in diameter and bears very large fascicle of spines when it is young. However, the trunk becomes naked when turning old. Young branches are red and leafy and often bear 5–7 black spines up to 1 cm in length. The spines reach 2 cm on the older stems. The leaves are thin, oblong to oblanceolate, glossy, and succulent, 6–21 cm long, and 2–7 cm wide [2]. The flowers are orange-red and grouped in 2–4 terminally and laterally. The fruits are yellow, thick walled, fleshy, and glossy and look like conical berries at maturity, up to 5 × 5 cm in size, turbinate, and containing 6–8 mm in diameter dark brown or black color seeds [1, 19, 31]. It can be propagated by stem cutting or seeds [12].

This species was collected by Bonpland during Humboldt's trip through the new world and was described and published by Kunth in 1823 [2]. In some older books and herbaria, it was confused with *Pereskia grandifolia* (*P. grandifolia*) [20] because both plants are vegetatively similar [31]. In addition, *P. bleo* and *P. grandifolia* are the only exceptions of *Pereskia* which grow in areas receiving considerably high annual rainfall more than 187 mm per wet month. Other *Pereskia* species grow in dry areas [3]. The two species can be distinguished by the leaves, flowers, and spines. *P. bleo* has thinner, corrugated leaves and orange-red flowers, with shorter spines compared to *P. grandifolia*. In contrast,

Table 2: Scientific and common names of *P. bleo*.

Names	References
Scientific names	
Cactus bleo Kunth	[2, 12, 17–19]
Pereskia bleo (Kunth) DC	[1, 2, 12, 17, 19–21]
Pereskia corrugata Cutak	[17, 21]
Pereskia panamensis F.A.C. Weber	[2, 17]
Rhodocactus bleo (Kunth) F.M. Kunth	[17, 19, 21]
Rhodocactus corrugatus (Cutak) Backeberg	[17]
Common names	
Butarrar (Kuna Indian)	[22]
Cak Sing Cam, Qi xing zhen (Chinese)	[1, 8, 23]
Chupa, Chupa melon, Najií, Najii De Culebra, Najú de esoubas, and Bleo de chupa (Spanish)	[2, 21, 24]
Perescia	[7]
Pokok Jarum Tujuh Bilah (Malay)	[2, 25]
Rose cactus, Bleo, Chinese rose, Spinach cactus, wax rose, and orange rose cactus (English)	[1, 6, 7, 21, 24, 26]

Table 3: Traditional usage and methods of preparation of *P. bleo*.

Purpose	Method of preparation	References
Detoxification and prevention of cancer	Making tea by boiling the leaves and/or the fruit and then drinking it warm or cool	[27–30]
Dietary purposes and health maintenance	Eating the raw leaf, flower, and fruit	[19, 28]
Health maintenance and revitalizing the body	Making juice from the leaves and boiling in water and drinking every morning	[30]
To alleviate muscleache	Making decoction from the leaves and then using as a warm bath for muscle ache	[29]
To alleviate stomachache	Preparing "ina kuamakalet": the inflorescence is mixed with the excrements of red ants by using a special mortar and then moistened with water. The resulted mass is moulded to oval shape objects which are dried in sun. When using the remedy, these balls are rubbed in a small container with a small amount of water.	[29]
To treat hemorrhoid, hypertension, diabetes, infections, headache, and inflammatory conditions (rheumatism and asthma)	No information is available in the literature.	[28, 31, 32]
To neutralize the effects of the snakebites	No information is available in the literature.	[33]

P. grandifolia has thicker, uncorrugated leaves, pink to purplish-pink flowers and longer but fewer spines on the stems [11]. Figure 1 shows the photographs of different parts of *P. bleo* and *P. grandifolia*. Although they are different species, anatomical similarities in these two species support the evolution theory for cactus family [18].

3.2. Traditional Usage. *P. bleo* has been used for various purposes. In some areas, it is used as a food spice [1, 7]. This plant has been eaten raw as vegetables by some people in Malaysia and China or taken as a concoction brewed from fresh leaves [19, 36]. In addition, it is taken for detoxification and revitalizing the body [27, 28, 40]. Its fruit is consumed by some ethnic groups in Panama as a wild fruit [26]. The leaves of *P. bleo* have been traditionally used to treat cancer, hemorrhoid, hypertension, diabetes [32, 40], infections, gastric pain, headache, ulcer, and inflammatory conditions like rheumatism and asthma [28, 31]. Indigenous Colombians have used *P. bleo* to neutralize the effects of snakebites [33], to relax spastic muscles, and to alleviate muscle aches [29]. Apart from dietary and medicinal uses, this plant is a suitable barrier hedge because of its sharp spines, strong stem, and insect repellant properties [21]. In Central America, Kuna Indians used the crushed leaves to clarify drinking water [12]. Different methods of preparation have been reported for the plant. It is usually taken raw or as a decoction of its fresh leaves. Table 3 shows the traditional usage and different preparation methods of *P. bleo*. To the best of our knowledge, information on the specific preparation methods for some of the indicated traditional usages is not available.

3.3. Phytochemistry. The leaves are the most commonly used part of *P. bleo* in traditional medicine. Hence, they have been more studied compared to the other plant parts. So far, 20

Table 4: Reported phytoconstituents in the leaves and fruits of *P. bleo*.

Plant part	Class of the constituents	Constituents	Reference
Leaves	Alkaloids	3,4-Dimethoxy-β-phenethylamine	[34]
		3-Methoxytyramine	[34]
		Tyramine	[34]
	Fatty acids	Methyl palmitate	[31]
		Methyl linoleate	
		Methyl α-linoleate	
	Flavonoid	Vitexin	[35]
	Phytosterol glycoside	β-Sitosterol glucoside	[35]
	Lactone	Dihydroactinidiolide	[28]
	Phenolic compounds	2,4-Ditert-butylphenol	[36]
		α-Tocopherol	[36, 37]
		Catechin	[37]
		Epicatechin	[37]
		Quercetin	[37]
		Myricetin	[37]
	Sterols	Campesterol	
		Stigmasterol	[28]
		β-Sitosterol	[36]
	Terpenoids	β-Carotene	[37]
		Phytol	[36]
Fruit	Carotenoids	Lutein (β,é-carotene-3,3′-diol)	[26, 37]
		Zeaxanthin (β,β-carotene-3,3′-diol)	

Table 5: Percentage (% w/w) of mineral contents in the leaves of *P. bleo* [38].

Mineral elements	Percentage weight (%)
Carbon	50.6
Oxygen	35.4
Magnesium	0.4
Phosphorus	0.4
Sulfur	1.5
Chlorine	1.2
Potassium	10.2
Aluminium	ND*
Calcium	0.3
Silicon	ND
Ferrum (Iron)	ND

*ND: not detected.

phytoconstituents have been reported in the leaves and two components from the fruit as shown in Table 4. These components include alkaloids, fatty acids, glycosides, lactones, phenolic, sterol, terpenoid, and carotenoid compounds. The major isolated component from *P. bleo* leaves is phytol [27]. In addition, Doetsch et al. [34] reported the isolation of three alkaloids, namely, 3,4-dimethoxy-β-phenethylamine (mescaline), 3-methoxytyramine, and tyramine, from the leaves of this plant. Vitamin E (α-tocopherol) [36, 37] which is well known for its antioxidant properties; 2,4-ditert-butylphenol and dihydroactinidiolide were isolated through bioassay-guided fractionation by Malek et al. [36]. Murillo et al. [26] analyzed the fruit of *P. bleo* for lutein and zeaxanthin contents. The total carotenoid content of the fruit was found to be 13.3 μg/g, making *P. bleo* fruit a high carotenoid food source among the wild fruits in Panama.

The mineral content of the leaves was also investigated by using energy-dispersive X-ray microanalysis. Table 5 shows the weight percentage of the minerals reported by Abbdewahab et al. [38]. As can be seen, *P. bleo* leaves are rich in potassium (10.16%). This is more than two times of the potassium content of tomato (4.5%), a vegetable known to be high in potassium [50]. It has been shown that a high potassium diet has an important role in lowering blood pressure [51]. Therefore, it might be one of the possible reasons for the traditional usage of *P. bleo* as a treatment for hypertension [31].

3.4. Pharmacological Properties. Pharmacological evaluation of plants is based on their traditional uses. Cancer is one of the main causes of mortality and morbidity. Since *P. bleo* is traditionally used to prevent and treat cancer [28, 30, 40], it has been most studied for its antiproliferative and cancer protective properties [8, 22, 28, 32, 36, 39, 40]. This is followed by investigations of its antimicrobial and antiparasitic effects *in vitro* [8, 38, 41–43, 52]. The snake

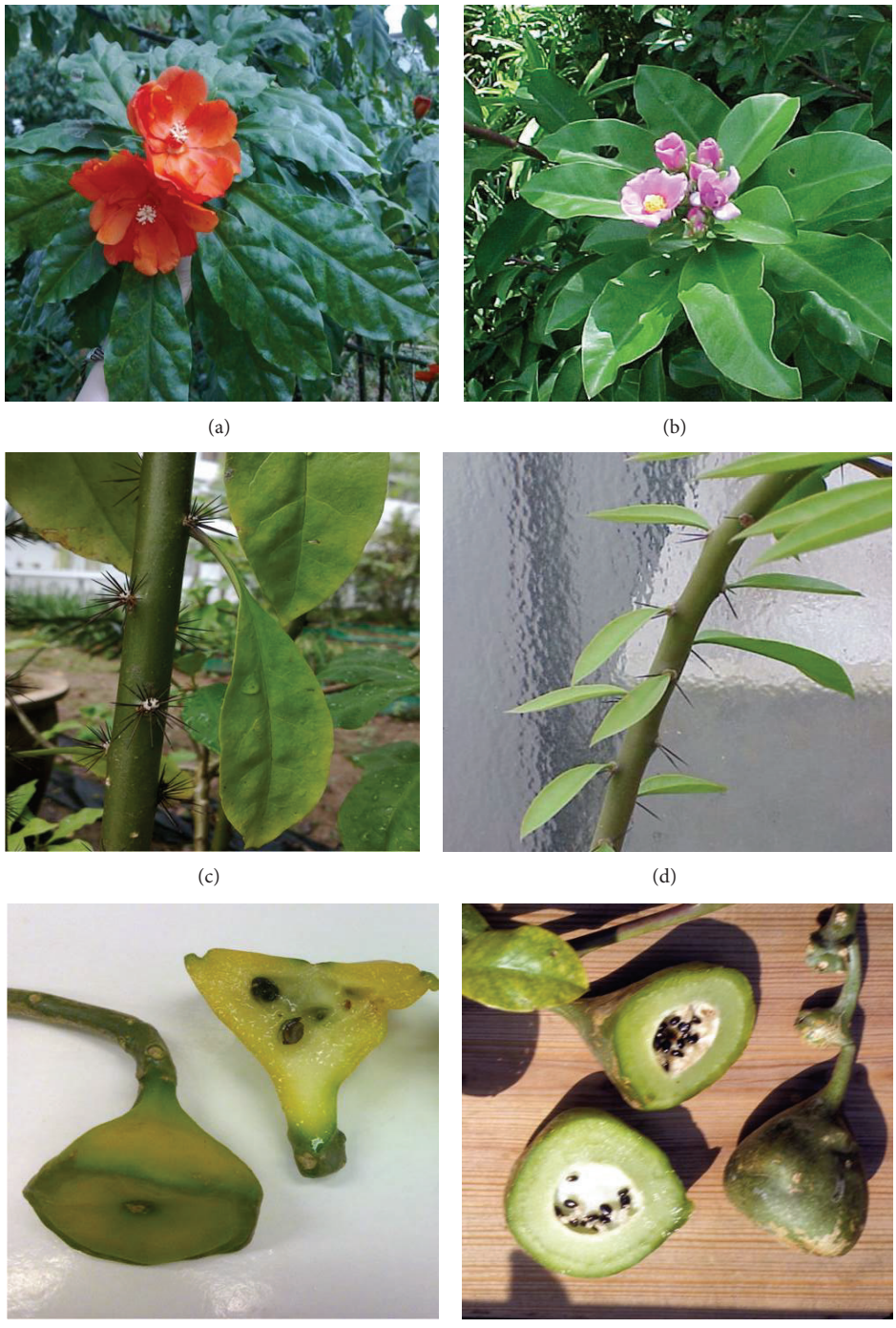

FIGURE 1: Photographs of different plant parts of *P. bleo* and *P. grandifolia*. (a) Flower of *P. bleo*, (b) lower of *P. grandifolia* [47], (c) stem and spines of *P. bleo*, (d) stem and spines of *P. grandifolia* [48], (e) ripe fruits and seeds of *P. bleo*, and (f) ripe fruits and seeds of *P. grandifolia* [49].

venom neutralizing properties [33], antinociceptive effects [35], and toxicity [22, 31] of this plant have been evaluated through *in vivo* studies.

3.4.1. Antiproliferative Properties. The effects of different *P. bleo* extracts have been reported on various cell lines *in vitro*. The crude methanol extract and its ethyl acetate fraction had significant cytotoxic effects against human nasopharyngeal epidermoid carcinoma cell line (KB) [36]. In addition, the ethyl acetate fraction was more active than the methanol extract against human colon carcinoma (HCT116) and hormone dependent breast carcinoma cell lines (MCF7) [36]. Table 6 shows the reported IC_{50} values (μg/mL) for the antiproliferative effects of *P. bleo* extracts and fractions.

Table 6: IC_{50} values (μg/mL) of *P. bleo* leaf extracts and fractions on different cell lines.

Cell line	Extracts and fractions (IC_{50}: μg/mL)					Positive control (IC_{50}: μg/mL)	Negative control	References
	Methanol	Water	Hexane	Dichloromethane	Ethylacetate			
4T1	>50	>50	NA	NA	NA	Cisplatin (NA)	NA	[32]
CasKi	40.5	—	89.5	NA	58	Doxorubicin (6×10^{-3})	NA	[36]
CEM-ss	—	NA	—	—	—	NA	VC	[8]
HT29 and HCT116	>30	NA	>30	>30	>30	NA	VC	[8]
	41.6	—	67.5	NA	22	Doxorubicin (3.6×10^{-1})	NA	[36]
KB	6.5	—	28	NA	4.5	Doxorubicin (1.2×10^{-2})	NA	[36]
MCF-7	>30	NA	>30	>30	>30	NA	VC	[8]
	39	—	25	NA	28	Doxorubicin (7.5×10^{-2})	NA	[36]
MRC-5	—	—	—	NA	—	Doxorubicin (5.5×10^{-1})	NA	[36]
NIH/3T3	≥200	≥200	NA	NA	NA	Cisplatin	NA	[32]
Saos-2	—	NA	NA	NA	NA	Cisplatin	NA	[39]
T-47D	2	NA	NA	NA	NA	DNase I	VC	[40]
V79	—	NA	NA	NA	NA	Nitracrine	VC	[22]

IC_{50}: 50% of maximum cell inhibition. $IC_{50} < 20$ μg/mL is considered active, $100 > IC_{50} > 20$ μg/mL is relatively active, and $IC_{50} > 100$ is not active [8].
(—): no activity.
4T1: mouse mammary cancer cell line; CasKi: human cervical carcinoma cell line; CEM-ss: human T-4 lymphoblastoid cell line; HT29 and HCT116: human colon carcinoma cell line; KB: human nasopharyngeal epidermoid carcinoma cell line; MCF-7: hormone dependent breast carcinoma cell line; MRC-5: normal human fibroblast cell lines; NIH/3T3: normal mouse fibroblast cell line; Saos-2: human osteosarcoma cell line; T-47D: human breast carcinoma cell line; V79: Chinese hamster lung fibroblasts.
NA: not available.
VC: vehicle control.

Table 7: Reported IC_{50} values (μg/mL) of selected *P. bleo* phytoconstituents on human cell lines [28].

Compound	IC_{50} (μg/mL) of different cell lines					
	KB	MCF7	CasKi	HCT 116	A549	MRC-5
Dihydroactinidiolide	6.7	30	40	5	97	91.3
β-sitosterol	>100	72	62	>100	78	>100
2,4-ditertbutylphenol	0.81	5.75	4.5	29	6	20
α-tocopherol	8	7.5	6	31	6	30.5
Phytol	7.1	34	18	100	31	74.1
Mixture of sterols	>100	>100	>100	>100	>100	>100
Doxorubicin	1.3×10^{-2}	7.6×10^{-2}	6.0×10^{-3}	3.6×10^{-1}	2.2×10^{-1}	5.5×10^{-1}

A549: human lung carcinoma cell line, CasKi: human cervical carcinoma cell Line, HCT116: human colon carcinoma cell Line, KB: human nasopharyngeal epidermoid carcinoma cell Line, MCF-7: hormone dependent breast carcinoma cell Line, MRC-5: normal human fibroblast cell Lines.

Gupta et al. [22] reported high tumor inhibition activity in "potato disc inhibition assay" using crown gall tumors (LC_{50} 77 ppm). Their result was accompanied by a significant DNA peak reduction in the DNA intercalation test for the methanol extract of the whole plant.

To date, no report is available on the *in vivo* antiproliferative activities of *P. bleo*.

(1) *Cytotoxic Components*. Some of the cytotoxic components in *P. bleo* have been reported. Table 7 shows the reported IC_{50} (μg/mL) values of these components in the different human cell lines. The effects of these compounds and the mixture of the isolated sterols were not as high as doxorubicin, that is, a chemotherapy drug [28]. In another study, phytol isolated from *P. bleo* leaves was found to have a significant antitumor activity against some mouse cancer cell lines [36].

(2) *Proposed Antiproliferative Mechanism*. The antiproliferative activity of the methanol extract of *P. bleo* against human breast carcinoma cell line (T-47D) was found to be apoptotic in nature through the activation of caspase-3 and c-myc pathways [40]. Caspase-3 and c-myc are frequently activated death proteases which catalyze the specific cleavage of many key cellular proteins. They are also essential for normal development of the tissues as well as apoptosis in the tissues and cell types [53]. Komiya et al. [54] reported the induction of apoptosis as a mechanism of action for cytotoxic activity of phytol. DNA intercalation is another proposed mechanism of antiproliferative activity for *P. bleo* [22]. However, in some studies, *P. bleo* did not show appreciable cytotoxic effect [32]. Differences in the sources of plants, extraction methods, assay methods, and cell lines can be the possible reasons for these discrepancies. On the other hand, *P. bleo* may contain some prodrugs which are metabolized to the active metabolites. Therefore, further studies are needed to better understand its antiproliferative activity.

Apart from the cytotoxic activities against cancer cell lines, crude methanol extract and its fractions (hexane, water, and ethyl acetate) did not show any cytotoxicity to the normal human fibroblast cell lines, MRC-5 [36].

3.4.2. Antioxidant Activity. The adverse effects of oxidative stress on human health have become a serious issue. Oxidative stress causes production of free radicals in the body that facilitate the development of degenerative diseases such as cardiovascular diseases, cancers, neurodegenerative disorders [55], Alzheimer's, and inflammatory diseases [56]. One solution to this problem is to supplement the diet with antioxidant compounds found in natural plant sources [57]. Hence, in the literature, the antioxidant effects of *P. bleo* were evaluated using different assays as follows.

2,2-Diphenyl-1-picrylhydrazyl Hydrate (DPPH) Assay. The methanol, dichloromethane, ethyl acetate, and hexane extracts of *P. bleo* leaves were tested [8, 25]. The hexane extract exhibited the most effective radical scavenging activity (EC_{50} 210 μg/mL) followed by the ethyl acetate extract (EC_{50} 225 μg/mL). This spectrophotometric assay uses a stable radical 2,2′-diphenylpicrylhydrazyl (DPPH) as a reagent [8, 25].

Ferric Reducing Antioxidant Potential Assay (FRAP). The hexane, water, and methanol extracts of *P. bleo* leaves were found to reduce Fe^{3+}/ferric cyanide complex to the ferrous form. Although the reduction was statistically significant, it was not more than ascorbic acid (vitamin C) and butylated hydroxyanisole (BHA) as positive controls [25]. Hassanbaglou et al. [37] compared the antioxidant activity of the ethyl acetate extract with that of hexane, ethanol, and methanol extracts. They showed that the ethyl acetate extract had significantly higher antioxidant properties compared to the rest of the tested extracts. FRAP measures the ability of test samples to reduce ferric ion to the ferrous form of TPTZ (2,4,6-tripyridyl-s-triazine).

β-Carotene-Linoleic Bleaching Assay. The ethyl acetate extract of *P. bleo* demonstrated the strongest antioxidant activity followed by the methanol extract reported by Sim et al. [25]. In this assay, the linoleate free radicals formed during the reaction are neutralized by antioxidants.

Table 8: Reported effects of *P. bleo* extracts on the growth of selected bacteria and fungi.

Organism	Antibacterial and antifungal effect of the extracts						Positive control	References
	Methanol	Water	Hexane	Dichloroethane	Ethyl acetate	Chloroform		
Bacillus subtilis[a]	–	NA	–	–	–	NA	Streptomycin*	[8]
	–	–	–	NA	–	NA	Gentamicin, ampicillin	[41]
Escherichia coli[b]	NA	NA	–	–	NA	NA	Streptomycin	[38]
	–	NA	NA	–	NA	NA	Streptomycin	[42]
Escherichia coli[a]	–	–	–	NA	–	NA	Gentamicin, ampicillin	[41]
Helicobacter pylori[b]	–	NA	NA	–	NA	NA	Streptomycin	[42]
Klebsiella pneumoniae[b]	–	NA	NA	–	NA	NA	Streptomycin	[42]
Methicillin resistant Staphylococcus aureus[a]	–	NA	–	+++	–	NA	Streptomycin*	[8]
	NA	NA	–	++	NA	NA	Streptomycin	[38]
Mycobacterium smegmatis[b]	–	NA	NA	–	NA	NA	Streptomycin	[42]
Pseudomonas aeruginosa[a]	++	NA	+++	+	+	NA	Streptomycin	[8]
	+	–	–	NA	+	NA	Gentamicin, ampicillin	[41]
Pseudomonas aeruginosa[b]	NA	NA	+++	+	NA	NA	Streptomycin*	[38]
	–	NA	NA	–	NA	NA	Streptomycin	[42]
Salmonella choleraesuis[a]	++	NA	+++	–	–	NA	Streptomycin*	[8]
	NA	NA	+++	–	NA	NA	Streptomycin	[38]
Staphylococcus aureus[b]	–	NA	NA	–	NA	NA	Streptomycin	[42]
Staphylococcus aureus[a]	–	–	–	NA	–	NA	Gentamicin, ampicillin	[41]
Candida albicans[c]	–	–	NA	NA	NA	–	Propiconazole, miconazole	[43]
Candida albicans[b]	–	NA	NA	–	NA	NA	Amphotericin B	[42]
Cladosporium cucumerinum[c]	+	+	NA	NA	NA	+	Propiconazole, miconazole	[43]

[a]The screening for antibacterial effect was carried out by determining the zone of inhibition using paper disc, + stands for activity between 6–9 mm, ++ stands for activity between 9–14 mm, +++ stands for activity more than 14 mm [38].

[b](+) stands for activity at 100 μg/mL for *E. coli*, *S. aureus*, *K. pneumoniae*, *M. smegmatis*, *C. albicance*, *P. aeruginosa* and at 12.5 μg/mL for *H. pylori*, (–) stands for inactive samples.

[c]agar overlay assay and (+) stands for active extracts at 50 μg/mL, (–) stands for inactive extract.

NA: not applicable as there is no report in the literature.

*Streptomycin showed 20 to 23 mm inhibition zone. The rest of the studies did not report the exact value of the inhibition for their positive controls.

In general, although different studies used plant materials from different sources and nonsimilar extraction methods, ethyl acetate and hexane extracts appear to be the strongest antioxidant extracts from the *P. bleo* leaves [8, 25, 37]. Moreover, this antioxidant capacity is strongly associated with the total phenolic compounds and flavonoid content of the plant leaves [25, 37, 58]. The above studies suggest that *P. bleo* has antioxidant properties which can be one of the possible reasons for its traditional usage for detoxification and prevention of cancer.

3.4.3. Antimicrobial Properties. *P. bleo* has been shown to possess antibacterial, antiviral, and antifungal properties *in vitro*. Table 8 shows the effect of *P. bleo* extracts on selected bacteria and fungi. As can be seen, the methanol and hexane extracts demonstrated great antibacterial activities against *Salmonella choleraesuis* and *Pseudomonas aeruginosa*. In addition, its dichloromethane extract showed promising antibacterial effect against *Methicillin resistant Staphylococcus aureus* [8, 38]. All of the mentioned bacteria are among the main causes of nosocomial infections and they have been developing antibiotic resistance [59–61]. Therefore, the potential antibacterial activity of *P. bleo* needs to be further investigated to identify the lead(s) antibacterial component(s).

The antifungal activity of the water and methanol extract of *P. bleo* leaves against *Cladosporium cucumerinum*, a plant pathogenic fungus, has been reported [43], but they were not active against *Candida albicans*, a common human pathogen [42, 43].

The antiviral properties of the water and methanol extracts of *P. bleo* leaves were evaluated against *Herpes Simplex Virus*-I (HSV-1) and *Human Immunodeficiency Virus* (HIV) by Matsuse et al. [62]. Both of the extracts demonstrated anti-HIV activity. However, the result of this study was not promising because of the low selectivity index of 0.94. Besides, in another study by Hattori et al. [63], the same extracts did not demonstrate any antiviral activity against HSV-1. In general, the available data on the antiviral activity of *P. bleo* is neither sufficient nor conclusive. Therefore, further research needs to be carried out.

3.4.4. Antiparasitic Properties. The only antiparasitic investigation on *P. bleo* was reported by Marston et al. [52]. In their study, the chloroform, methanol, and water extracts of this plant did not exert any antiparasitic activity against schistosomiasis.

3.4.5. Neutralizing Snake Venom. Otero et al. [33] evaluated the neutralizing effect of the ethanol extract of *P. bleo* on hemorrhagic activity of "*Bothrops atrox* venom" in mice. This extract did not show any neutralizing effect against the tested venom.

3.4.6. Antinociceptive Properties. Wahab et al. [35] evaluated the antinociceptive activity of the ethanol extract and its fractions using two *in vivo* analgesic models: peripheral formalin-induced licking and acetic acid-induced abdominal writhing. They showed that the ethanol extract, hexane fraction, dichloromethane fraction, and ethyl acetate fraction of *P. bleo* had moderate antinociceptive effects. However, no compound was identified in their study.

3.5. Toxicity Studies. Acute toxicity effect of the leave's extracts of *P. bleo* was evaluated by *in vitro* and *in vivo* studies. Er et al. [32] showed that the water extract may form mutagenic compound(s) upon metabolization by the liver enzymes *in vitro*. In another study by Gupta et al. [22], the methanol extract of the whole plant had moderate toxicity in brine shrimp toxicity assay (LD_{50} 77 ppm). In the only *in vivo* study by Sim et al. [31], the methanol extract did not have any toxicity effect on ICR mice (LD_{50} > 2500 mg/kg). Although animal models have around 70–80% predictability for human toxicities [64, 65], the long term toxicity and the mutagenicity of metabolites of *P. bleo* should be further investigated.

4. Conclusion

A comprehensive review on *Pereskia bleo* has been presented. It provides an overview of the botanical characteristics, traditional usage, phytoconstituents, pharmacological activities, and safety of *P. bleo*. The current review highlights the association between the traditional usage of the plant and the reported anticancer, antibacterial, and antinociceptive effects tested in different studies. Although *P. bleo* has been traditionally used for a variety of therapeutic and prophylactic purposes, only a few of them has been investigated. Hence, more research is warranted to further study its biological activities and chemical properties to understand its traditional usage and to develop novel therapeutics. Understanding the traditional uses, knowing the available scientific evidences, and identifying the gaps in research will allow the proper translation of promising research results into a safe and efficacious usage of herbal medicine and discovery of new therapeutics. It will also assist in setting appropriate policy and guidelines in the usage of herbal medicine.

Conflict of Interests

All authors declare that there is no conflict of interests regarding the publication of this paper.

Acknowledgments

Funding from the National University of Singapore (NUS) research Grant (R-148-000-137-112 to KHL) and Leeward Pacific Pte Ltd. (R-148-000-140-592 to KHL) and research scholarship from the Singapore International Graduate Award (SINGA, SZ) are acknowledged.

References

[1] C. Wiart, *Medicinal Plants of Asia and the Pacific: Drugs of the Future*, World Scientific, Singapore, 2006.

[2] N. L. Britton and J. N. Rose, *The Cactaceae, Descriptions and Illustrations of Plants of the Cactus Family*, Dover Publications, Washington, DC, USA, 2009.

[3] E. J. Edwards and M. J. Donoghue, "Pereskia and the origin of the cactus life-form," *American Naturalist*, vol. 167, no. 6, pp. 777–793, 2006.

[4] E. J. Edwards, R. Nyffeler, and M. J. Donoghue, "Basal cactus phylogeny: implications of *Pereskia* (Cactaceae) paraphyly for the transition to the cactus life form," *American Journal of Botany*, vol. 92, no. 7, pp. 1177–1188, 2005.

[5] R. M. Ogburn and E. J. Edwards, "Anatomical variation in Cactaceae and relatives: trait lability and evolutionary innovation," *American Journal of Botany*, vol. 96, no. 2, pp. 391–408, 2009.

[6] C. M. Boo, C. L. Ou-Yang, and K. Omar-Hor, *1001 Garden Plants in Singapore*, National Parks Board, Singapore, 2nd edition, 2007.

[7] Singapore Npark Board, NParks Flora&Founa web, 2010, https://florafaunaweb.nparks.gov.sg/Special-Pages/plant-detail.aspx?id=2324#.

[8] S. I. A. Wahab, A. B. Abdul, S. M. Mohan, A. S. Al-Zubairi, M. M. Elhassan, and M. Y. Ibrahim, "Biological activities of *Pereskia bleo* extracts," *International Journal of Pharmacology*, vol. 5, no. 1, pp. 71–75, 2009.

[9] R. T. Bárcenas, C. Yesson, and J. A. Hawkins, "Molecular systematics of the Cactaceae," *Cladistics*, vol. 27, no. 5, pp. 470–489, 2011.

[10] K. Y. Chong, H. T. Tan, and R. T. Corlett, *A Checklist of the Total Vascular Plant Flora of Singapore: Native, Naturalised and Cultivated Species*, Raffles Museum of Biodiversity Research, National University of Singapore, Singapore, 2009, http://rmbr.nus.edu.sg/raffles_museum_pub/flora_of_singapore_tc.pdf.

[11] A. M. Sri Nurestri, K. S. Sim, and A. W. Norhanom, "Phytochemical and cytotoxic investigations of *Pereskia grandifolia* Haw. (Cactaceae) leaves," *Journal of Biological Sciences*, vol. 9, no. 5, pp. 488–493, 2009.

[12] E. Anderson, *The Cactus Family*, pp. 566–568, Timber Press, Puritana, Ore, USA, 1st edition, 2001.

[13] R. P. Wunderlin and B. F. Hansen, "Atlas of Florida Vascular Plants," 2008, http://www.plantatlas.usf.edu/.

[14] N. P. Taylor, D. Zappi, P. Braun, and M. Machado, "*Pereskia aculeata*. Iucn Red List of Threatened Species. Version 2013. 2," 2013, http://www.iucnredlist.org.

[15] E. Pooley, *A Field Guide to Wild Flowers KwaZulu Natal and the Eastern Region*, Natal Flora Publications Trust, Durban, South Africa, 1999.

[16] A. G. I. Natural Heritage Trust, "Weed Management Guide, Leaf cactus, *Pereskia aculeata*," 2003, http://www.environment.gov.au/biodiversity/invasive/weeds/publications/guidelines/alert/pubs/p-aculeata.pdf.

[17] Tropicos, "Missouri Botanical Garden (MBG)," 2012, http://www.tropicos.org/Name/5100482.

[18] B. E. Leuenberger, "*Pereskia*, Maihuenia, and Blossfeldia-taxonomic history, updates, and notes," *Haseltonia*, no. 14, pp. 54–93, 2008.

[19] J. Nugent, "Permaculture Plants, agaves and cacti," 2007, http://books.google.com.sg/books?id=YVwMM2OdO34C&q=Pereskia+bleo#v=snippet&q=Pereskia%20bleo&f=false.

[20] B. E. Leuenberger, "Humboldt & Bonpland's Cactaceae in the herbaria at Paris and Berlin," *Willdenowia*, vol. 32, pp. 137–153, 2002.

[21] K. A. Liamas, *Tropical Flowering Plants: A Guide to Identification and Cultivation*, Timber Press, Portland, Ore, USA, 2003.

[22] M. P. Gupta, A. Monge, G. A. Karikas et al., "Screening of Panamanian medicinal plants for brine shrimp toxicity, crown gall tumor inhibition, cytotoxicity and DNA intercalation," *Pharmaceutical Biology*, vol. 34, no. 1, pp. 19–27, 1996.

[23] C. C. Kazama, D. T. Uchida, K. N. Canzi et al., "Involvement of arginine-vasopressin in the diuretic and hypotensive effects of *Pereskia grandifolia* Haw. (Cactaceae)," *Journal of Ethnopharmacology*, vol. 144, no. 1, pp. 86–93, 2012.

[24] USDA, "National Genetic Resources Program, Germplasm Resources Information Network—(GRIN)," [Online Database], 2012, http://www.ars-grin.gov/cgi-bin/npgs/html/tax_search.pl?Pereskia+bleo%.

[25] K. S. Sim, A. M. Sri Nurestri, and A. W. Norhanom, "Phenolic content and antioxidant activity of crude and fractionated extracts of *Pereskia bleo* (Kunth) DC. (Cactaceae)," *African Journal of Pharmacy and Pharmacology*, vol. 4, no. 5, pp. 193–201, 2010.

[26] E. Murillo, A. J. Meléndez-Martínez, and F. Portugal, "Screening of vegetables and fruits from Panama for rich sources of lutein and zeaxanthin," *Food Chemistry*, vol. 122, no. 1, pp. 167–172, 2010.

[27] K. Hostettmann, A. Marston, M. Maillard, and M. Hamburger, *Phytochemistry of Plants Used in Traditional Medicine*, pp. 373–376, Oxford University Press, Oxford, UK, 1995.

[28] S. N. A. Malek, S. K. Shin, N. A. Wahab, and H. Yaacob, "Cytotoxic components of *Pereskia bleo* (Kunth) DC. (Cactaceae) leaves," *Molecules*, vol. 14, no. 5, pp. 1713–1724, 2009.

[29] M. P. Gupta, A. Correa, D. Mireya et al., "Medicinal plant inventory of Kuna Indians: part 1," *Journal of Ethnopharmacology*, vol. 40, no. 2, pp. 77–109, 1993.

[30] A. Rahmat, F. P. Saib, and N. A. Buslima, "Comparing the effect of ficus benjamina extract and *Pereskia* saecnarosa extract on tthe level of micro and macro minerals in normal and induced liver cancer rats," in *Proceedings of the 4th International Conference on Biomedical Engineering in Vietnam*, pp. 208–212, 1980.

[31] K. S. Sim, A. M. Sri Nurestri, S. K. Sinniah, K. H. Kim, and A. W. Norhanom, "Acute oral toxicity of *Pereskia bleo* and *Pereskia grandifolia* in mice," *Pharmacognosy Magazine*, vol. 6, no. 21, pp. 67–70, 2010.

[32] H. M. Er, E. Cheng, and A. K. Radhakrishnan, "Anti-proliferative and mutagenic activities of aqueous and methanol extracts of leaves from *Pereskia bleo* (Kunth) DC (Cactaceae)," *Journal of Ethnopharmacology*, vol. 113, no. 3, pp. 448–456, 2007.

[33] R. Otero, V. Núñez, J. Barona et al., "Snakebites and ethnobotany in the northwest region of Colombia, part III: neutralization of the haemorrhagic effect of Bothrops atrox venom," *Journal of Ethnopharmacology*, vol. 73, no. 1-2, pp. 233–241, 2000.

[34] P. W. Doetsch, J. M. Cassady, and J. L. McLaughlin, "Cactus alkaloids: XL. Identification of mescaline and other β-phenethylamines in *Pereskia*, Pereskiopsis and Islaya by use of fluorescamine conjugates," *Journal of Chromatography A*, vol. 189, no. 1, pp. 79–85, 1980.

[35] I. R. A. Wahab, C. C. Guilhon, P. D. Fernandes, and F. Boylan, "Anti-nociceptive activity of *Pereskia bleo* Kunth. (Cactaceae) leaves extracts," *Journal of Ethnopharmacology*, vol. 144, no. 3, pp. 741–746, 2012.

[36] S. N. A. Malek, N. A. Wahab, H. Yaacob et al., "Cytotoxic activity of *Pereskia bleo* (Cactaceae) against selected human cell lines," *International Journal of Cancer Research*, vol. 4, no. 1, pp. 20–27, 2008.

[37] B. Hassanbaglou, A. A. Hamid, A. Roheeyati et al., "Antioxidant activity of different extracts from leaves of *Pereskia bleo* (Cactaceae)," *Journal of Meidinal Plants Research*, vol. 6, no. 15, pp. 2932–2937, 2012.

[38] S. I. Abbdewahab, N. M. Ain, A. B. Abdul, M. M. E. Taha, and T. A. T. Ibrahim, "Energy-dispersive X-ray microanalysis of elements' content and antimicrobial properties of *Pereskia bleo* and *Goniothalamus umbrosus*," *African Journal of Biotechnology*, vol. 8, no. 10, pp. 2375–2378, 2009.

[39] S. Y. Liew, E. J. Stanbridge, K. Yusoff, and N. Shafee, "Hypoxia affects cellular responses to plant extracts," *Journal of Ethnopharmacology*, vol. 144, no. 2, pp. 453–456, 2012.

[40] M. L. Tan, S. F. Sulaiman, N. Najimuddin, M. R. Samian, and T. S. T. Muhammad, "Methanolic extract of *Pereskia bleo* (Kunth) DC. (Cactaceae) induces apoptosis in breast carcinoma, T47-D cell line," *Journal of Ethnopharmacology*, vol. 96, no. 1-2, pp. 287–294, 2005.

[41] K. Philip, S. N. A. Malek, W. Sani et al., "Antimicrobial activity of some medicinal plants from Malaysia," *American Journal of Applied Sciences*, vol. 6, no. 8, pp. 1613–1617, 2009.

[42] T. Rüegg, A. I. Calderón, E. F. Queiroz et al., "3-farnesyl-2-hydroxybenzoic acid is a new anti-Helicobacter pylori compound from *Piper multiplinervium*," *Journal of Ethnopharmacology*, vol. 103, no. 3, pp. 461–467, 2006.

[43] L. Rahalison, M. Hamburger, K. Hostettmann et al., "Screening for antifungal activity of Panamanian plants," *International Journal of Pharmacognosy*, vol. 31, no. 1, pp. 68–76, 1993.

[44] A. P. D. Candolle, "*Pereskia bleo* (Kunth) DC," 2011, http://www.tropicos.org/Name/5100482.

[45] USDA, "Taxon: *Pereskia bleo*," 2013, http://www.ars-grin.gov/cgi-bin/npgs/html/tax_search.pl?Pereskia+bleo%.

[46] IPNI, "International Plant Names Index," 2005, http://www.ipni.org/ipni/plantNameByVersion.do?id=273592-2&version=1.3.

[47] M. Gardener, "Tropical plants library online," 2014, http://mgonline.com/articles/exotics.aspx.

[48] S. Kurt, "Stem of *P. grandifolia*," 2014, http://www.biolib.de/.

[49] NRCS, "Natural Resources and Conservation Service of USDA, Plant profile of *P. grandifolia* Haw," 2013, http://plants.usda.gov/core/profile?symbol=PEGR14#.

[50] D. C. Sanders, A. S. Grayson, and T. J. Monaco, "Mineral content of tomato (*Lycopersicon esculentum*) and four competing weed species," *Weed Science*, vol. 29, no. 5, pp. 590–593, 1981.

[51] J. M. Geleijnse, J. C. Witteman, A. A. Bak, J. H. den Breeijen, and D. E. Grobbee, "Reduction in blood pressure with a low sodium, high potassium, high magnesium salt in older subjects with mild to moderate hypertension," *British Medical Journal*, vol. 309, no. 6952, pp. 436–440, 1994.

[52] A. Marston, G. Dudan, M. P. Gupta, P. N. Solis, M. D. Correa, and K. Hostettmann, "Screening of Panamanian plants for molluscicidal activity," *Pharmaceutical Biology*, vol. 34, no. 1, pp. 15–18, 1996.

[53] A. G. Porter and R. U. Jänicke, "Emerging roles of caspase-3 in apoptosis," *Cell Death and Differentiation*, vol. 6, no. 2, pp. 99–104, 1999.

[54] T. Komiya, M. Kyohkon, S. Ohwaki et al., "Phytol induces programmed cell death in human lymphoid leukemia Molt 4B cells," *International Journal of Molecular Medicine*, vol. 4, no. 4, pp. 377–380, 1999.

[55] M. Gerber, M. C. Boutron-Ruault, S. Hercberg, E. Riboli, A. Scalbert, and M. H. Siess, "Food and cancer: state of the art about the protective effect of fruits and vegetables," *Bulletin du Cancer*, vol. 89, no. 3, pp. 293–312, 2002.

[56] V. di Matteo and E. Esposito, "Biochemical and therapeutic effects of antioxidants in the treatment of Alzheimer's disease, Parkinson's disease, and amyotrophic lateral sclerosis," *Current Drug Targets-CNS & Neurological Disorders*, vol. 2, no. 2, pp. 95–107, 2003.

[57] P. Knekt, R. Jarvinen, A. Reunanen, and J. Maatela, "Flavonoid intake and coronary mortality in Finland: a cohort study," *British Medical Journal*, vol. 312, no. 7029, pp. 478–481, 1996.

[58] R. A. Mustafa, A. Abdul Hamid, S. Mohamed, and F. A. Bakar, "Total phenolic compounds, flavonoids, and radical scavenging activity of 21 selected tropical plants," *Journal of Food Science*, vol. 75, no. 1, pp. C28–C35, 2010.

[59] E. B. Breidenstein, C. de la Fuente-Núñez, and R. E. Hancock, "Pseudomonas aeruginosa: all roads lead to resistance," *Trends in Microbiology*, vol. 19, no. 8, pp. 419–426, 2011.

[60] C. Chu, C.-H. Chiu, W.-Y. Wu, C.-H. Chu, T.-P. Liu, and J. T. Ou, "Large drug resistance virulence plasmids of clinical isolates of *Salmonella enterica* serovar *Choleraesuis*," *Antimicrobial Agents and Chemotherapy*, vol. 45, no. 8, pp. 2299–2303, 2001.

[61] K. Hiramatsu, H. Hanaki, T. Ino, K. Yabuta, T. Oguri, and F. Tenover, "Methicillin-resistant *Staphylococcus aureus* clinical strain with reduced vancomycin susceptibility," *Journal of Antimicrobial Chemotherapy*, vol. 40, no. 1, pp. 135–136, 1997.

[62] I. T. Matsuse, Y. A. Lim, M. Hattori, M. Correa, and M. P. Gupta, "A search for anti-viral properties in Panamanian medicinal plants: the effects on HIV and its essential enzymes," *Journal of Ethnopharmacology*, vol. 64, no. 1, pp. 15–22, 1998.

[63] M. Hattori, T. Nakabayashi, Y. A. Lim et al., "Inhibitory effects of various Ayurvedic and Panamanian medicinal plants on the infection of herpes simplex virus-1 *in vitro* and *in vivo*," *Phytotherapy Research*, vol. 9, no. 4, pp. 270–276, 1995.

[64] I. Kola and J. Landis, "Can the pharmaceutical industry reduce attrition rates?" *Nature Reviews Drug Discovery*, vol. 3, no. 8, pp. 711–716, 2004.

[65] H. Olson, G. Betton, D. Robinson et al., "Concordance of the toxicity of pharmaceuticals in humans and in animals," *Regulatory Toxicology and Pharmacology*, vol. 32, no. 1, pp. 56–67, 2000.

Hindawi Publishing Corporation
Evidence-Based Complementary and Alternative Medicine
Volume 2014, Article ID 586857, 8 pages
http://dx.doi.org/10.1155/2014/586857

Research Article

The Traditional Kampo Medicine Tokishakuyakusan Increases Ocular Blood Flow in Healthy Subjects

Shin Takayama,[1,2] Yukihiro Shiga,[3] Taiki Kokubun,[3] Hideyuki Konno,[3] Noriko Himori,[3] Morin Ryu,[3] Takehiro Numata,[4] Soichiro Kaneko,[4] Hitoshi Kuroda,[5] Junichi Tanaka,[2] Seiki Kanemura,[2] Tadashi Ishii,[2] Nobuo Yaegashi,[4] and Toru Nakazawa[3]

[1] *Comprehensive Education Center for Community Medicine, Tohoku University Graduate School of Medicine, 2-1 Seiryo-Machi, Aoba Ward, Sendai City 980-8575, Japan*
[2] *Department of Education and Support for Community Medicine, Tohoku University Hospital, 1-1 Seiryo-Machi, Aoba Ward, Sendai City 980-8574, Japan*
[3] *Department of Ophthalmology, Tohoku University Graduate School of Medicine, 1-1 Seiryo-Machi, Aoba Ward, Sendai City 980-8574, Japan*
[4] *Department of Obstetrics and Gynecology, Tohoku University Graduate School of Medicine, 1-1 Seiryo-Machi, Aoba Ward, Sendai City 980-8574, Japan*
[5] *Division of General Medicine, Saitama Medical Center, Jichi Medical University, 1-847 Amanumacho, Omiya Ward, Saitama City 330-8503, Japan*

Correspondence should be addressed to Shin Takayama; tatahara1492@gmail.com

Received 21 February 2014; Accepted 22 March 2014; Published 24 April 2014

Academic Editor: Wei Jia

The aim of this study was to examine the effects of oral administration of kampo medical formulas on ocular blood flow (OBF). A crossover protocol was used to randomly administer five grams of yokukansan, tokishakuyakusan (TSS), keishibukuryogan, or hachimijiogan to 13 healthy blinded subjects (mean age: 37.3 ± 12.3 years). The mean blur rate, a quantitative OBF index obtained with laser speckle flowgraphy, was measured at the optic nerve head before and 30 minutes after administration. Blood pressure (BP) and intraocular pressure (IOP) were also recorded. No significant changes were observed in mean BP or IOP after the administration of any of the kampo medical formulas. There was a significant increase in OBF 30 minutes after administration of TSS (100% to 103.6 ± 6.9%, $P < 0.01$). Next, TSS was administered to 19 healthy subjects (mean age: 32.0 ± 11.0 years) and OBF was measured before and 15, 30, 45, and 60 minutes after administration. Plain water was used as a control. OBF increased significantly after TSS administration compared to control ($P < 0.01$) and also increased from 30 to 60 minutes after administration compared to baseline ($P < 0.05$). These results suggest that TSS can increase OBF without affecting BP or IOP in healthy subjects.

1. Introduction

Ocular blood flow (OBF) abnormalities have been reported to play an important role in the pathogenesis of many ocular diseases, including glaucoma and diabetic retinopathy [1–4]. An understanding of these abnormalities is therefore of critical importance in determining the pathophysiological features of these diseases and finding novel treatments.

Japanese kampo medicine has a history spanning more than 1500 years. Kampo medical formulas have been used to treat a variety of physical illnesses and diseases [5], including ocular conditions such as dry eye, blurred vision, decreased visual acuity, and visual field defects [6]. However, the clinical efficacy of kampo medicine has traditionally been evaluated with subjective assessments of symptoms, and there is little quantitative information on the effects of kampo medical

formulas on the eye [7]. A few such studies have suggested that yokukansan (YKS) has an influence on blood flow in the short posterior ciliary artery in rabbits [8] and that hachimijiogan (HJG) has an effect on blood flow in the central retinal artery in humans [9]. Other studies have reported that tokishakuyakusan (TSS) has an inhibitory effect on platelet aggregation and a relaxative effect on vascular smooth muscle [10, 11]. Additionally, a study of erythrocyte aggregability and deformability found that keishibukuryogan (KBG) had an influence on microcirculation [12, 13]. These four kampo medical formulas thus have the potential to influence ocular circulation, but so far, no studies have been conducted to evaluate their effects.

Recently, we have reported that laser speckle flowgraphy (LSFG) and color Doppler imaging can be used to assess the effects of topical medications or acupuncture on OBF, including circulation in the optic nerve head (ONH) and retrobulbar space [14–16]. LSFG allows us to quantify microcirculation in the ONH, the choroid, and the retina simultaneously [17]. It is a noncontact technique based on the laser speckle phenomenon and has been shown to be reliable and reproducible in human eyes, especially in the ONH [18–20]. Furthermore, it can acquire an image of OBF in just a few seconds [17]. We believe that these characteristics make LSFG a suitable instrument for this study's evaluation of dynamic OBF alterations in healthy eyes after the administration of kampo formulas.

Thus, the object of this study was to investigate, with healthy volunteers and LSFG, the effects on OBF of kampo formulas (YKS, TSS, KBG, and HJG) traditionally used for the treatment of eye disease.

2. Methods

2.1. Experiment 1 (Ex. 1)

2.1.1. Subjects. Healthy, nonsmoking volunteers ranging from 20 to 70 years old were recruited from respondents to a poster campaign at Tohoku University Hospital, Miyagi, Japan, between April 2013 and November 2013. Subjects were included in this experiment if baseline intraocular pressure (IOP) was below 22 mmHg in both eyes in a Goldmann applanation tonometry examination, findings were normal in slit lamp and funduscopic examinations, and refractive error was within a range of −8.5 to −0.5 diopters (mean of the included subjects: −2.2 ± 2.0). Subjects were excluded if they had a history of ophthalmic or general disorders, had ocular laser or incisional surgery in either eye, or were receiving systemic or topical medication. Subjects abstained from alcohol and caffeine for at least six hours before the measurements. Both eyes of each participant were monitored. The procedures in all experiments followed the tenets of the Declaration of Helsinki and were approved by the committee of Tohoku University Graduate School of Medicine. Written informed consent was obtained from all participants. Overall, 26 eyes of 13 healthy volunteers (mean age, 37.3 ± 12.3 years; 6 men and 7 women) were included in this experiment.

2.1.2. Study Design. This was a randomized, double-blinded, crossover experiment.

2.1.3. Randomization. No participants or examiners had any knowledge of kampo medicine and they were blinded to the order of administration of the formulas, which was randomized. The washout period between administrations of the formulas was at least one week. All four formulas were administered to each participant over the course of two months.

2.1.4. Measurement of Clinical Parameters. IOP was determined with Goldmann applanation tonometry. Both systemic blood pressure (BP) and pulse rate (PR) were conventionally measured from the left brachial artery at the height of the heart with an automated BP monitor (HEM-759 E, Omron Corporation, Kyoto, Japan). Mean arterial blood pressure (MBP) was calculated from systolic BP (SBP) and diastolic BP (DBP) according to the following formula: MBP = DBP + 0.42 (SBP−DBP) [21–23].

2.1.5. LSFG. The principles of LSFG have previously been described in detail [24, 25]. Briefly, this instrument consists of a fundus camera equipped with a diode laser (830 nm wavelength) and an ordinary charge-coupled device sensor (750 × 360 pixels). This study used the LSFG-NAVI device (Softcare Co., Ltd., Fukutsu, Japan), which has been approved by the Pharmaceuticals and Medical Devices Agency in Japan. Mean blur rate (MBR), a measurement of relative OBF expressed in arbitrary units, is determined using the pattern of speckle contrast produced by the interference of a laser scattered by blood cells moving in the ocular fundus [26]. The MBR images are acquired continuously at the rate of 30 frames per second over a 4-second period. The accompanying analysis software (LSFG Analyzer, version 3.0.43.0) combines all captured images into a composite map of OBF. In this study, we identified the ONH margin and set this area as the region of interest in the software. The software then automatically calculated the MBR in the ONH from the OBF map, as we have described in a previous report [16].

2.1.6. Intervention. One of the four kampo medical formulas was prepared in 50 mL of plain hot water and orally administered to the subject. The kampo medical formulas included YKS, TSS, KBG, and HJG. All were produced by Tsumura and Co. (Tokyo, Japan). The compositions of the formulas, which are all mixtures of dried herbs registered in the Pharmacopoeia of Japan, are as follows. YKS contains 4.0 g Atractylodis Lanceae Rhizoma, 4.0 g Poria, 3.0 g Cnidii Rhizoma, 3.0 g Angelicae Radix, 2.0 g Bupleuri Radix, 1.5 g Glycyrrhizae Radix, and 3.0 g Uncariae Uncis Cum Ramulus; TSS contains 4.0 g Paeoniae Radix, 4.0 g Atractylodis Lanceae Rhizoma, 4.0 g Alismatis Rhizoma, 4.0 g Poria, 3.0 g Cnidii Rhizome, and 3.0 g Angelicae Radix; KBG contains 3.0 g Cinnamomi Cortex, 3.0 g Paeoniae Radix, 3.0 g Persicae Semen, 3.0 g Poria, and 3.0 g Moutan bark; and HJG contains 6.0 g Rehmanniae Radix, 3.0 g Corni Fructus, 3.0 g Dioscoreae Rhizoma, 3.0 g Alismatis Rhizoma, 3.0 g Poria, 2.5 g Moutan Cortex, 1.0 g Cinnamomi Cortex, and 0.5 g Aconiti Tuber.

2.1.7. Testing Protocol. All tests were performed between 6:00 and 8:00 p.m. at an ambient room temperature of 25 degrees

Table 1: Baseline variables in the four study groups (Experiment 1).

Variable	YKS	TSS	KBG	HJG	*P* value
OBF (AU)	24.5 ± 3.5	22.8 ± 2.8	23.4 ± 3.8	23.6 ± 3.8	0.48
IOP (mmHg)	12.9 ± 2.5	14.2 ± 2.4	13.6 ± 2.5	13.2 ± 2.7	0.28
SBP (mmHg)	109.7 ± 10.9	113.3 ± 10.9	111.8 ± 9.2	112.0 ± 14.4	0.95
DBP (mmHg)	64.8 ± 12.0	66.6 ± 9.9	67.3 ± 10.3	64.4 ± 7.6	0.75
MBP (mmHg)	83.7 ± 10.7	85.4 ± 10.0	86.0 ± 9.0	84.4 ± 9.8	0.90
PR (beats/min)	73.6 ± 7.7	75.5 ± 10.7	71.0 ± 8.2	77.2 ± 6.8	0.28

Data are expressed as mean ± standard deviation. Differences between groups were assessed with the Kruskal-Wallis test.

Celsius. On the day of the test, after a slit lamp examination, 0.4% tropicamide (Mydrin M; Santen Pharmaceutical Co., Ltd., Osaka, Japan) was used to dilate the pupil. All subjects received a funduscopic examination, and IOP was measured with Goldmann applanation tonometry. To ensure that systemic hemodynamic conditions in each subject were consistent, all subjects rested in a sitting position for 10 minutes before the start of the investigation, in accordance with previous studies [16–20]. Immediately after the 10-minute rest period, systemic BP, PR, and IOP were recorded, and triplicate measurements of OBF were made with LSFG. The formula was administered, and after 30 minutes, triplicate OBF measurements were made again. The entire procedure took place in a darkened room. Normalized MBR was used for the statistical analysis.

2.1.8. Statistical Analysis. The analysis used percentage values (%) calculated by defining the baseline measurement variables as 100%. The values were the mean ± standard deviation. Measurements of baseline variables made on different days were compared with the Kruskal-Wallis test. The Wilcoxon signed-rank test was used to assess differences in the values before and after kampo administration. All statistical analyses were performed with JMP software (Pro version 10.0.2; SAS Institute Japan, Inc., Tokyo, Japan). The difference was considered significant when the *P* value was less than 0.05.

2.2. Experiment 2 (Ex. 2)

2.2.1. Subjects. The inclusion criteria, recruitment of subjects, and procedures of the test were the same as those in Ex. 1. Overall, 38 eyes of 19 healthy volunteers (mean age: 32.0 ± 11.0 years, male : female = 8 : 11) were included in this experiment.

2.2.2. Study Design. This was a double-blinded, controlled experiment.

2.2.3. Measurement of Clinical Parameters. Measurement of IOP, BP, PR, and OBF was the same as in Ex. 1.

2.2.4. Intervention. Five grams of TSS prepared in 50 mL of hot water was administered to each subject. As a control, 50 mL of plain hot water was also administered to each subject on a different day, with a washout period of at least one week between the administration of TSS and water.

2.2.5. Kampo Diagnostic Questionnaire. A questionnaire was given to the subjects to determine their scores for "qi," "blood," and "fluid," traditional diagnostic criteria used in kampo medicine. The questionnaire was obtained from a kampo manual written by Terasawa [27]. "Qi," "blood," and "fluid" are considered fundamental components of the human body in kampo medicine, and disorders and disease are associated with imbalances of these components. These imbalances are classified as "qi deficiency," "qi stagnation," "qi counter flow," "blood deficiency," "blood stasis," and "fluid retention." [28].

2.2.6. Testing Protocol. The procedures of the test were the same as in Ex. 1. Systemic BP, PR, and OBF were measured just before and 15, 30, 45, and 60 minutes after administration of TSS or water. IOP was recorded before and 60 minutes after administration.

2.2.7. Statistical Analysis. The determination of baseline values was with the same method as in Ex. 1. LSFG values after administration of TSS and water were compared at each time point with a two-way analysis of variance (ANOVA). The repeated ANOVA values and post hoc Dunnett's test were used for a statistical comparison of baseline and postadministration values. Differences were considered significant with a *P* value of less than 0.05.

3. Results

3.1. Ex. 1

3.1.1. Comparison of Baseline Variables of the Subjects. Table 1 summarizes the measurements of the baseline variables in the subjects before the administration of each formula. There were no significant differences in OBF, IOP, SBP, DBP, MBP, or PR between the subjects before they were administered any of the formulas.

3.1.2. Alteration of Systemic Variables, IOP, and OBF after Administration of Each Kampo Formula. No significant changes were observed in IOP or MBP after the administration of any of the kampo formulas. PR significantly decreased after the administration of YKS, TSS, and HJG (Table 2). Thirty minutes after the administration of TSS, LSFG measurements of OBF revealed significant increases (100% to 103.6 ± 6.9%, $P < 0.01$). By contrast, 30 minutes after the administration

Table 2: Alteration of IOP and systemic variables in response to administration of each kampo formula (Experiment 1).

	Variable	Baseline	30 minutes after treatment	P value
YKS	OBF change (%)	100.0 ± 0.0	96.9 ± 6.7	0.05
	IOP (mmHg)	12.9 ± 2.5	13.0 ± 2.9	0.73
	MBP (mmHg)	83.7 ± 10.7	87.8 ± 8.2	0.13
	PR (beats/min)	73.6 ± 7.7	66.9 ± 7.8	<0.01
TSS	OBF change (%)	100.0 ± 0.0	103.6 ± 6.9	<0.01
	IOP (mmHg)	14.2 ± 2.4	14.1 ± 2.5	0.98
	MBP (mmHg)	85.4 ± 10.0	86.8 ± 4.9	0.27
	PR (beats/min)	75.5 ± 10.7	67.0 ± 8.0	<0.01
KBG	OBF change (%)	100.0 ± 0.0	101.8 ± 6.9	0.35
	IOP (mmHg)	13.6 ± 2.5	13.3 ± 2.9	0.17
	MBP (mmHg)	86.0 ± 9.0	86.9 ± 8.9	0.74
	PR (beats/min)	71.0 ± 8.2	66.6 ± 7.9	0.05
HJG	OBF changc (%)	100.0 ± 0.0	100.0 ± 6.9	0.89
	IOP (mmHg)	13.2 ± 2.7	13.1 ± 2.5	0.81
	MBP (mmHg)	84.4 ± 9.8	85.9 ± 6.0	0.74
	PR (beats/min)	77.2 ± 6.8	67.2 ± 7.7	<0.01

Data are expressed as mean ± standard deviation. The Wilcoxon signed-rank test was applied to assess differences in the values before and after kampo administration.

of YKS, KBG, or HJG there were no significant changes in OBF. Additionally, there were no adverse events from administration of any of the kampo medical formulas during the experiment.

3.2. Ex. 2

3.2.1. Comparison of Baseline Variables in the Subjects. Table 3 summarizes the baseline variables of the subjects before administration of water or TSS. There were no significant differences in OBF, SBP, DBP, MBP, or PR, before the administration of either substance, although there was a small, though statistically significant, difference in IOP.

3.2.2. Alteration in OBF after Administration. OBF after the administration of TSS or water was significantly different ($P < 0.01$) (Table 4). OBF increased significantly 30, 45, and 60 minutes after administration of TSS (100% to 104.1 ± 5.3%; $P < 0.05$, 104.2 ± 4.8%; $P < 0.05$, 104.0 ± 5.5%; $P < 0.05$) (Figure 1). According to the results of the kampo diagnostic questionnaire, 5 subjects had "qi deficiency," 3 subjects had "qi stagnation," 6 subjects had "qi counter flow," 4 subjects had "blood deficiency," 10 subjects had "blood stasis," and 8 subjects had "fluid retention." OBF increased significantly 15 to 60 minutes after the administration of TSS in the group of subjects with "blood deficiency" and "blood stasis" (15 minutes, $P < 0.05$; 30 minutes, $P < 0.05$; 45 minutes, $P < 0.05$; 60 minutes, $P < 0.05$) and in the group with "blood deficiency" and "fluid retention" (15 minutes, $P < 0.05$; 30 minutes, $P < 0.05$; 45 minutes, $P < 0.05$; 60 minutes, $P < 0.05$) (Figures 2(a) and 2(b)). Figure 3 shows a representative image of OBF in the ONH before administration of TSS, as well as 30 and 60 minutes after administration.

Table 3: Baseline variables in the 2 study groups (Experiment 2).

Variable	Control	TSS	P value
OBF (AU)	25.1 ± 4.3	24.7 ± 4.6	0.25
IOP (mmHg)	12.8 ± 2.2	13.8 ± 2.0	<0.01
SBP (mmHg)	106.2 ± 11.4	110.1 ± 14.2	0.16
DBP (mmHg)	64.9 ± 8.4	67.9 ± 10.8	0.09
MBP (mmHg)	82.3 ± 9.1	85.7 ± 11.7	0.11
PR (beats/min)	73.1 ± 13.1	73.2 ± 9.5	0.65

Data are expressed as mean ± standard deviation. Differences between groups were assessed with the Kruskal-Wallis test.

4. Discussion

Ex. 1 revealed that, of four candidate kampo formulas, only TSS had the effect of increasing OBF. This was somewhat in contrast to previous studies, which have found that YKS has an influence on blood flow in the short posterior ciliary artery in rabbits [8] and that HJG has an effect on blood flow in the central retinal artery in humans [9]. This may be due to differences in OBF measurement technique and location between these previous studies and the present one. The previous studies evaluated OBF from the retrobulbar side, whereas this study evaluated OBF from the ocular side, in the ONH.

The mechanism of the effects of TSS and KBG on circulation has been described in several reports. Nasu et al. reported that TSS had an inhibitory effect on platelet aggregation [10]. KBG has been reported to improve endothelial function in patients with metabolic syndrome [29]. Additionally, an evaluation of erythrocyte aggregability and deformability in patients with multiple old lacunar infarctions found that KBG improved microcirculation [12, 13]. TSS has a number of

Table 4: Alteration of ocular blood flow and clinical variables in response to administration of kampo formula (Experiment 2).

	Variable	Baseline	15 minutes after treatment	30 minutes after treatment	45 minutes after treatment	60 minutes after treatment	P value
Control	OBF change (%)	100.0 ± 0.0	99.3 ± 8.0	99.8 ± 8.1	101.7 ± 7.6	101.4 ± 8.1	0.49
	IOP (mmHg)	12.8 ± 2.2				12.4 ± 2.1	0.11
	SBP (mmHg)	106.2 ± 11.4	106.9 ± 11.5	106.2 ± 10.2	108.0 ± 13.0	108.1 ± 13.5	0.98
	DBP (mmHg)	64.9 ± 8.4	67.5 ± 12.0	65.3 ± 7.4	65.8 ± 7.4	66.9 ± 8.4	0.90
	MBP (mmHg)	82.3 ± 9.1	84.1 ± 11.0	82.5 ± 8.3	83.5 ± 9.0	84.2 ± 10.0	0.96
	PR (beats/min)	73.1 ± 13.1	66.7 ± 8.1	65.7 ± 7.5	67.7 ± 7.8	66.3 ± 8.1	0.12
TSS	OBF change (%)	100.0 ± 0.0	102.7 ± 7.0	104.1 ± 5.3	104.2 ± 4.8	104.0 ± 5.5	<0.01
	IOP (mmHg)	13.8 ± 2.0				13.6 ± 1.8	0.41
	SBP (mmHg)	110.1 ± 14.2	110.1 ± 10.0	108.6 ± 10.3	108.3 ± 11.5	109.0 ± 10.7	0.98
	DBP (mmHg)	67.9 ± 10.8	69.3 ± 9.8	68.3 ± 8.4	69.3 ± 9.2	71.0 ± 10.8	0.90
	MBP (mmHg)	85.7 ± 11.7	86.4 ± 9.1	85.2 ± 8.5	85.7 ± 9.1	87.0 ± 10.1	0.45
	PR (beats/min)	67.9 ± 10.8	69.3 ± 9.8	68.3 ± 8.4	69.3 ± 9.2	71.0 ± 10.8	0.19

Data are expressed as mean ± standard deviation. The Wilcoxon signed-rank test was applied to assess differences in IOP before and after kampo administration. A one-way analysis of variance was used to assess differences in other values before and after kampo administration.

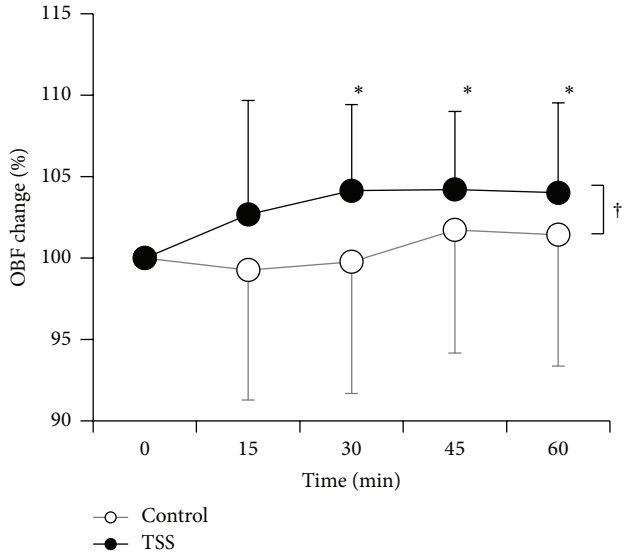

Figure 1: Dynamic OBF changes in response to administration of TSS (●) and control (○). Data are expressed as mean ± standard deviation. The dagger indicates a statistically significant difference between TSS and control (two-way analysis of variance; ANOVA). The asterisk indicates a statistically significant difference from the baseline (repeated measurements of ANOVA, with post hoc Dunnett's test).

components in common with YKS, KBG, and HJG. Atractylodis Lanceae Rhizoma, included in YKS and TSS, has been reported to inhibit platelet aggregation [10]. Poria, included in YKS, TSS, KBG, and HJG, has been reported to have a similar effect [10]. Paeoniae Radix, included in TSS and KBG, has been reported to relax vascular smooth muscle [11]. Polyphenols of Cinnamomi Cortex or cinnamaldehyde, included in KBG and HJG, have been reported to have an endothelium-dependent relaxative effect [30–33]. Moreover, these four kampo formulas include multiple physiologically active substances that have yet to be fully identified. The interactions between them are also not yet fully understood.

In Ex. 2, we found that TSS increased OBF without affecting BP or IOP. This additional experiment supported the preliminary results of Ex. 1. In kampo practice, TSS is used to treat "blood deficiency," "fluid retention," and "blood stasis" [34], which are part of six conditions used in kampo practice and described by Terasawa. These conditions also include "qi deficiency," "qi stagnation," and "qi counter flow." Classification of patients depends on their symptoms and a physical examination [27, 28, 34]. "Blood deficiency" and "blood stasis" are believed to be associated with general symptoms of eye disease such as blurred vision, decreased visual acuity, and visual field defects, while increased IOP is believed to be associated with "fluid retention" and "qi stagnation." Kampo formulas are chosen based on the patient's symptoms and the results of a physical examination in a clinical setting, a methodology that has been in use since ancient times. Patients with combined "blood deficiency" and "blood stasis" or combined "blood deficiency" and "fluid retention" are considered suitable cases for treatment with TSS in kampo practice, and in Ex. 2 of this study, the OBF increase was in fact most remarkable in subjects with these conditions. This result supports the existence of a relationship between the effectiveness of kampo formulas in practice and diagnoses made according to kampo theory. The effectiveness of the formulas has traditionally been judged only by subjectively measured improvements, with quantitative and objective reports of the effects of kampo formulas on ocular circulation being very limited. The present study sought to alleviate this deficiency. We believe our results indicate that, to be most effective, kampo formulas should be chosen after patients are evaluated by both traditional kampo diagnostic practices and western medical techniques.

The authors have previously reported that 60 minutes after administration of topical tafluprost, LSFG measurements of OBF increased significantly in the eyes of normal subjects and patients with normal tension glaucoma (NTG)

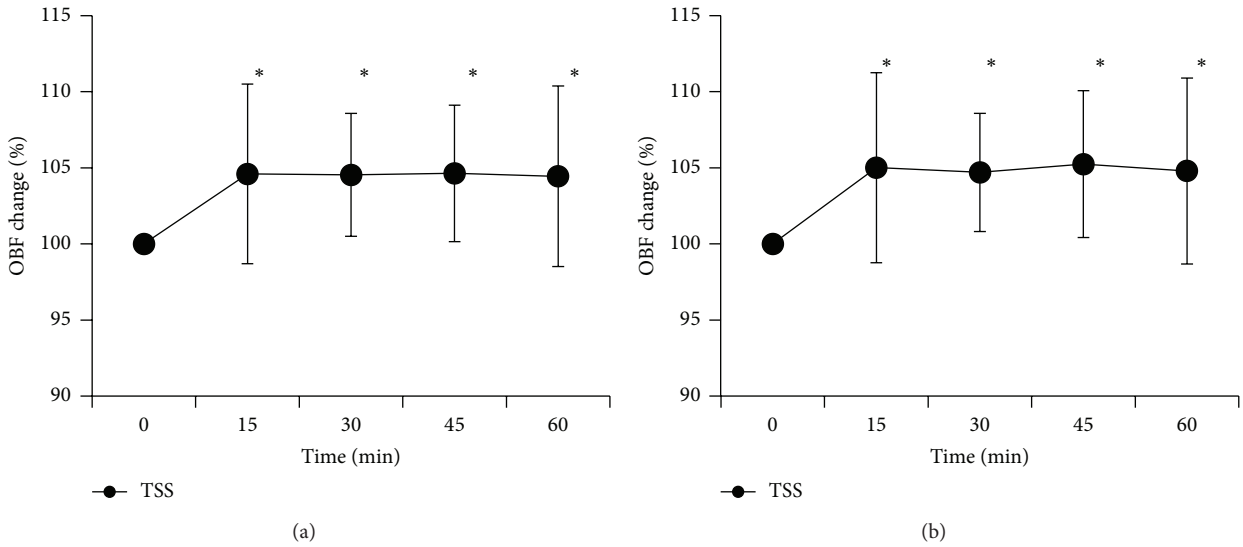

Figure 2: Dynamic OBF changes in subjects with blood deficiency and blood stasis (a) and with blood deficiency and fluid retention (b) in response to administration of TSS. Data are expressed as mean ± standard deviation. The asterisk indicates a statistically significant difference from the baseline (repeated measurements of ANOVA, with post hoc Dunnett's test).

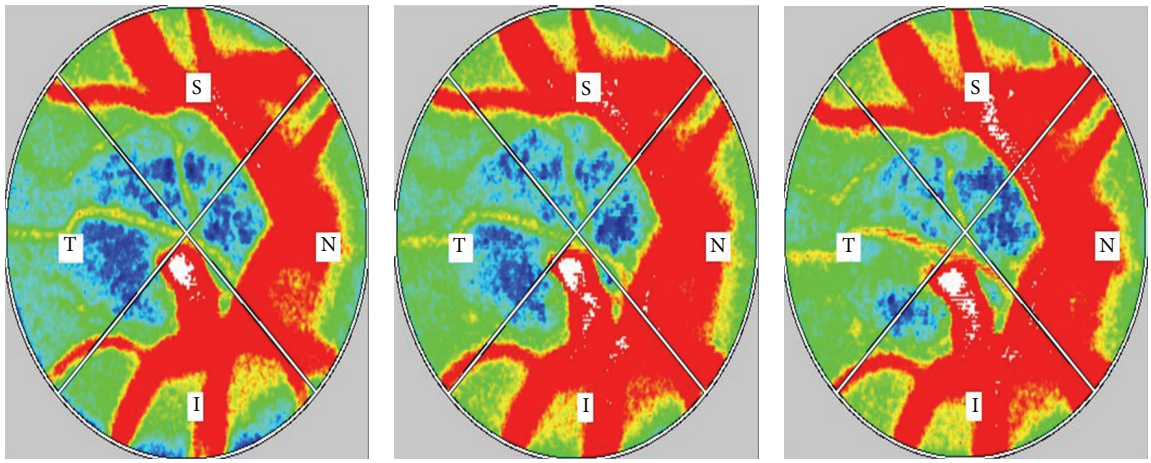

Figure 3: Representative MBR images of the entire ONH before administration and 30 and 60 minutes after the administration of TSS in healthy subjects (right eye). (a) Composite blood flow map of the ONH before the administration of TSS. The MBR value is 21.2. (b) Composite blood flow map of the ONH 30 minutes after the administration of TSS. The MBR value is 24.8. (c) Composite blood flow map of the ONH 60 minutes after the administration of TSS. The MBR value is 26.1.

(100% to 104.3 ± 6.6%, $P < 0.01$) [16]. This study revealed that TSS had a similar ability to significantly increase OBF in a similar timeframe. In addition, while tafluprost led to a significant decrease in IOP, TSS had no effect on IOP. Recently, it has been suggested that impaired ocular circulation may contribute to the progression of glaucomatous damage [35, 36]. New drugs or interventions to improve ocular hemodynamics have thus become a promising target of research. Hypotension often coincides with NTG [37], and as oral vasodilators are difficult to use, to both improve OBF and treat hypotension, TSS administration, alone and in combination with topical medications such as tafluprost, may be an effective strategy to improve fundus circulation in glaucoma patients, especially those with NTG.

Limitations. We found that PR decreased after the administration of YKS, TSS, KBG, and HJG. Moreover, this decrease occurred in all groups of subjects including those who were administered a control substance, leading us to believe that it was a nonspecific response. The subjects waited in a quiet, darkened room for over 30 minutes, and the observed decrease in PR may have been an effect of relaxation. The other limitation of this study was the small number of healthy subjects included and the short observation time. In the

future, we hope to conduct a longitudinal clinical study to determine the effectiveness of TSS in patients with eye disease, especially NTG.

5. Conclusions

TSS increased OBF without affecting BP or IOP in healthy subjects. Further study will be needed to investigate the effect of TSS in patients with eye disease.

Abbreviations

OBF: Ocular blood flow
YKS: Yokukansan
TSS: Tokishakuyakusan
KBG: Keishibukuryogan
HJG: Hachimijiogan
LSFG: Laser speckle flowgraphy
ONH: Optic nerve head
Ex.: Experiment
IOP: Intraocular pressure
BP: Blood pressure
PR: Pulse rate
MBP: Mean arterial blood pressure
SBP: Systolic BP
DBP: Diastolic BP
MBR: Mean blur rate
NTG: Normal tension glaucoma.

Conflict of Interests

The authors declare that they have no conflict of interests.

Authors' Contribution

Shin Takayama and Yukihiro Shiga equally contributed to this work. Shin Takayama took part in planning the study, randomized the order of administration of the kampo medical formulas, and wrote the paper. Yukihiro Shiga took part in planning the study, performed the measurements, and wrote the paper. Taiki Kokubun, Hideyuki Konno, Noriko Himori, and Morin Ryu took part in planning the study and performed the measurements. Takehiro Numata performed the statistical analysis. Soichiro Kaneko took part in planning the study and provided advice for the statistical analysis. Hitoshi Kuroda, Junichi Tanaka, Seiki Kanemura, Tadashi Ishii, and Toru Nakazawa provided advice for the protocol and the paper. Tadashi Ishii, Nobuo Yaegashi, and Toru Nakazawa were responsible for the study design and execution and assisted in writing the paper.

Acknowledgments

The authors thank Seri Takahashi, Shiori Suzuki, and Haruka Sato for technical support and thank Tim Hilts for reviewing the paper. Tohoku University Graduate School of Medicine did receive a grant from Tsumura, a Japanese manufacturer of kampo medicine.

References

[1] F. Berisha, G. T. Feke, T. Hirose, J. W. McMeel, and L. R. Pasquale, "Retinal blood flow and nerve fiber layer measurements in early-stage open-angle glaucoma," *American Journal of Ophthalmology*, vol. 146, no. 3, pp. 466–472, 2008.

[2] J. E. Grunwald, A. J. Brucker, S. E. Grunwald, and C. E. Riva, "Retinal hemodynamics in proliferative diabetic retinopathy: a laser Doppler velocimetry study," *Investigative Ophthalmology & Visual Science*, vol. 34, no. 1, pp. 66–71, 1993.

[3] E. M. Kohner, "Dynamic changes in the microcirculation of diabetics as related to diabetic microangiopathy," *Acta Medica Scandinavica, Supplement*, vol. 578, pp. 41–47, 1975.

[4] J. E. Grunwald, C. E. Riva, and R. A. Stone, "Retinal autoregulation in open-angle glaucoma," *Ophthalmology*, vol. 91, no. 12, pp. 1690–1694, 1984.

[5] Y. Sato, *Introduction to Kampo*, The Japan Society for Oriental Medicine, Elsevier, pp. 6–8, 2005.

[6] Y. Sato, *Introduction to Kampo*, The Japan Society for Oriental Medicine, Elsevier, pp. 165–168, 2005.

[7] S. Hayasaka, T. Kodama, and A. Ohira, "Traditional Japanese herbal (kampo) medicines and treatment of ocular diseases: a review," *The American Journal of Chinese Medicine*, vol. 40, no. 5, pp. 887–904, 2012.

[8] R. Yamada, "Hemodynamic examination on short posterior ciliary artery of the rabbit after the administration of yokukansan," *Kampo and the Newest Therapy*, vol. 20, no. 2, pp. 175–178, 2011.

[9] H. Isobe, K. Yamamoto, and J.-C. Cyong, "Effects of Hachimijio-gan (Ba-wei-di-huang-wan) on blood flow in the human central retinal artery," *The American Journal of Chinese Medicine*, vol. 31, no. 3, pp. 425–435, 2003.

[10] Y. Nasu, M. Iwashita, M. Saito, S. Fushiya, and N. Nakahata, "Inhibitory effects of Atractylodis Lanceae Rhizoma and Poria on collagenor thromboxane A2-induced aggregation in rabbit platelets," *Biological and Pharmaceutical Bulletin*, vol. 32, no. 5, pp. 856–860, 2009.

[11] H. Goto, Y. Shimada, Y. Akechi, K. Kohta, M. Hattori, and K. Terasawa, "Endothelium-dependent vasodilator effect of extract prepared from the roots of Paeonia lactiflora on isolated rat aorta," *Planta Medica*, vol. 62, no. 5, pp. 436–439, 1996.

[12] T. Itoh, K. Terasawa, K. Kohta, N. Shibahara, H. Tosa, and Y. Hiyama, "Effects of Keishi-bukuryo-gan and trapidil on the microcirculation in patients with cerebro-spinal vascular disease," *Journal of Medical and Pharmaceutical Society For WAKAN-YAKU*, vol. 9, no. 1, pp. 40–46, 1992.

[13] H. Hikiami, H. Goto, N. Sekiya et al., "Comparative efficacy of Keishi-bukuryo-gan and pentoxifylline on RBC deformability in patients with "oketsu" syndrome," *Phytomedicine*, vol. 10, no. 6-7, pp. 459–466, 2003.

[14] S. Takayama, M. Watanabe, H. Kusuyama et al., "Evaluation of the effects of acupuncture on blood flow in humans with ultrasound color Doppler imaging," *Evidence-Based Complementary and Alternative Medicine*, vol. 2012, Article ID 513638, 8 pages, 2012.

[15] T. Seki, S. Takayama, T. Nakazawa et al., "Short-term effects of acupuncture on open-angle glaucoma in retrobulbar circulation: additional therapy to standard medication," *Evidence-based Complementary and Alternative Medicine*, vol. 2011, Article ID 157090, 6 pages, 2011.

[16] S. Tsuda, Y. Yokoyama, N. Chiba et al., "Effect of topical tafluprost on optic nerve head blood flow in patients with myopic disc type," *Journal of Glaucoma*, vol. 22, no. 5, pp. 398–403, 2013.

[17] T. Sugiyama, M. Araie, C. E. Riva, L. Schmetterer, and S. Orgul, "Use of laser speckle flowgraphy in ocular blood flow research," *Acta Ophthalmologica*, vol. 88, no. 7, pp. 723–729, 2010.

[18] N. Aizawa, Y. Yokoyama, N. Chiba et al., "Reproducibility of retinal circulation measurements obtained using laser speckle flowgraphy-NAVI in patients with glaucoma," *Clinical Ophthalmology*, vol. 5, no. 1, pp. 1171–1176, 2011.

[19] Y. Shiga, M. Shimura, T. Asano et al., "The influence of posture change on ocular blood flow in normal subjects, measured by laser speckle flowgraphy," *Current Eye Research*, vol. 38, no. 6, pp. 691–698, 2013.

[20] Y. Shiga, K. Omodaka, H. Kunikata et al., "Waveform analysis of ocular blood flow and the early detection of normal tension glaucoma," *Investigative Ophthalmology & Visual Science*, vol. 54, no. 12, pp. 7699–7706, 2013.

[21] F. N. Sayegh and E. Weigelin, "Functional ophthalmodynamometry: comparison between brachial and ophthalmic blood pressure in sitting and supine position," *Angiology*, vol. 34, no. 3, pp. 176–182, 1983.

[22] A. Longo, M. H. Geiser, and C. E. Riva, "Posture changes and subfoveal choroidal blood flow," *Investigative Ophthalmology & Visual Science*, vol. 45, no. 2, pp. 546–551, 2004.

[23] P. Kaeser, S. Orgül, C. Zawinka, G. Reinhard, and J. Flammer, "Influence of change in body position on choroidal blood flow in normal subjects," *The British Journal of Ophthalmology*, vol. 89, no. 10, pp. 1302–1305, 2005.

[24] Y. Tamaki, M. Araie, K. Tomita, M. Nagahara, A. Tomidokoro, and H. Fujii, "Non-contact, two-dimensional measurement of tissue circulation in choroid and optic nerve head using laser speckle phenomenon," *Experimental Eye Research*, vol. 60, no. 4, pp. 373–383, 1995.

[25] H. Isono, S. Kishi, Y. Kimura, N. Hagiwara, N. Konishi, and H. Fujii, "Observation of choroidal circulation using index of erythrocytic velocity," *Archives of Ophthalmology*, vol. 121, no. 2, pp. 225–231, 2003.

[26] N. Konishi, Y. Tokimoto, K. Kohra, and H. Fujii, "New laser speckle flowgraphy system using CCD camera," *Optical Review*, vol. 9, no. 4, pp. 163–169, 2002.

[27] K. Terasawa, *Shoreikaramanabu Wakanshinryogaku*, Igakushoin, Tokyo, Japan, 3rd edition, 2011.

[28] M. Arai, K. Arai, C. Hioki et al., "Evaluation of medical students using the, "qi, blood, and fluid" system of Kampo medicine," *The Tokai Journal of Experimental and Clinical Medicine*, vol. 38, no. 1, pp. 37–41, 2013.

[29] Y. Nagata, H. Goto, H. Hikiami et al., "Effect of keishibukuryogan on endothelial function in patients with at least one component of the diagnostic criteria for metabolic syndrome: a controlled clinical trial with crossover design," *Evidence-Based Complementary and Alternative Medicine*, vol. 2012, Article ID 359282, 10 pages, 2012.

[30] L. Gongwang, *Fundamentals of Formulas of Chinese Medicine*, Hua Xia, 2002.

[31] K. Tanikawa, H. Goto, N. Nakamura et al., "Endotheliumdependent vasodilator effect of tannin extract from Cinnamonomi Cortex on isolated rat aorta," *Journal of Medical and Pharmaceutical Society for WAKAN-YAKU*, vol. 16, pp. 45–50, 1999.

[32] H. Goto, Y. Shimada, Y. Akechi, K. Kohta, M. Hattori, and K. Terasawa, "Endothelium-dependent vasodilator effect of extract prepared from the roots of Paeonia lactiflora on isolated rat aorta," *Planta Medica*, vol. 62, no. 5, pp. 436–439, 1996.

[33] A. Yanaga, H. Goto, T. Nakagawa, H. Hikiami, N. Shibahara, and Y. Shimada, "Cinnamaldehyde induces endothelium-dependent and -independent vasorelaxant action on isolated rat aorta," *Biological and Pharmaceutical Bulletin*, vol. 29, no. 12, pp. 2415–2418, 2006.

[34] Y.-L. Xue, H.-X. Shi, F. Murad, and K. Bian, "Vasodilatory effects of cinnamaldehyde and its mechanism of action in the rat aorta," *Vascular Health and Risk Management*, vol. 7, pp. 273–280, 2011.

[35] M. Satilmis, S. Orgül, B. Doubler, and J. Flammer, "Rate of progression of glaucoma correlates with retrobulbar circulation and intraocular pressure," *American Journal of Ophthalmology*, vol. 135, no. 5, pp. 664–669, 2003.

[36] J. Schumann, S. Orgül, K. Gugleta, B. Dubler, and J. Flammer, "Interocular difference in progression of glaucoma correlates with interocular differences in retrobulbar circulation," *American Journal of Ophthalmology*, vol. 129, no. 6, pp. 728–733, 2000.

[37] V. P. Costa, E. S. Arcieri, and A. Harris, "Blood pressure and glaucoma," *British Journal of Ophthalmology*, vol. 93, no. 10, pp. 1276–1282, 2009.